GENERAL DYNAMICS
CORPORATION

GA-1030
MA-S89-1

MARITIME GAS-COOLED REACTOR PROGRAM

QUARTERLY PROGRESS REPORT
FOR THE PERIOD ENDING MARCH 31, 1959

Contract AT(04-3)-187

U.S. ATOMIC ENERGY COMMISSION

and

MARITIME ADMINISTRATION

GENERAL ATOMIC and
ELECTRIC BOAT DIVISIONS

LEGAL NOTICE

Printed in USA. Price $2.75.

Available from the Office of Technical Services,
Department of Commerce,
Washington 25, D.C.

GENERAL DYNAMICS
CORPORATION

GA-1030
Reactors—Power
TID-4500 (15th ed.)

MARITIME GAS-COOLED REACTOR PROGRAM

QUARTERLY PROGRESS REPORT

FOR THE PERIOD ENDING MARCH 31, 1959

Contract AT(04-3)-187

U.S. ATOMIC ENERGY COMMISSION

and

MARITIME ADMINISTRATION







GENERAL ATOMIC and
ELECTRIC BOAT DIVISIONS

MGCR QUARTERLY REPORT SERIES

GA-744 October, November, December, 1958

SUMMARY

Turbomachinery considerations indicate that it would be desirable to reduce the cycle pressure from 1,000 psia to 800 psia. Although this change does not affect the over-all efficiency, it necessitates the revision of certain cycle conditions. Preliminary design calculations based on these new conditions have been made.

The problem of determining the temperature distribution and the resulting thermal-stress pattern within the graphite has been considered. An analytical solution was found for the case in which the thermal conductivity throughout the fuel element is constant, i. e., assuming there is no discontinuity between the fuel body and the cladding or between the cladding and the graphite. A code is being developed to permit calculation of the temperature pattern for the case in which the conductivity is not constant.

Preliminary designs for a heterogeneous fuel element and a semihomogeneous fuel element were developed. At the present time, all problems associated with the design of a satisfactory semihomogeneous fuel element appear to be solvable. The tentative design of an electrically heated, high-temperature, high-pressure helium test loop for testing fuel-element performance is being developed for cost estimation. Since such a loop would be a major item in regard to both cost and effort, other methods of testing are also being considered.

A decision has been reached to utilize the Hanford in-pile gas loop as soon as possible. Although the loop will operate at a helium pressure somewhat less than the MGCR operating conditions, it is anticipated that the test samples will attain the power densities and temperatures predicted for the MGCR; first tests are scheduled for August, 1959. Extensive testing was carried out during the quarter to firm up the design of the test model. In this connection, a nuclear mockup of the test element was fabricated and sent to Hanford for preliminary tests in the Hanford test pile.

Two-group PDQ calculations were run to estimate control-rod worth for the preliminary design core under cold, clean conditions. Calculations were run in the XY-geometry with the rods in the form of thermally black cruciforms; axial bucklings for the cases were derived from axial flux distributions obtained in PDQ calculations of the unrodded core in RZ-geometry. The results of these calculations are included in this report.

Curves of rod worth versus position were developed for the hot, clean and the cold, clean preliminary design core. Normalized curves of the fraction of rod worth versus fraction of rod length inserted are given. These curves demonstrate the higher incremental worth of the rods in the cold core as compared to that in the hot core.

Revision of the estimated core life was made by introducing corrections to the equivalent resonance escape probability and thermal nonleakage probability for a reactor in the analytical burnup model. For the preliminary design core, the lifetime at full power was reduced from 603 to 572 days.

A detailed lifetime calculation was made for the preliminary design heterogeneous core; for purposes of this calculation, 428 g of natural boron was considered to be uniformly distributed throughout the fuel elements. Variations in K_{eff} versus days at full power for a core with and without boron for hot and cold conditions are presented.

Fuel-cycle costs were estimated on the basis of the effect of boron in the fuel elements. In all cases, the fuel-cycle costs vary less than 10% for the lifetime and loading ranges considered.

It is presently planned to locate the critical facility in the buildings originally constructed for General Atomic's CIRGA experiments. The schedule for the critical experiments is based on establishing the pressure-vessel requirements in the spring of 1960. To achieve this aim, the critical facility should be ready for operation by late 1959, and the experiments are expected to be completed six months later. The design of the facility is 50% complete, and the procurement of materials and equipment has been started. Work has begun on the preparation of the safeguards report,

and a vendor has been selected to fabricate the fuel.

To augment the present experimental program, it is proposed that a series of experiments be performed in the Lawrence Radiation Laboratory "hot box" facility. Specifically, the use of elements containing U^{238} and rare earths is proposed. These elements would be in groups of various sizes and compositions, so that the influence of both "lumping" and temperature could be evaluated.

The speed of the main turbine shaft has been tentatively set at approximately 12,200 rpm--a factor of 2.75 times the first critical speed. Although a higher factor could be tolerated, it is felt that other considerations preclude the use of critical speed ratios as high as those that are used in open-cycle practice.

The design and fabrication of a test stand to evaluate shaft seals and seal systems has been completed and trial runs have been made. First tests will be made on bushings and face seals. Later tests will involve other seals, including the floating-ring and floating-labyrinth types of seal.

The effects of minor heat transfer due to heat leakage, fluid flow, and thermodynamic phenomena on MGCR full-load cycle performance were studied. The variables and results are presented in Section IV of this report.

The heat-exchanger test facility was assembled and prepared for operation, despite serious delays encountered by the late arrival and fabrication deficiencies of the model heat exchanger. Some of the operating characteristics of the facility are described.

A critical review was conducted on the desirability of using concentric ducts and valves. The prototype design is based on the use of concentric ducts and concentric valves between the reactor and the propulsion system. Pressure-loss studies have been conducted for various configurations of ducting. The preliminary design for the heat barrier in straight-duct sections is now essentially complete.

Work is continuing on various control systems. Block diagrams

outlining reactor power level, reactor outlet temperature, and plant inventory control are presented.

Differential equations which permit the dynamic analysis of a closed-cycle gas-turbine plant were programed for numerical solution on a digital computer. Response to disturbances resulting from changes in reactor power and changes in plant load has been obtained. Equations have been determined for the transient behavior of the regenerator.

Descriptions have been prepared for each fluid-mechanical system. Preliminary sizing of all principal system components has been completed, and a preliminary arrangement study has been made.

Several methods of purifying helium in both the storage bank and the main loop have been investigated. Of these, low-temperature adsorption and high-temperature gettering have been selected for laboratory study.

Task descriptions have been drafted for all 18 propulsion-plant electrical systems, and block diagrams have been prepared. Investigations into the maximum operating temperatures of the various electrical equipment indicate that ambient temperatures up to 140°F can be tolerated.

Arrangement studies of plant structure and shielding are continuing. The main effort has been directed toward the elimination or minimizing of the relative thermal expansion of the various components.

The emergency cooling system is under study. Preliminary design work has been carried out on a cool-down system which uses a stored inert coolant, such as nitrogen, CO_2, or steam.

Work on the irradiation stability of fuel materials is continuing at Battelle Memorial Institute. Results indicate that conversion from the monocarbide to the dicarbide can take place at temperatures as low as 2,350°F in graphite bodies which contain uranium monocarbide.

A program has been initiated to study the sintering properties of alumina in a hydrogen atmosphere. Sintered-pellet densities as high as 96.6% of theoretical values have been produced.

Apparatus has been put into operation to measure the fission-product

xenon released from irradiated UO_2 granules of controlled particle size. Results are given for a wide range of particle size.

The hot cells under construction at General Atomic will be completed approximately on schedule; however, a strike at the vendor's plant that is supplying the manipulators will limit the use of the cells for an unknown length of time.

Progress has been made in the development of high-temperature x-ray diffraction techniques. A camera has been developed for use in studying uranium oxide ceramic systems at temperatures up to 2,000°C.

The cladding of graphite is under study. So far, niobium, nickel, nickel-copper, Monel, and stainless steels have been considered, with nickel and alloys of nickel and copper showing the most promise.

Corrosion and mass-transport tests in helium have begun. Apparatus for this work is described and some preliminary results are presented.

Exploratory tests were conducted to investigate the effects of coolant and impurities in the coolant on plant materials and the effects of gettering on inhibiting reactions. Tests were run for 1,000 hr with graphite at temperatures of 810°C. Significant changes in the hardness of niobium and niobium-zirconium alloys were observed. No carburization was observed in the stainless steel samples.

Economic studies are continuing with the objective of determining the optimum size and power ranges for both nuclear and conventionally powered ships. Total costs for a ton of cargo carried are shown for the New York-to-Kuwait round trip. Present estimated costs for the first seagoing nuclear tankers are somewhat higher than those for conventional ships.

MGCR DESIGN DATA

Power	
At propeller	22,000 shp (max)
Reactor thermal output	54 Mw (max)
Auxiliaries	750 kw
Net shaft efficiency	30%
Cycle efficiency	32%
Reactor	
Moderator and reflector	Graphite
Core dimensions (active lattice)	
Diameter	6.4 ft
Height	6.4 ft
Reflector thickness	1 ft
Vessel	
Outside diameter	10.4 ft
Height	25.5 ft
Wall thickness	5.75 in.
Fuel	Enriched uranium, 128 kg U^{235}
Fuel element	
Heterogeneous	19-rod bundle, 1/4-in. rods of UO_2 in BeO or Al_2O_3, stainless steel clad
Semihomogeneous	Graphite flat plates 1 in. thick, 6 in. wide, 6.4 ft long, containing metal-clad rods of UC in graphite or of UO_2 in BeO
Fuel loading	Uniform
Number of control rods	16
Core life at full power	500 days (approx)
Coolant	Helium
Coolant pressure	800 psia from high-pressure compressor; 308 psia into low-pressure compressor
Reactor inlet temperature	730°F
Reactor outlet temperature	1,300°F
Turbomachinery	
Turbocompressor speed	13,450 rpm
Power-turbine speed	8,000 rpm
Turbomachinery stages	
High-pressure turbines	7
Low-pressure (power) turbines	6
Low-pressure compressors	15
High-pressure compressors	19
Over-all length	30 ft

Shielding	
Primary	40 in. of lead, iron, and water
Secondary (integral with containment)	3.0 in. of iron, 24.0 in. of fuel oil (for emergency diesel plant)
Power-plant weight, including containment and auxiliaries	2,020 long tons

CONTENTS

I. REACTOR DEVELOPMENT

THERMAL AND HYDRODYNAMIC ANALYSIS OF REACTOR CORE
(S. A. Bernsen and R. Katz)

During this quarterly period, turbomachinery considerations indicated a decrease in cycle pressure level from 1,000 to 800 psia. This brought about a revision of cycle conditions to those listed below:

Core pressure	760 psia
Inlet temperature	730°F
Outlet temperature	1,300°F
Maximum surface temperature	1,500°F
Coolant flow	72.78 lb/sec
Power level	54.2 Mw

Preliminary design calculations based on these new conditions have been made for cores using semihomogeneous and heterogeneous fuel elements. Tables 1.1 and 1.2 list some characteristics for several possible parameters for these cores.

FUEL-ELEMENT DESIGN (R. Katz)

Semihomogeneous Element

Since the external surfaces of the semihomogeneous fuel element are flat plates which are parallel to the direction of flow of the working fluid, the exterior heat-transfer and hydrodynamic performance is easily calculable. The interior geometry consists of metal-clad cylindrical fuel rods imbedded in flat graphite slabs, with different degrees of thermal bond between the fuel body and the cladding and between the cladding and

Table 1.1

TYPICAL SEMIHOMOGENEOUS CORE PARAMETERS

	Core Design				
	A	B	C	D	E
Number of assemblies in core	120	120	68	68	68
Fuel-element size (in.)	6 x 6	6 x 6	8 x 8	8 x 8	8 x 8
Plates per assembly	5	6	6	7	8
Fuel pellets per plate	6	7	7	8	9
Plate thickness (in.)	0.687	0.550	0.887	0.741	0.632
Fuel-pellet diameter (in.)	0.442	0.354	0.571	0.476	0.407
Coolant gap (in.)	0.113	0.117	0.113	0.116	0.118
Core void fraction	0.0591	0.0733	0.0601	0.0721	0.0842
Heat-transfer area (ft^2)	2,650	2,970	2,720	3,030	3,320
Average flux (Btu/(ft^2)(hr))	69,800	62,200	68,000	61,000	55,700
Pressure drop (psia)	28.3	17.9	28.5	18.1	13.1

Table 1.2

TYPICAL HETEROGENEOUS CORE PARAMETERS

	Core Design			
	A	B	C	D
Number of assemblies in core	400	450	500	550
Fuel rods per assembly	19	19	19	19
Fuel-rod diameter (in.)	0.250	0.250	0.250	0.250
Minimum spacing between rods (in.)	0.049	0.051	0.052	0.053
Core void fraction	0.0611	0.0706	0.0798	0.0899
Heat-transfer area (ft^2)	3,160	3,560	3,950	4,350
Average flux (Btu/(ft^2)(hr))	58,500	52,000	46,800	42,500
Pressure drop (psia)	46.4	33.7	27.4	21.6

the graphite. This poses a difficult problem in determining the temperature distribution and the resulting thermal-stress pattern within the graphite. If a satisfactory fuel element is to be obtained, it is necessary to know these quantities in order to stay within the limits imposed by strength and carburization properties of the cladding and the graphite.

An analytical solution to this problem has been found for the special case in which the thermal conductivity throughout the entire fuel element--both fuel body and graphite--is a constant; i.e., where no discontinuity exists between the fuel body and the cladding or between the cladding and the graphite. Under this condition, any combination of fuel-body diameter and spacing and graphite slab thickness can be calculated. Figure 1.1 shows the results of one such calculation where the dimensionless isotherms, T^*, have been plotted in one quadrant of a semihomogeneous fuel element in which the spacing of fuel bodies is equal to the graphite slab thickness and the fuel-body diameter is equal to one half the slab thickness.

Calculations based on the constant-conductivity model are useful for relative comparison of fuel elements, but a more refined approach is needed to accurately evaluate the temperature and thermal stress in a given fuel element. A code is being developed to permit calculation of the temperature pattern for cases where conductivity is not constant, and a second code is under study which will enable thermal stresses to be calculated.

At the present time, all problems associated with the design of a satisfactory semihomogeneous fuel element appear to be soluble. It is obvious that thermal stresses will impose limits on power density, and the maximum allowable power density is to be determined.

Heterogeneous Element

The developmental work on this type of fuel element is described under "Fuel-element Thermal Performance Experiments."

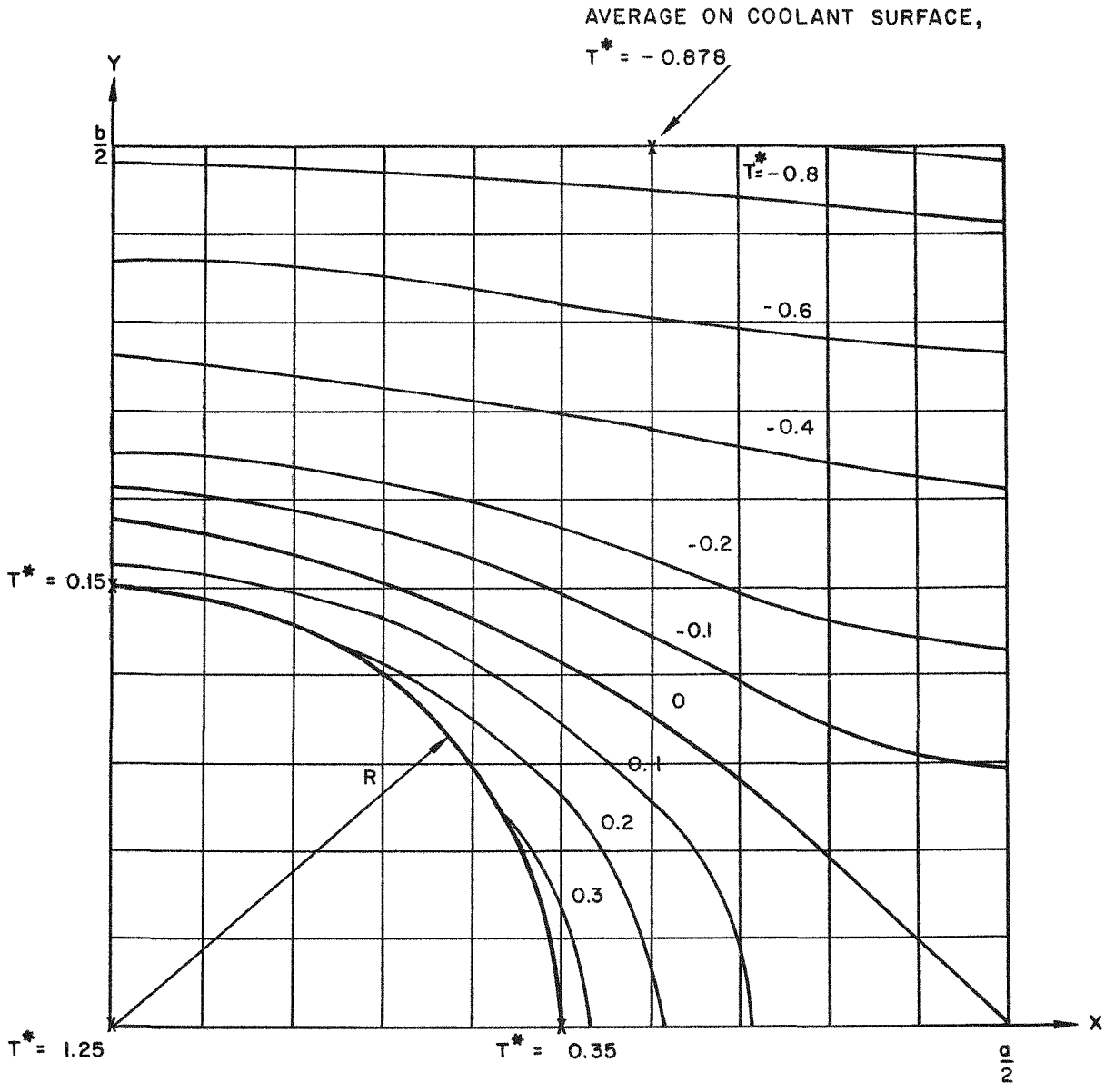

$$T^* = \frac{T}{qR^2/2k} - \left(\frac{\pi}{a}\frac{k}{h} + \frac{\pi}{2}\frac{b}{a} - \ln 2\right)$$

T^* = DIMENSIONLESS TEMPERATURE

T = TEMPERATURE (°F)

q = POWER DENSITY (BTU/(FT^3)(HR))

R = FUEL - PELLET RADIUS (FT)

k = THERMAL CONDUCTIVITY (BTU/(FT)(HR)(°F))

h = HEAT - TRANSFER COEFFICIENT (BTU/(FT^2)(HR)(°F))

Fig. 1.1--Temperature distribution in semihomogeneous fuel element

FUEL-ELEMENT THERMAL PERFORMANCE EXPERIMENTS

(H. C. Hopkins, Jr.)

The construction of an air-flow test stand for determining heat transfer and fluid-flow performance of fuel elements proceeded rapidly during the quarter. A blower was received and when tested, was found to operate satisfactorily over the required range of flow. The installation of the electric power supply for heating the simulated fuel elements and their associated instrumentation was nearing completion at the end of the quarter.

The temperature instrumentation, which is designed especially for measurement of temperature differences, consists of a precision potentiometer and an automatically balancing potentiometer with a variable range and zero point. Different parts of the test stand are shown in Figs. 1.2 through 1.4.

The first fuel element to be tested will be a mockup of the 19-rod bundle element described in the previous quarterly report (GA-744). Design of a modification of the 19-rod bundle and purchase of equipment that would permit a probe to scan for axial and circumferential temperature variation was begun. One or more rods would consist of hollow thin-wall tubes which are resistance heated and equipped with an internal movable temperature probe.

Although this test facility was designed to test the rod-bundle, heterogeneous type of fuel element, it is not necessarily limited to this type. The facility could be modified to test the semihomogeneous type of fuel elements. In either case, it would be most valuable as a means of quick comparison of hydrodynamic performance and, to a lesser extent, of heat transfer between different fuel elements. It is particularly limited in testing the graphite-encased semihomogeneous elements since it uses air. With such elements, temperatures and heat fluxes must be limited to prevent burning of the graphite in the air stream.

The in-pile loop at Hanford produces approximately design heat fluxes in

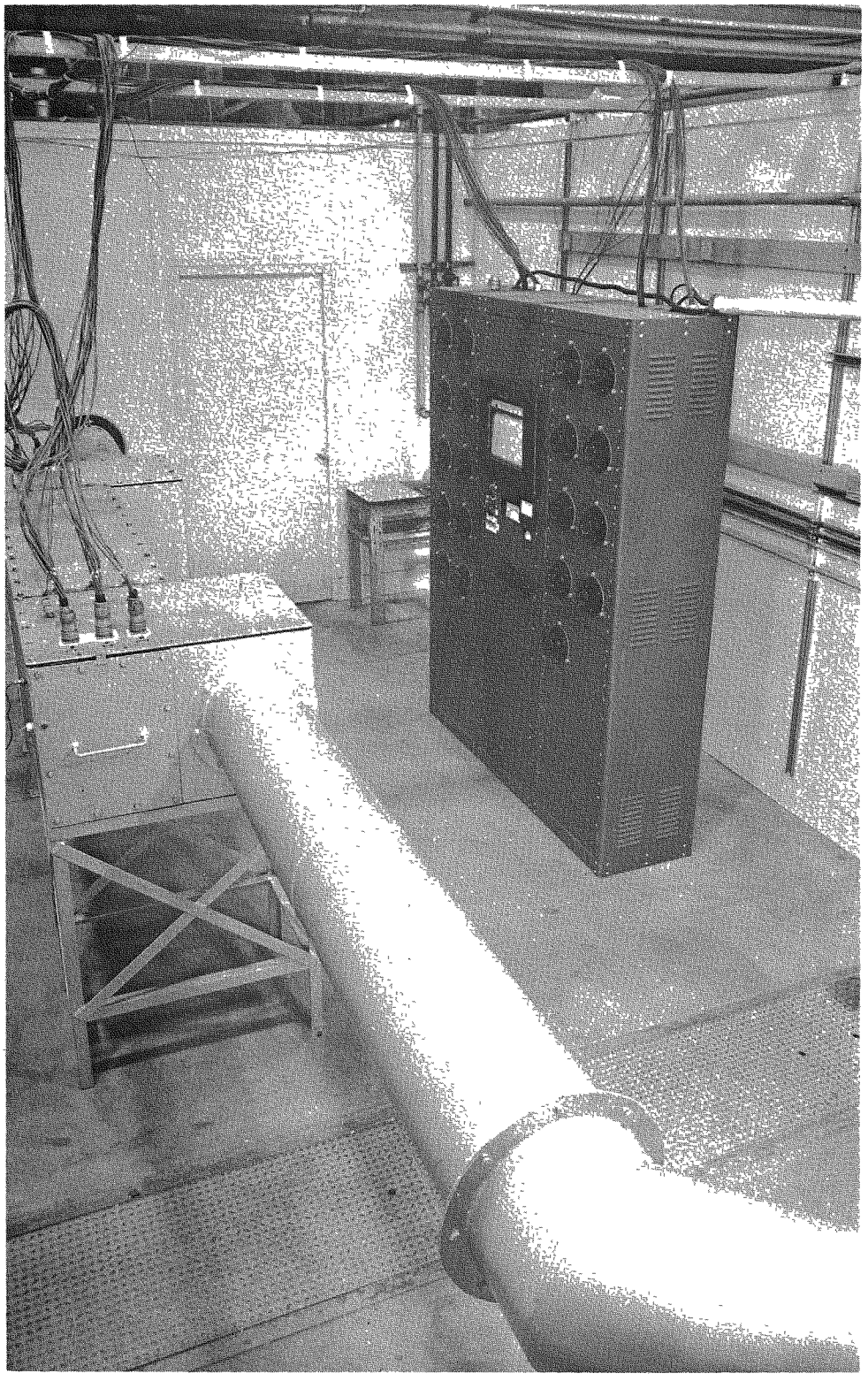

Fig. 1.2--Air-flow test stand

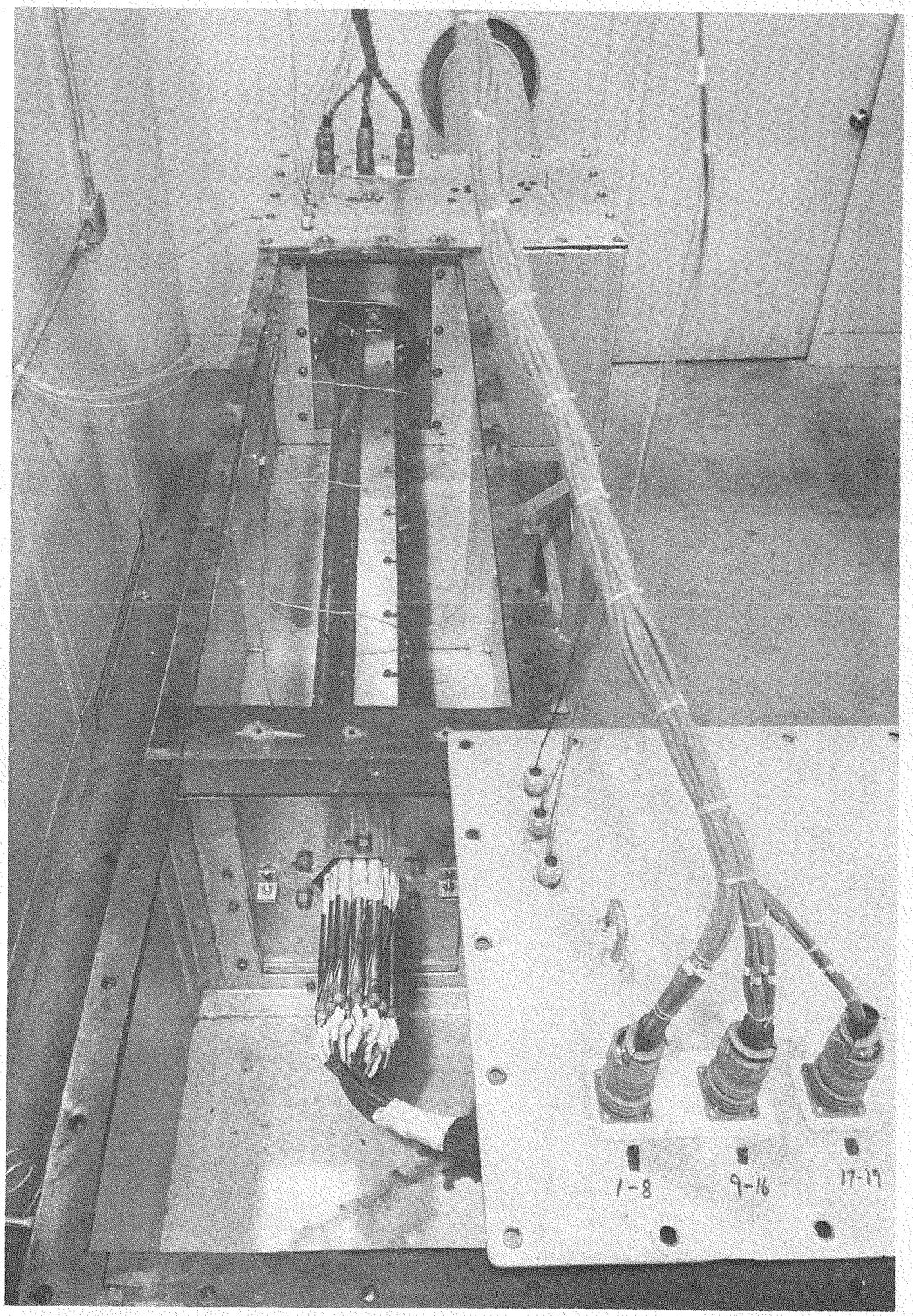

Fig. 1.3--Test section assembled in air-flow test stand

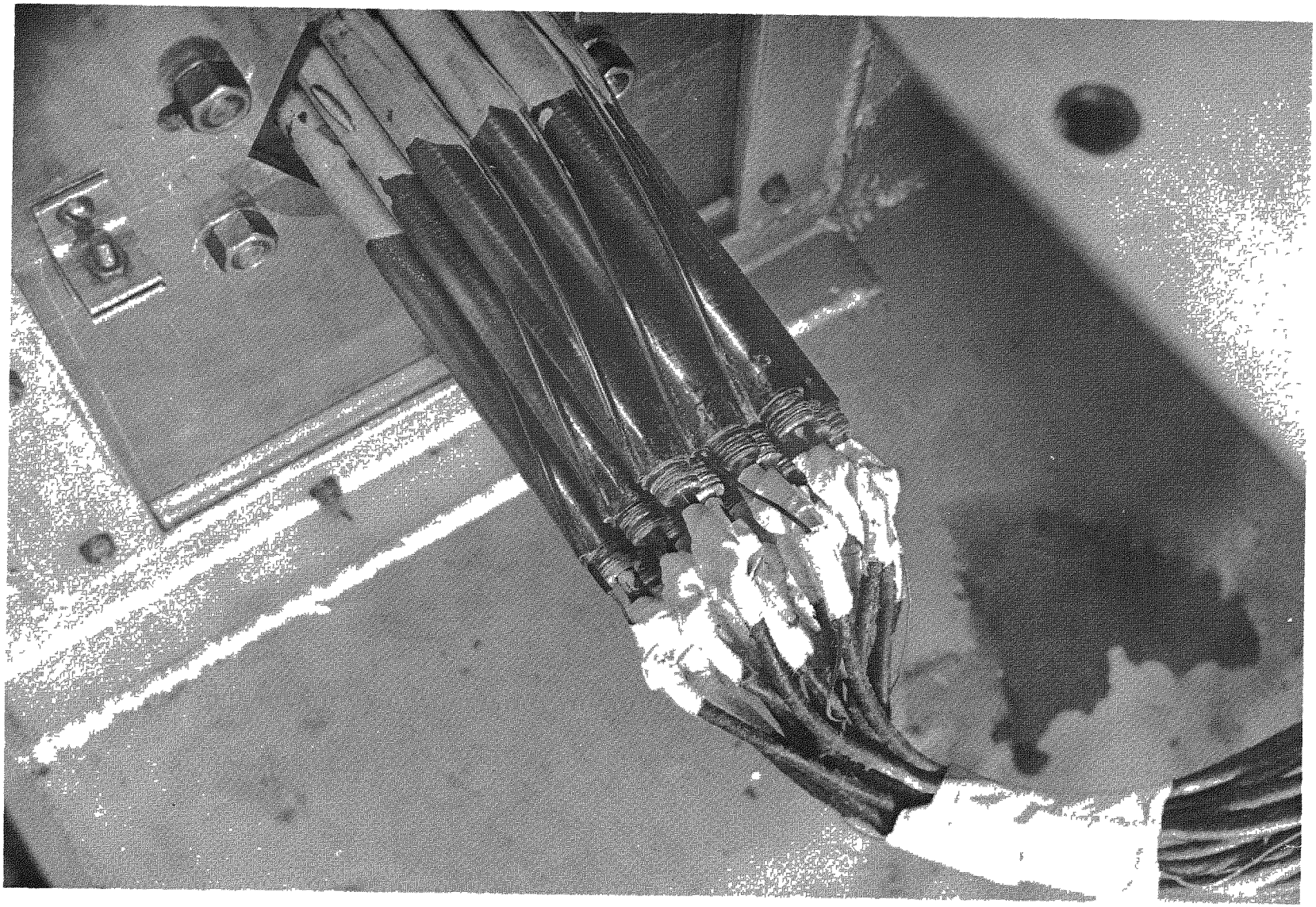

Fig. 1.4--Heater rods assembled in air-flow test section

a helium atmosphere, but size of the test specimen is limited to a small part of a fuel element.

One method of testing performance of fuel elements with respect to fluid flow, heat transfer, and structural integrity at reactor operating conditions would be to construct a high-pressure helium test loop equipped to handle a full-size, electrically heated fuel element. The tentative design of such a loop is being developed for cost-estimation purposes. Since such a facility would be a major item with regard to both cost and effort, alternative methods of developing fuel elements are also being studied.

HANFORD-LOOP EXPERIMENT (R. C. Howard and R. Katz)

Early in this quarterly period, a decision was reached to utilize as soon as possible the Hanford DR reactor gas loop for the MGCR program. The loop, which will operate with helium at 200 psi, will first be employed to test a portion of a semihomogeneous fuel plate 1-1/2 in. wide, 3/4 in. thick, and 18 in. long. It will be possible to operate this plate at the maximum power densities and temperatures anticipated in the MGCR. It is expected that the loop will be ready for operation in July, 1959, and that the first test will begin on schedule early in August.

Previously, the majority of the effort on the semihomogeneous element had been concentrated on design and theoretical analysis. In order to prove the feasibility of an in-pile semihomogeneous test element, an accelerated experimental program has been undertaken. This program includes the development of fabrication techniques and tests of components under simulated in-pile loop conditions. Figure 1.5 shows some of the details of the model to be tested and Fig. 1.6 shows the expected in-pile performance of the test model at varying loop conditions.

Extensive testing was carried out during the quarter to firm up the design of the test model and study techniques of fabrication and

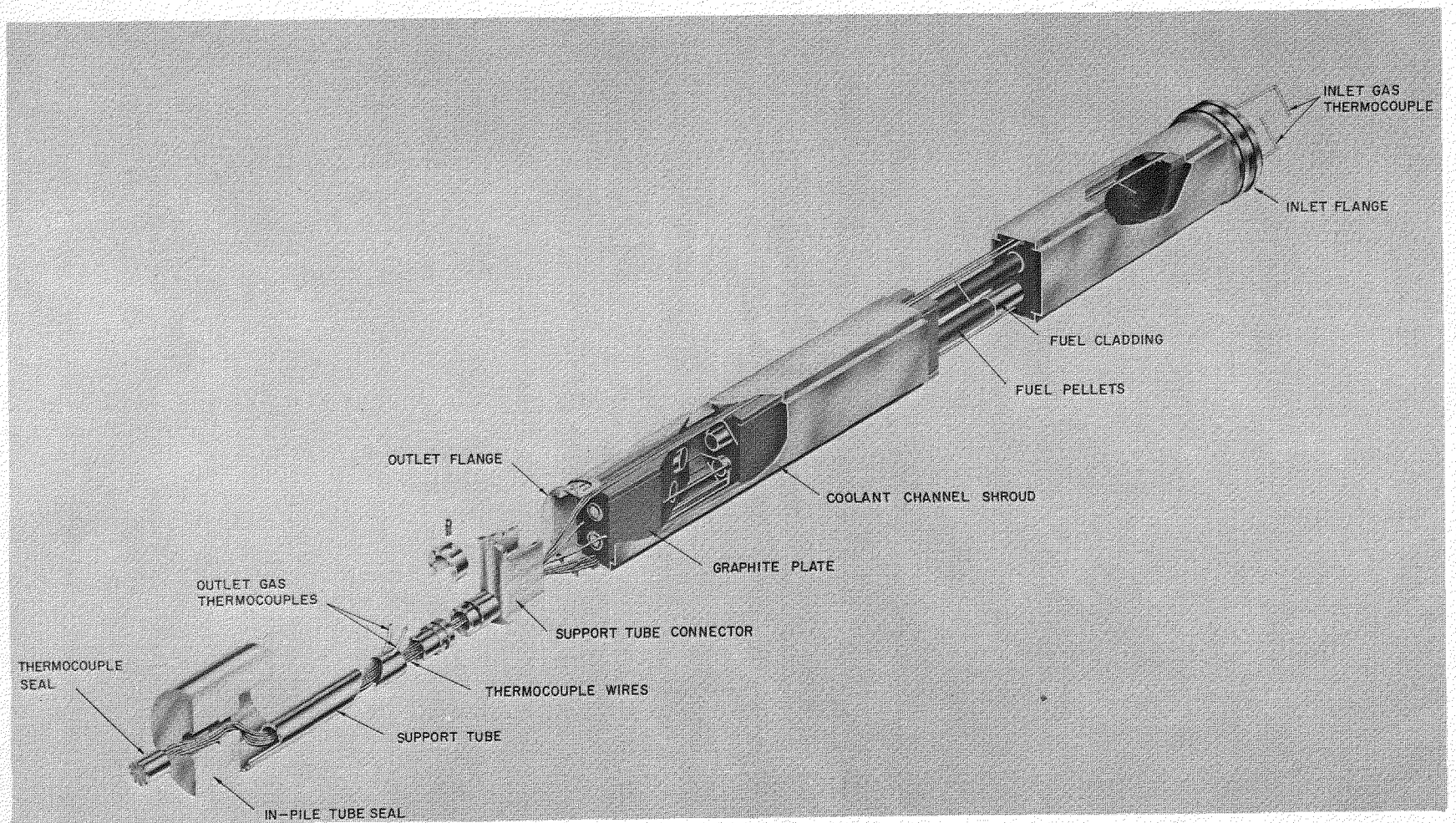

Fig. 1.5--Hanford loop test element

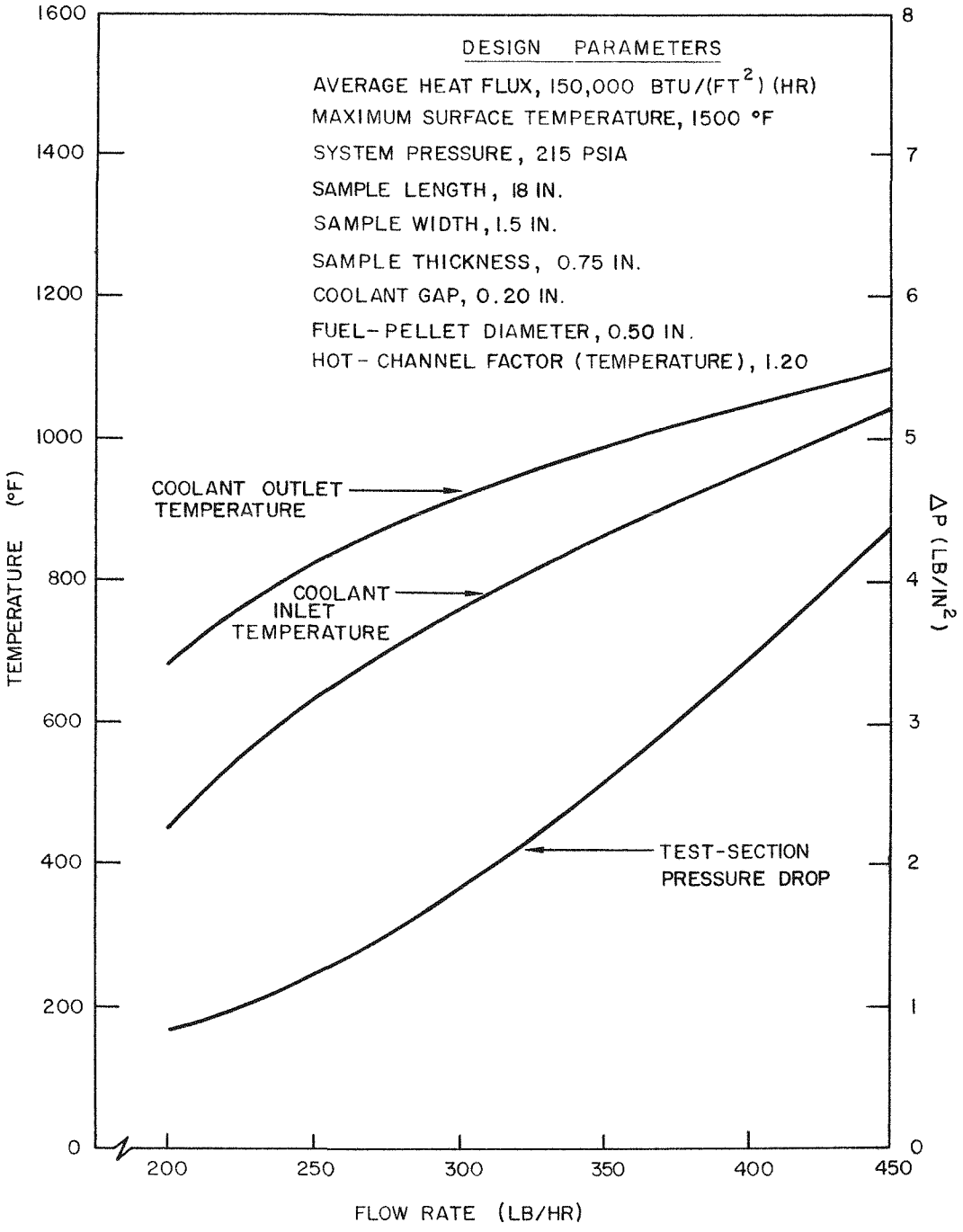

Fig. 1.6--Expected performance of test element (Hanford loop)

instrumentation. The following data were derived:

If 100% of the fission gases are released from the in-pile loop test element, it is conceivable that the pressure could build up as high as 150 psi. Graphite plates tested thus far have not failed until the pressure has exceeded 350 psi, and some have not failed as high as 450 psi. Figure 1.7 shows a typical plate failure which occurred at 430 psi.

A nuclear mockup of the test element (see Fig. 1.8) was fabricated at General Atomic and shipped to Hanford for experiments in the Hanford test pile. These tests will determine the fuel loading required to obtain the desired thermal performance.

Autoclaves for performing thermal cycling and pressure cycling were designed. One is already in operation and a second will be in operation in 1960. These tests have been started.

Furnaces have been set up to determine an acceptable type of piston-ring seal to employ between the test element and the in-pile tube. These tests are essential for determining whether any welding between the ring and the in-pile tube will occur during operation as a result of the nonoxidizing environment of the loop.

Various types of thermocouples have been selected for test and delivery is expected soon. These tests are essential to determine whether carburization will have deleterious effects on metal-clad thermocouples.

Seven sets of nonfueled parts were fabricated for use in the in-pile experiments and preliminary tests.

Ceramic fuel bodies were prepared for use in in-pile tests to determine the physics constants and fuel loading for the test model. The nominal fuel loadings for these tests were 5, 10, 20, and 30 g of U^{235} per foot of pellet-column length. These loadings correspond to 6.1, 12.2, 24.4, and 36.6 g of fully enriched UO_2, respectively. The process used in fabricating these bodies is described in Section IV of this report. In addition, an assortment of nonfueled alumina bodies was

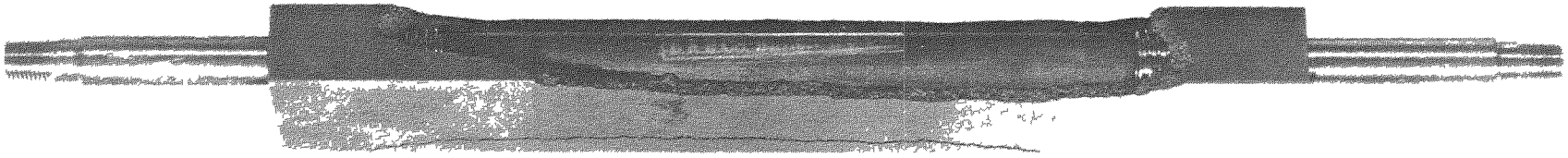

Fig. 1.7--Typical plate failure in graphite strength test

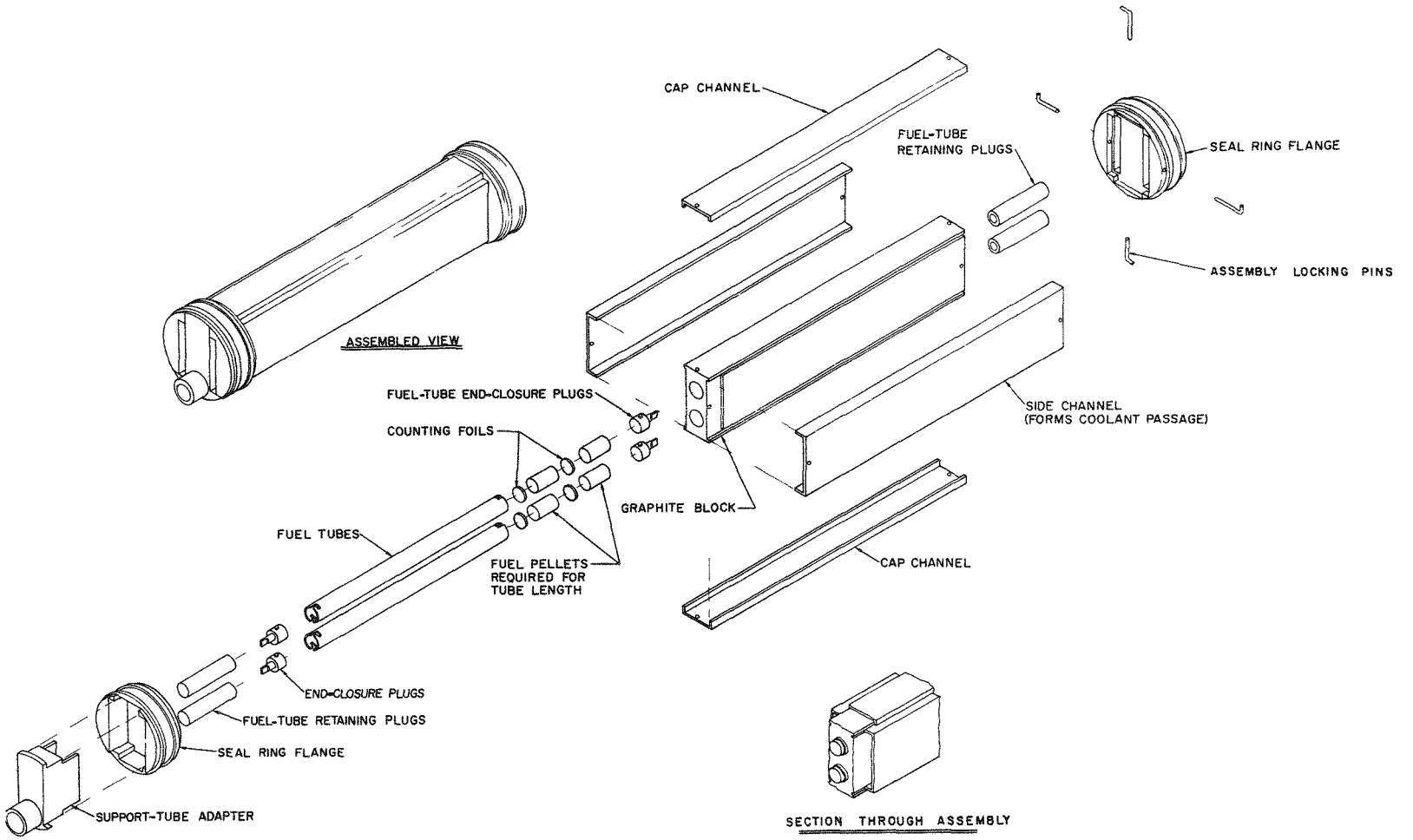

Fig. 1.8--Assembly drawing of nuclear mockup

prepared to simulate fuel-bearing pellets in thermal-expansion and thermal-cycling tests.

Four lots of fuel bodies were prepared from graphite containing enriched UO_2. Each lot consisted of 3 ln ft of pellets with equivalent loadings of 5, 10, 20, and 30 g of U^{235} per foot of column length. Analytical results supplied by the General Atomic chemistry department for two of the lots indicate that a uniform distribution of oxide was obtained.

A dimensional mockup, shown in Figs. 1.9 through 1.11, is being fabricated to allow the Hanford people to check their method of handling and cutting the test model. Another mockup of the test model is to be built for thermal-cycling tests.

Vendors have been selected for fabrication of the fuel bodies to be used in the final test model. Two orders for fuel-bearing beryllia bodies and two orders for fuel-bearing graphite bodies have been placed. Fuel-bearing alumina bodies will be fabricated at General Atomic.

MECHANICAL DESIGN OF REACTOR CORE (S. A. Bernsen)

Preliminary designs for a heterogeneous fuel element and a semihomogeneous fuel element were developed (see Figs. 1.12 and 1.13). The heterogeneous fuel element would fit into moderator blocks which are dimensionally identical to those in the semihomogeneous fuel assembly. End fittings would be identical to permit utilization of the same fuel-element loading tool. In Figs. 1.12 and 1.13, a removable orifice plate is shown held in place in the top end fitting by an internal snap ring. The semi-homogeneous fuel element or the moderator block for the heterogeneous core would seat and seal in the lower support structure. The heterogeneous fuel element would be contained in holes within the moderator block.

PRESSURE-VESSEL DESIGN (S. A. Bernsen and H. C. Hopkins, Jr.)

Work was started on establishing the design requirements for the pressure vessel. Several concepts were sketched in an effort to better

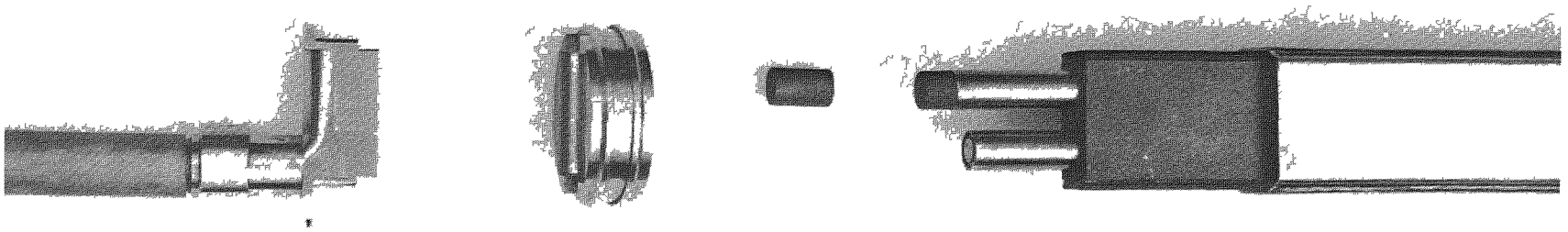

Fig. 1.9--End assembly details (dimensional mockup)

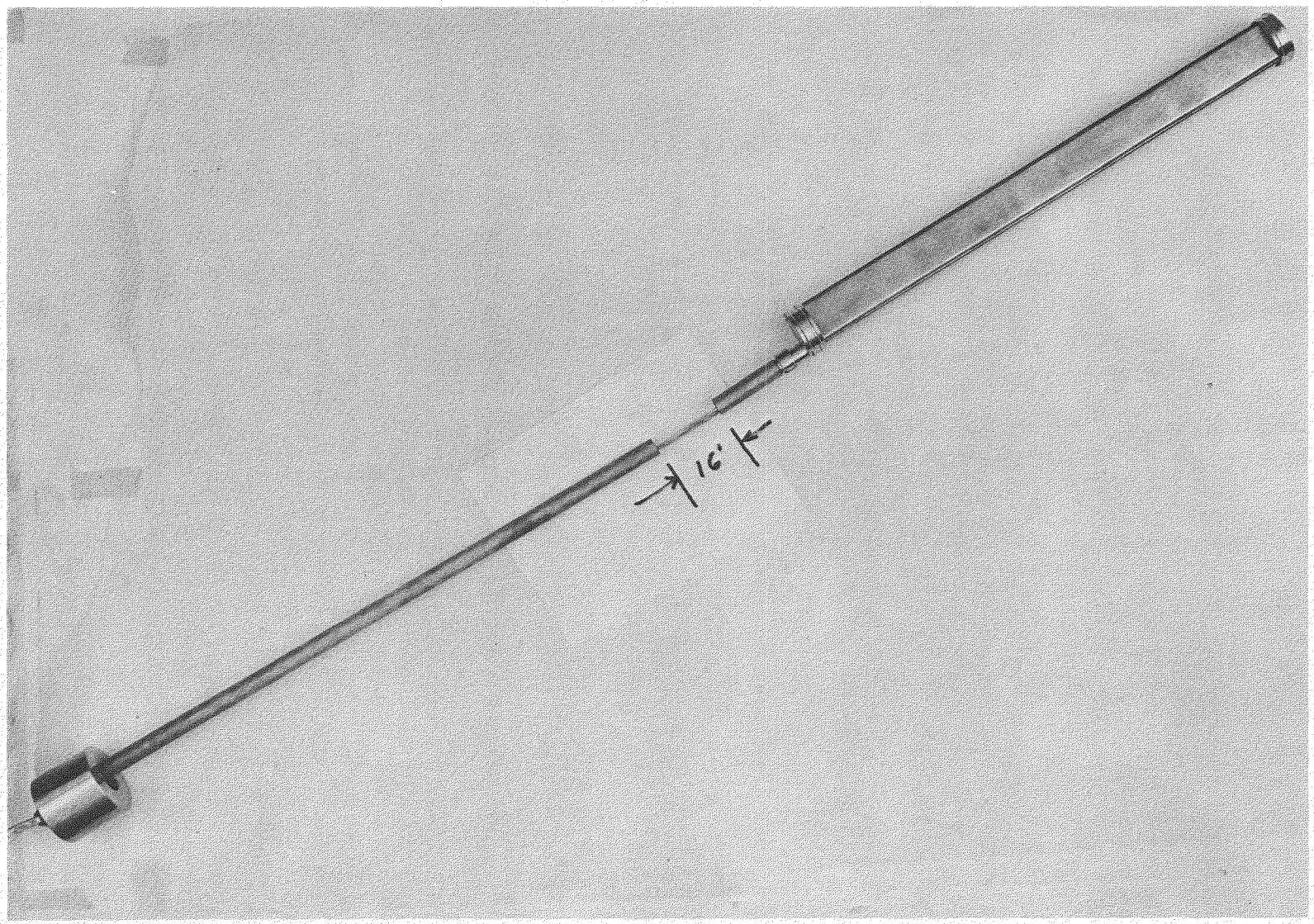

Fig. 1.10--Dimensional mockup assembly

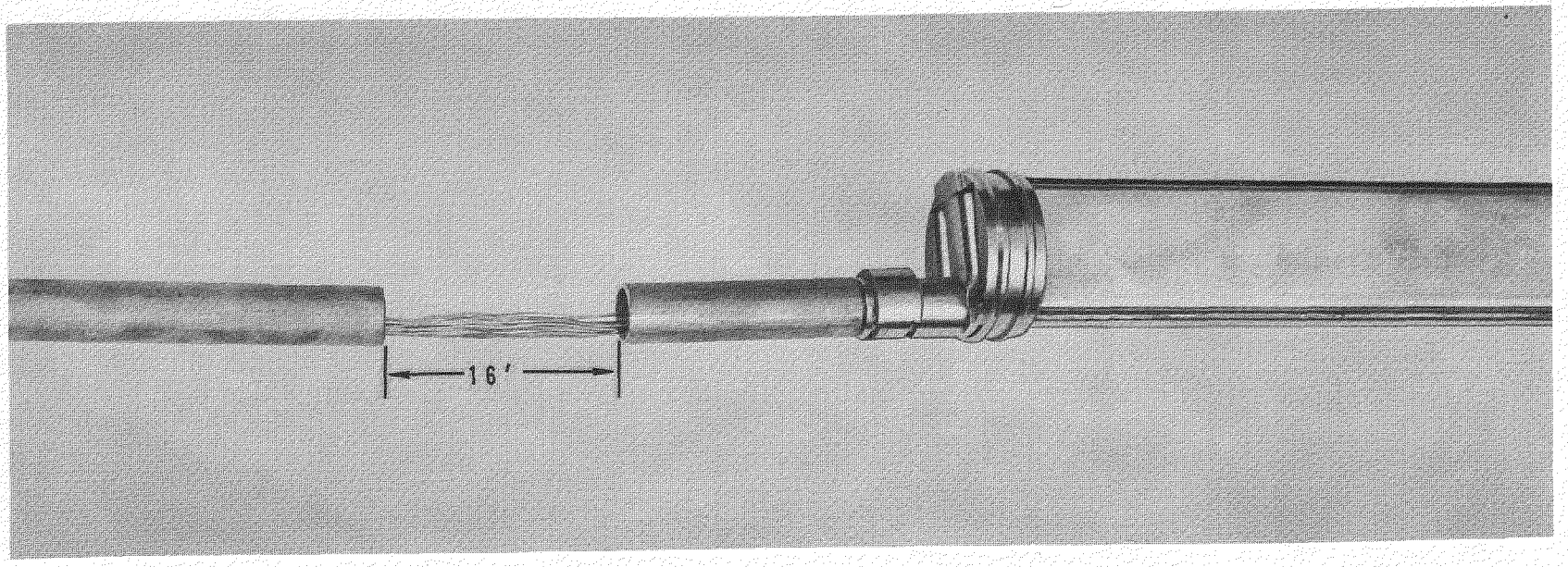

Fig. 1.11--Support tube end of dimensional mockup

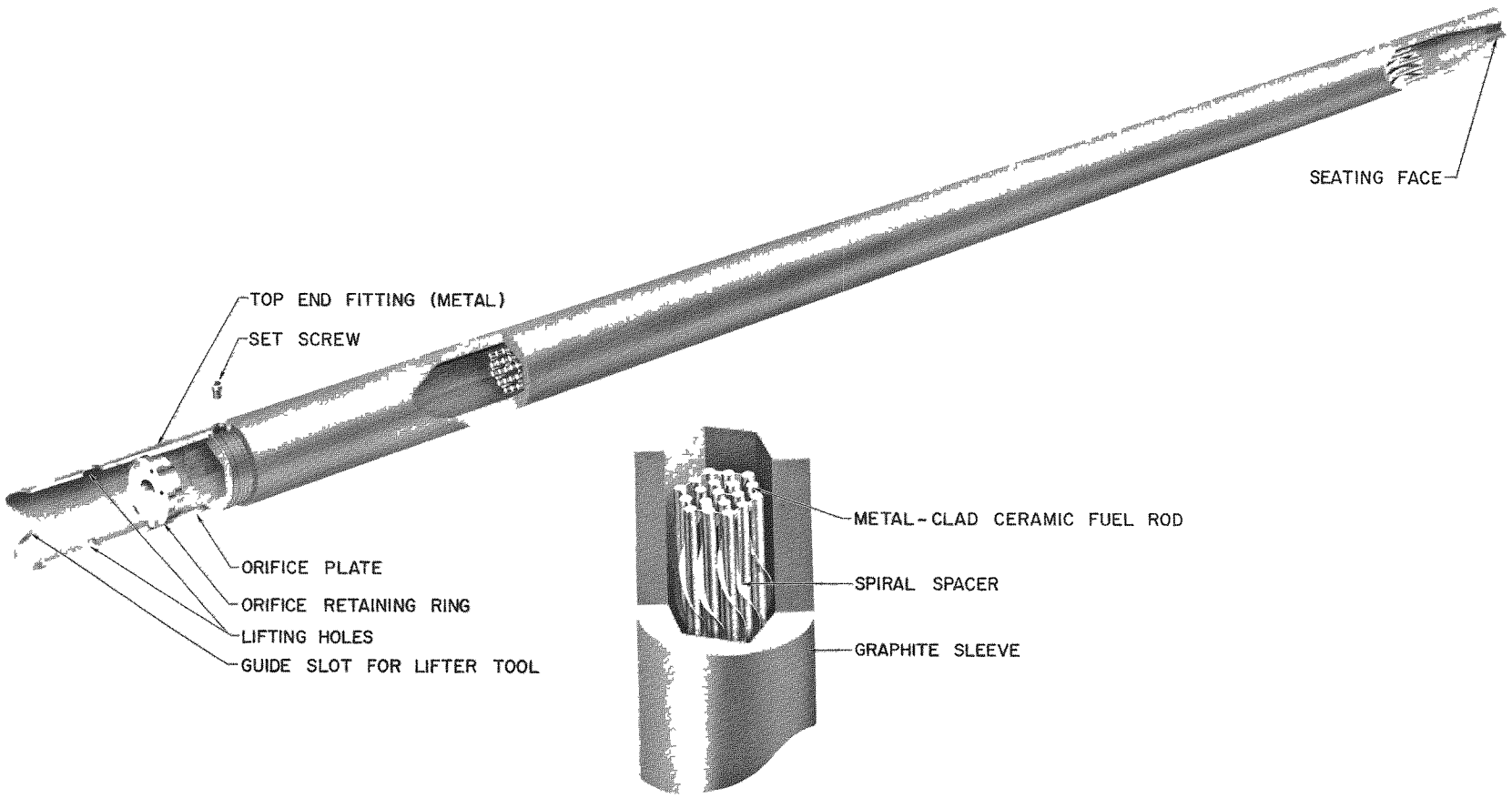

Fig. 1.12--Heterogeneous fuel assembly

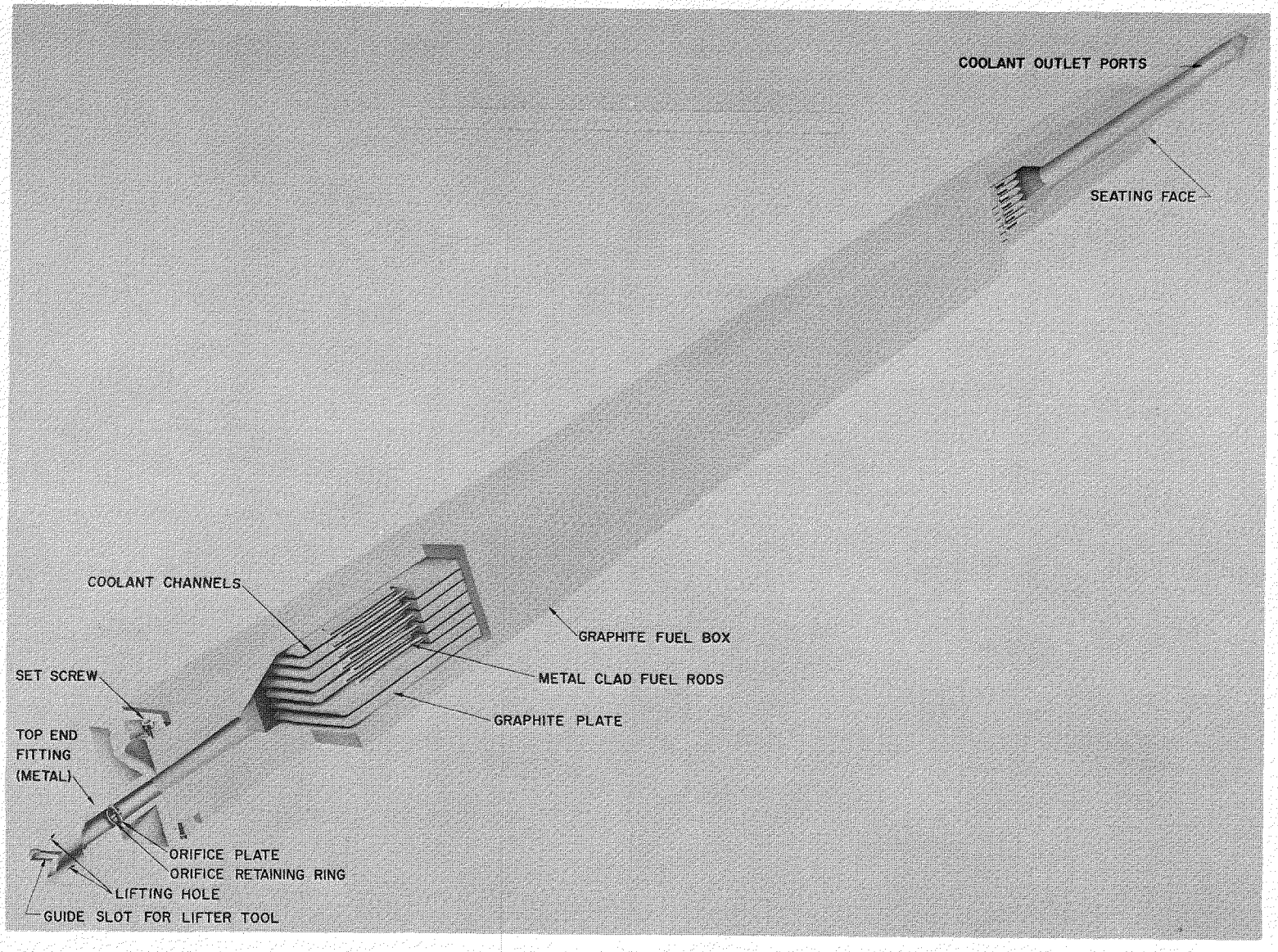

Fig. 1.13--Semihomogeneous fuel assembly

evaluate the magnitude of some of the problems. Specific procedures are being evolved which will permit a reliable and orderly investigation into each problem. Both a concentric and a nonconcentric duct system for the primary loop are being considered.

Since work has just begun in this area, the number and magnitude of the problems associated with the pressure-vessel design are not fully known. It may prove desirable to employ an internal insulation to the reactor vessel wall in order to reduce the operating wall temperature to a level where adequate strength can be obtained without excessive wall thickness.

The conductivity of insulating materials is usually given in an air atmosphere. There is indication that conductivity is increased if the atmosphere is helium. Since insufficient data are available on the conductivity of insulating materials in helium, a series of tests is being set up to obtain the necessary information to assess the suitability of different types of internal insulation.

Tests will be run on a large scale in an autoclave approximately 12 in. OD and 6 ft long. These tests will also provide general information on the ease of fabrication and dimensional stability of a clad insulation blanket. The first tests will be run on Refrasil, a rather pure silica-wool product. Subsequently, stainless steel wool and other types will be tested. The design for the test stand is virtually complete, and the majority of the materials have been ordered.

Other schemes to keep the vessel cool, such as directing the inlet coolant around the vessel surface prior to passing it through the core, are under consideration.

Analytical effort is being devoted to design problems associated with supporting the reactor core. However, before much progress can be made in this area, many features of the design of the vessel and its internal components must be more firmly established.

CONTROL-ROD DRIVES (F. Liederbach)

Preliminary tests were made with a simple pneumatic dashpot to survey the possibility of using this kind of technique to arrest the motion of the scram rod. These rather simple tests indicated that a pneumatic system may be feasible. A more sophisticated series of experiments will be developed and conducted. At the same time, other snubbing schemes will be investigated. The problem of design is complicated by the fact that the snubber must be capable of functioning over a wide range of pressures and of temperatures. For example, the snubber must be effective at zero pressure, as well as at the predicted operating pressure of 800 psi. It also must be effective at cold start-up conditions, as well as at the predicted operating temperature of 1,200°F.

II. FLUID SYSTEMS AND PLANT ARRANGEMENT

Preliminary results from a detailed study of rotating machinery by Westinghouse Electric Corporation showed a critical condition in the high-pressure compressor which could be alleviated by dropping the over-all system pressure. Since reduced pressure operation would increase the heat-transfer area required in the reactor core, and consequently the cost of the nuclear fuel, further studies are in progress to see whether the pressure can be increased by increasing the prototype power level. This study is of basic importance because the results will have a strong bearing on the feasible power level for a closed-cycle gas-turbine power plant.

Pending the completion of these studies, the reference design maximum pressure level has been set at 800 psi and the design power level has been kept at 20,000 shp.

TURBOMACHINERY (A. C. McClure, H. E. Holmes, F. E. McDonald, T. M. Silks, and D. F. Putnam)

Analytical and preliminary design work by personnel of the machinery subcontractor has progressed to the point where decisions regarding basic design of the several major components are rapidly being "firmed up." A design report was issued by Westinghouse Electric Corporation on March 31.*

Mechanical Designs

As a result of the various studies carried out to date, the speed of the main shaft will be held to approximately 12,200 rpm, which allows a factor of approximately 2.75 times first critical speed. Although a higher

*Westinghouse Electric Corporation, Steam Division, Engineering Report No. GTM-55, March 31, 1959.

factor could be tolerated, it was felt that other design considerations, such as minimum hub diameter, stage work, number of stages, shaft stiffness, made optimization at the foregoing speed highly desirable. In addition, the required seal welding of casing joints and the generally limited access to the shaft, after operation of the machinery, preclude any fine "field balancing"; therefore, it is believed advisable to keep the ratio of operating speed to critical speed within the limits of experience.

Compressors

Subsequent to analysis of various possible stage types, the symmetrical-staging, constant-axial-velocity, free-vortex design appears to be best for the application.

With this stage type, one or, at the most, two master blade patterns will be sufficient for blading each compressor. Design of both compressors is proceeding rapidly.

Turbines

As was done with the compressors, decisions favoring the free-vortex, symmetrical-staging design having constant axial velocity, with slight divergence along the tip diameter, have been made for the high-pressure machine.

Further study is being made on the low-pressure, or power, turbine because of additional problems. Because the power turbine must be capable of variable speed, it is desired to hold maximum design speed below the first critical speed. However, as design speed is reduced the required number of stages is increased, thus increasing the shaft length and lowering the first critical speed. Simultaneously, however, the speed ratio and size of the reduction gear are reduced. Since the reduction gear is a major power-plant item from the standpoint of both cost and weight, this tends to offset the increased number of turbine stages. Optimization studies of the low-pressure turbine design are continuing.

The design concepts will permit each turbine to be bladed with one or two master blades, and this will lower the cost and shorten the procurement time.

Power Absorber

The prototype power plant will not have a marine reduction gear and propeller; therefore, some other means must be provided to absorb the output power. Power absorber devices which are currently being considered include an air turbocompressor, an electric system, and a water brake.

Bearings, Seals, and Lubricants for Rotating Machinery

The design and fabrication of a test stand to evaluate shaft seals and seal systems has been completed, and trial runs, using commercial bushing seals, were made in March to check the test-stand operation. Generally satisfactory performance of the test stand was obtained, although some alterations were required before starting the test program. The bushing seals performed well during the checkout runs.

Face-type and commercial seals are being installed and tests to evaluate the bushing and face seals are scheduled for the week of April 6, 1959.

The test stand consists of a high-pressure housing, containing adapters to hold the seals in position, and a shaft, with required collars and sleeves, driven by a 5:1 gear-speed increaser through a flexible coupling. A 200-hp dc motor drives the test shaft at speeds from 0 to 20,000 rpm. Complete lubricating oil, seal gas, and cooling-water systems are provided. Maximum operating pressure is 1,000 psi, which is well above expected seal pressures. A gauge board contains two 24-channel thermocouple recorders, gas and oil pressure gauges, differential pressure gauges, and gas, oil, and water flow meters. Pressure regulators maintain the desired gas and oil pressures and provide a means for studying

the effect of pressure transients on the sealing systems. All of the systems have been operated satisfactorily after adjustment and minor alterations.

Other types of seals are being investigated for later tests, including floating ring and floating labyrinth seals. The latter seals can be designed with closer clearance and potentially lower leakage than stationary labyrinths, with longer life and greater dependability than the face-type seals.

Detailed designs are nearly complete on sealing systems incorporating a double floating labyrinth to separate oil and gas at small differential pressure, with a sleeve-type oil seal for the main pressure breakdown. Several materials appear promising for the floating labyrinth, including carbon, bronze, and cast iron. Vendors have been invited to submit seals of this type for testing to supplement those to be made by Electric Boat. These will be the subject of future tests.

Lubricating-oil Selection

An oil-gas separator was designed to handle the lubrication oil after it leaves the high-pressure regions. This unit was designed to remove gas bubbles from the oil stream and to remove oil entrainment and oil vapor from the helium stream. This equipment can be operated in conjunction with the seal test stand.

A number of suggested lubricating oils, both natural and synthetic, were compared on the basis of viscosity, vapor pressure, composition of base oil, nature of additives, radiation stability, and price. Based on these data, a lubrication-oil test program was planned for the following three natural oils and two synthetic oils:

Teresso 43	paraffin base,
Mobil Oil DTE 797	paraffin base,
Gulf Crest 44	paraffin base,
Esso Turbo 35	synthetic,
Union Carbide UCON DLB-200	ex-synthetic.

Other oils may be added at a later date.

The tests proposed are

1. Solubility of helium in oil,
2. Effect of dissolved helium on viscosity of oil,
3. Foaming characteristics after decompression,
4. Vapor pressure.

A rolling-ball viscosimeter has been designed and construction is almost complete. This is a simple device designed to demonstrate possible gross changes in viscosity due to helium entrainment. Equipment for the other tests is being studied. In all cases, emphasis will be placed on obtaining results of sufficient accuracy for engineering design.

Cycle Analysis (A. C. McClure, T. M. Silks, D. R. Olding, and J. J. Kearns, Jr.)

The effects of minor heat transfer,* fluid flow, and thermodynamic phenomena on MGCR full-load cycle performance were studied. Among the variables considered were

1. Fluid leak in regenerator,
2. Fluid leak in concentric duct,
3. Heat leak in concentric duct,
4. Fluid leaks from the plant,
5. Change in turbine inlet temperature,
6. Bleed flows from compressor discharge to compressor suction and turbine inlet.

The results are presented in Figs. 2.1 and 2.2.

All new information generated in the last three months was considered in an optimization of the power plant, which included optimizing heat exchangers with regard to the capital recovery factor. This optimization verified the parameter selection made in the previous quarter to initially establish the working cycle.

*Heat leakage from one stream to another within the system.

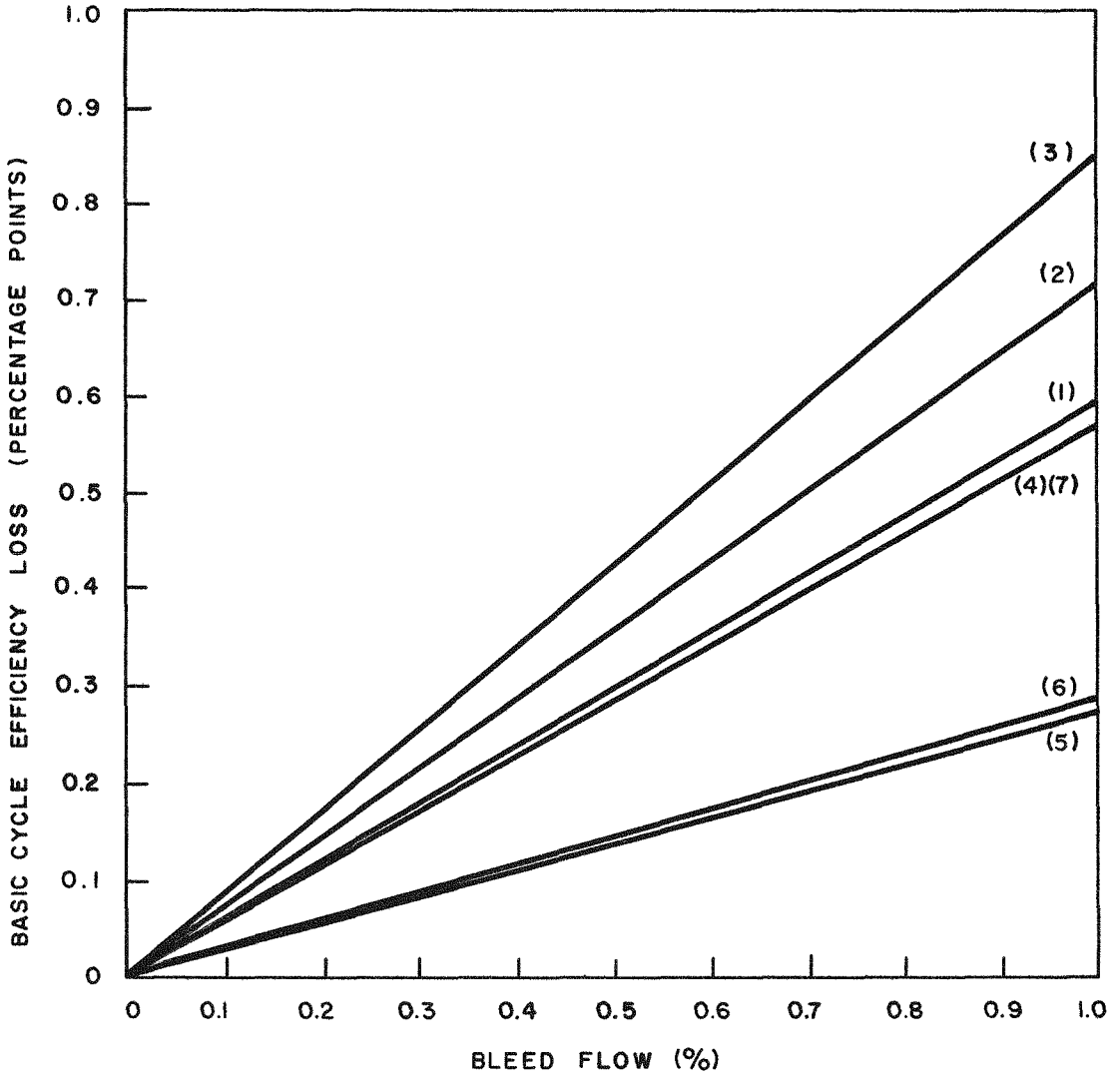

(1) BLEED FLOW FROM HPC OUTLET TO HPT INLET

(2) BLEED FLOW FROM HPC OUTLET TO LPT INLET

(3) BLEED FLOW FROM HPC OUTLET TO LPT OUTLET

(4) BLEED FLOW FROM HPC OUTLET TO LPC INLET

(5) BLEED FLOW FROM HPC OUTLET TO HPC INLET

(6) FLUID LEAK IN CONCENTRIC DUCT

(7) FLUID LEAK IN REGENERATOR

Fig. 2.1--The effect of minor bleed flows on cycle performance (helium plant)

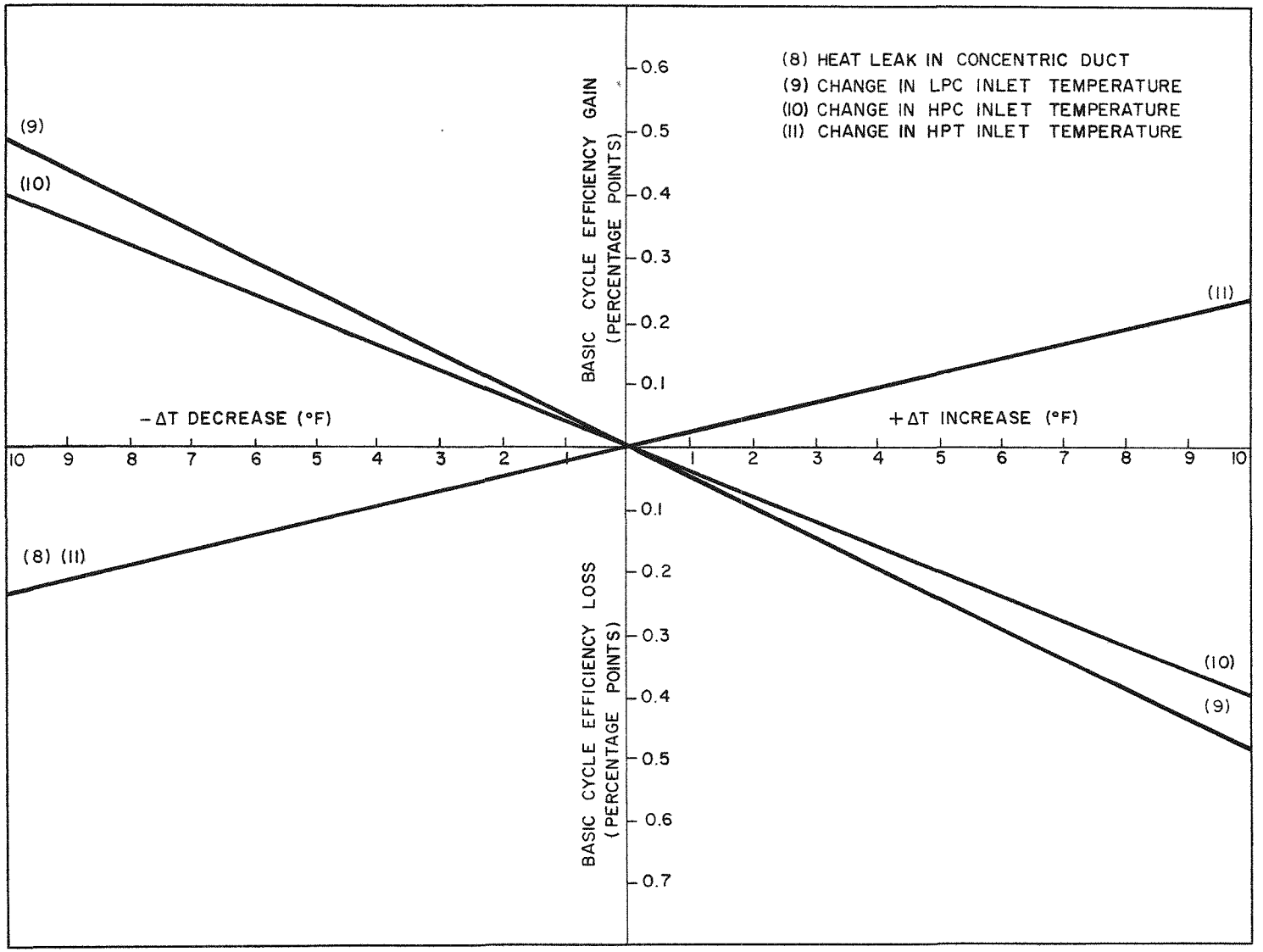

Fig. 2.2--The effect of minor heat transfer and thermodynamic phenomena on cycle performance (helium plant)

The parameters of the working cycle are as follows:

Shaft horsepower, rated	20,000
Reactor outlet temperature	1,300°F
Cycle refrigeration temperature	85°F
Peak cycle pressure	800 psia
Pressure ratio	2.6
Compressor split, p_{LPC}/p_{HPC}	1.1
Regeneration	85%
Flow rate	72.8 lb/sec
Bleed flow, approximate total	2%
Total fraction pressure drop	0.12
Compressor blade path efficiency	86%
Turbine blade path efficiency	90%
Auxiliary power generation (20% efficient steam cycle)	600 kw
Over-all cycle efficiency	30.3%

The extent of inventory control was selected as a compromise between the maximum cycle efficiency at the half-load condition and the necessary range of high-efficiency operation based on an analysis of tanker application. The current system would require an accumulator with a volume of 750 ft^3. This accumulator will provide inventory control in the prototype plant down to about 64% load; this would give essentially full-load efficiency from 64% load to full load, and thereby give the MGCR plant an advantage in applications requiring a high part-load efficiency (see Fig. 2.3).

A new set of curves describing the off-design performance of the plant has been drawn based on the most recent arrangement and working cycle. No appreciable difference was noted between these curves and earlier versions, except in the low power range.

The equations used to compute off-design heat balances were expanded to include two bleed flows, a power turbine bypass, and a steam generator.

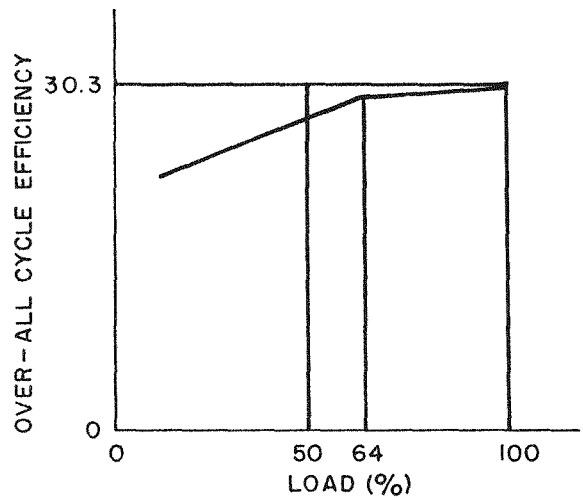

Fig. 2.3--Cycle versus load efficiency

In addition, flow through the turbines is being approximated in a slightly different manner from that which was used previously. Studies in progress utilizing the equations include determination of temperature fluctuations during maneuvering and establishing control-system accuracy requirements.

HEAT-EXCHANGER TEST PROGRAM (B. Lund, H. C. Paulsen, II, F. B. Anderson, and L. Casellini)

During this quarter, the heat-exchanger test facility was assembled completely and placed in readiness for test operations. Activities consisted of the final assembly and operational checkout of the blower and its appurtenances, installation of the heat exchanger in the loop, final installation of instrument panels, calibration of instruments, and the installation and checkout of pressure and temperature probes. Means for measurement and control of impurities were also developed.

Serious program delays occurred when the model heat exchanger arrived at Electric Boat Division behind schedule and there were so many fabrication deficiencies that major reworking became necessary to make it suitable for experimental test work. It was necessary to rebuild the tube shrouds, remachine the main flanges of the shell, and relocate some of the instrument connections. A special cleaning solution had to be devised to remove rust from the tube surfaces.

By employing a dummy loop, it was possible to perform mechanical and initial aerodynamic performance tests on the blower and its associated systems. This unit was tested at speeds up to 16,000 rpm with nitrogen at pressures up to 600 psig. Performance exceeded expectations, and the seal-oil and bearing-oil systems operated satisfactorily.

The gas in the heat-exchanger test loop can become contaminated from oil used in the blower or from water leaks in the heat exchangers. Contamination from either of these sources is undesirable, since this would result in the deposition of a film on the tubes of the model heat exchanger, which would introduce an error in the heat-transfer measurements.

Specifications were set for the maximum allowable contamination levels at 10 ppm for oil and 1,000 ppm for water. An oil removal bypass loop was designed which consisted of the following units in series: (a) a water-cooled heat exchanger, (b) an entrainment separator, and (c) an activated carbon adsorption bed. This system was given preliminary operational and flow tests.

Several methods were considered for water removal, but all of the designs considered resulted in equipment costs higher than desirable. It was therefore decided that a water-removal system would not be built until a need for it was clearly demonstrated. A magnetic particle trap was installed in the loop to remove iron oxide dust without introducing an unnecessary pressure drop. A combination air purifier and drier was installed to supply high-pressure air of acceptable purity to the test loop for the initial series of tests which are scheduled with air.

A number of methods were considered for the measurement of oil and water in the test-loop stream. An infrared method was selected for the analysis of oil. This method utilizes the following steps: (a) a large helium sample is bubbled through analytical-grade carbon tetrachloride to collect the oil, (b) the carbon tetrachloride is evaporated to dryness, (c) the oil residue is dissolved in a known small volume of carbon tetrachloride, and (d) the quantity of oil is determined by infrared spectroscopy. An inexpensive dew-point indicator was installed for measurement of moisture in the loop.

CONCENTRIC-DUCT DESIGN DEVELOPMENT AND TEST (H. Curtis and and B. Lund)

A critical review was conducted on the desirability of the concentric valve and ducts and on the present design and technological status. The prototype design will be based on the use of concentric ducts and a concentric valve between the reactor and the propulsion system, pending further studies of the feasibility of this system and of an alternative internally insulated system. The latter would avoid a hot pressure-vessel wall, and the resulting transients, during emergency operation.

Pressure-loss studies for straight concentric ducting have been conducted in order to determine the optimum ratio of inner to outer duct diameter. For an outer duct diameter of 28 in. and an inner duct wall thickness of 0.7 in., including insulation, the optimum ratio of diameters is 0.658. With this size of ducting, the total power loss due to friction in the main coolant concentric ducting is about 1.48 hp/ft of pipe.

Pressure-loss studies for the bends or elbows in the concentric ducting have been completed. Various configurations of long radius and short radius elbows and mitered bends were considered with vanes and without vanes. The pressure losses for each of the configurations considered are so small that the effect on basic cycle efficiency is negligible. Consequently, it was concluded that the bend configuration used should be

that of the simplest and least expensive construction.

Calculations which predict the probable heat-transfer performance of the heat barrier inside the inner duct have been completed. Two basic configurations of radiation baffling were considered, one incorporating a single radiation shield and the other featuring two radiation shields in series. The results of the calculations indicate that, although the temperature of the inner duct pressure wall is approximately the same for both of the basic configurations, the heat loss is about 40% greater for the single baffle than for the double baffle arrangement.

Based on the results of the heat-transfer calculations, design studies are being conducted on various arrangements of double or multiple radiation baffles. The reference design for the heat barrier in straight-duct sections is now essentially complete, but further studies are necessary to perfect the design of the baffling in elbows and tees and in those areas where instrumentation connections must penetrate the heat barrier.

CONTROL SYSTEM ANALYSIS (A. C. McClure, T. M. Silks, and J. J. Kearns, Jr.)

Power Turbine Bypass Control

The greater part of the control work during the period January 1, 1959, through April 1, 1959, was devoted to the development of a control for the cycle gas flow in the vicinity of the low-pressure turbine. The philosophy of control in this area* was revised somewhat to accommodate a steam generator which would continuously supply steam for generation of electric power. Formerly a generator coupled to the turbomachinery shaft provided the electric power. However, it was found that available variable-speed couplings were very inefficient or did not have proven reliability. The use of a steam generator for supplying power to turbine

*Evaluation of Coolant and Moderator for the MGCR, General Atomic Report GA-570, Chapter 9.

generator sets has an advantage in that the bypass cooler is used both as a heat sink for maneuvering and as a steam generator and is kept hot and in operating condition, ready for emergency use without penalty.

The steam generator is mounted between the low-pressure turbine and the regenerator, with the low-pressure turbine exhaust gas furnishing the heat. A fractional part of the exhaust helium is drawn off and passed through the steam generator, where the gas gives up its heat to the steam. After it leaves the steam generator, the gas rejoins the main exhaust stream and mixes with it just prior to entry into the regenerator shell.

A means for dumping heat when the low-pressure turbine is by-passed is still required. The possibility existed for utilizing the steam generator as this heat sink, and such a system was devised and examined in some detail.

A conceptual design of the steam generator was made in order that a computer study could be made of the proposed system to determine its characteristics under both steady-state and maneuvering operating conditions. The steam generator is a vertical recirculation unit, with the helium flowing through a U-tube bundle and with the water boiling on the outside of the tubes.

Computer runs were made on a digital computer for a number of cycle gas inventories and at varying degress of low-pressure turbine bypass. It was indicated that the controllers for some of the valves were rather complex, though not necessarily impractical. Accordingly, alternative systems which might simplify valve control are being investigated. These systems, in general, utilize separate tubes for the steam generator and bypass cooler, and they appear to offer an improvement over the system previously studied.

The requirement for maximum plant efficiency makes it essential that pressure loss around the loop be kept to the economic minimum. The allowable pressure drop between the low-pressure turbine exhaust flange and the regenerator shell inlet is a fraction of a pound per square inch.

The steam generator is mounted between these two points, and investigation showed that the pressure drop through the steam generator and associated valves might be as great as 3 psi. However, a venturi, or jet pump, inserted in the exhaust line to supply the required 3-psi pumping head to force the flow through the steam generator and valves, with an efficient diffuser installed between the venturi throat and the regenerator, recovered part of this pressure drop; this seemed to be a satisfactory solution.

Reactor Outlet Temperature and Plant Inventory Control System

The reactor power-level control system and the reactor outlet temperature and helium inventory control system are shown in the block diagrams of Figs. 2.4 and 2.5.

It is proposed that each of the three operations function independently of each other. Power level is determined by measuring flow rate and coolant temperature rise across the reactor. Power level is controlled by automatically moving control rods when the measured power level differs from the ordered power level. Reactor outlet temperature is continuously monitored, and whenever it varies from its ordered value, gas is admitted to or withdrawn from the cycle in order to return the temperature to its ordered value.

Proper plant inventory is maintained by comparing actual with design accumulator pressure and by manual valve operation, eliminating any difference by gas transfer to or from the storage and handling system.

Work is currently in progress to specify the requirements for the components of this system.

System Transient Studies

Differential equations which permit the dynamic analysis of a closed-cycle gas-turbine plant were programmed for numerical solution on a digital computer.

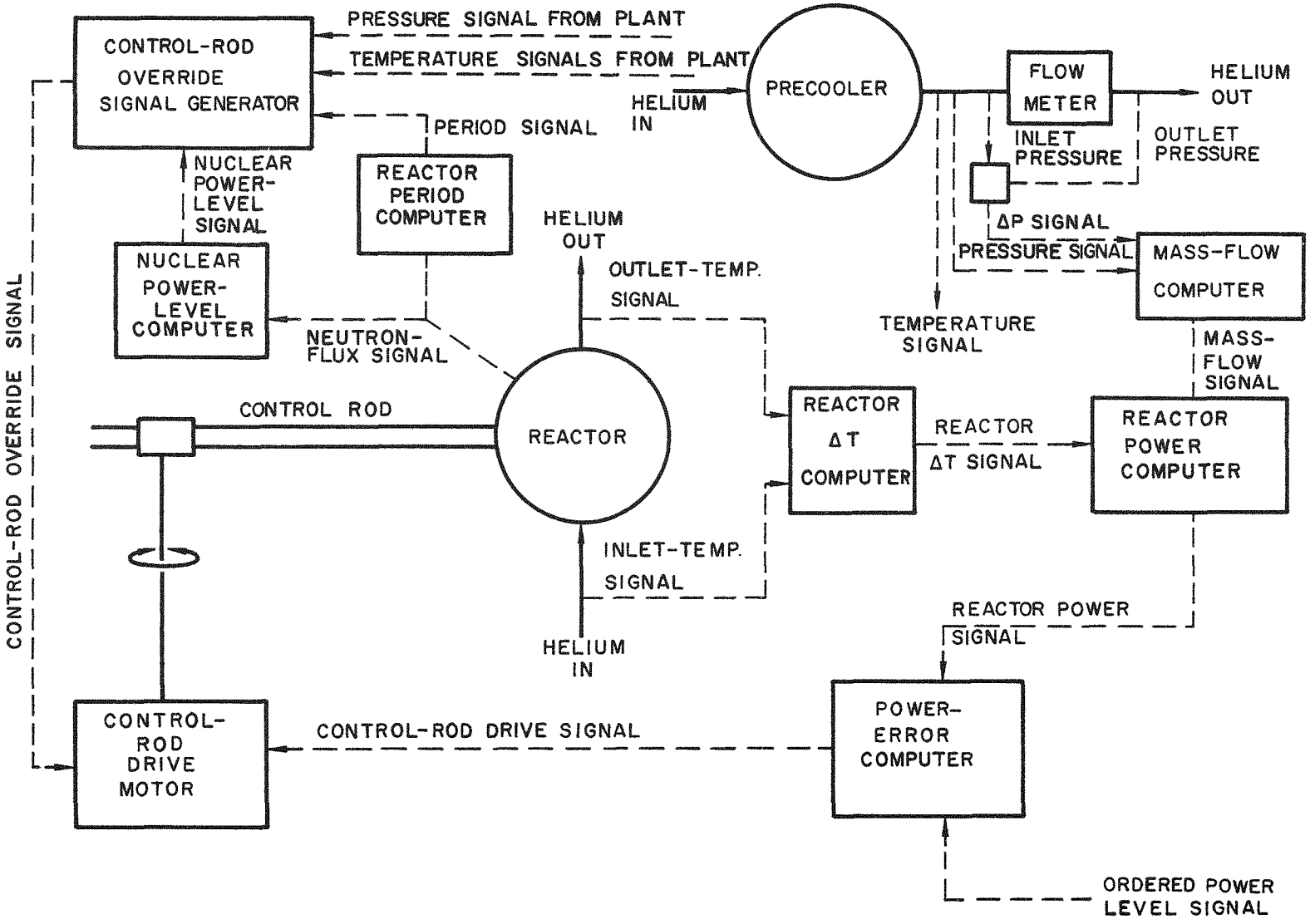

Fig. 2.4--Reactor power-level control system

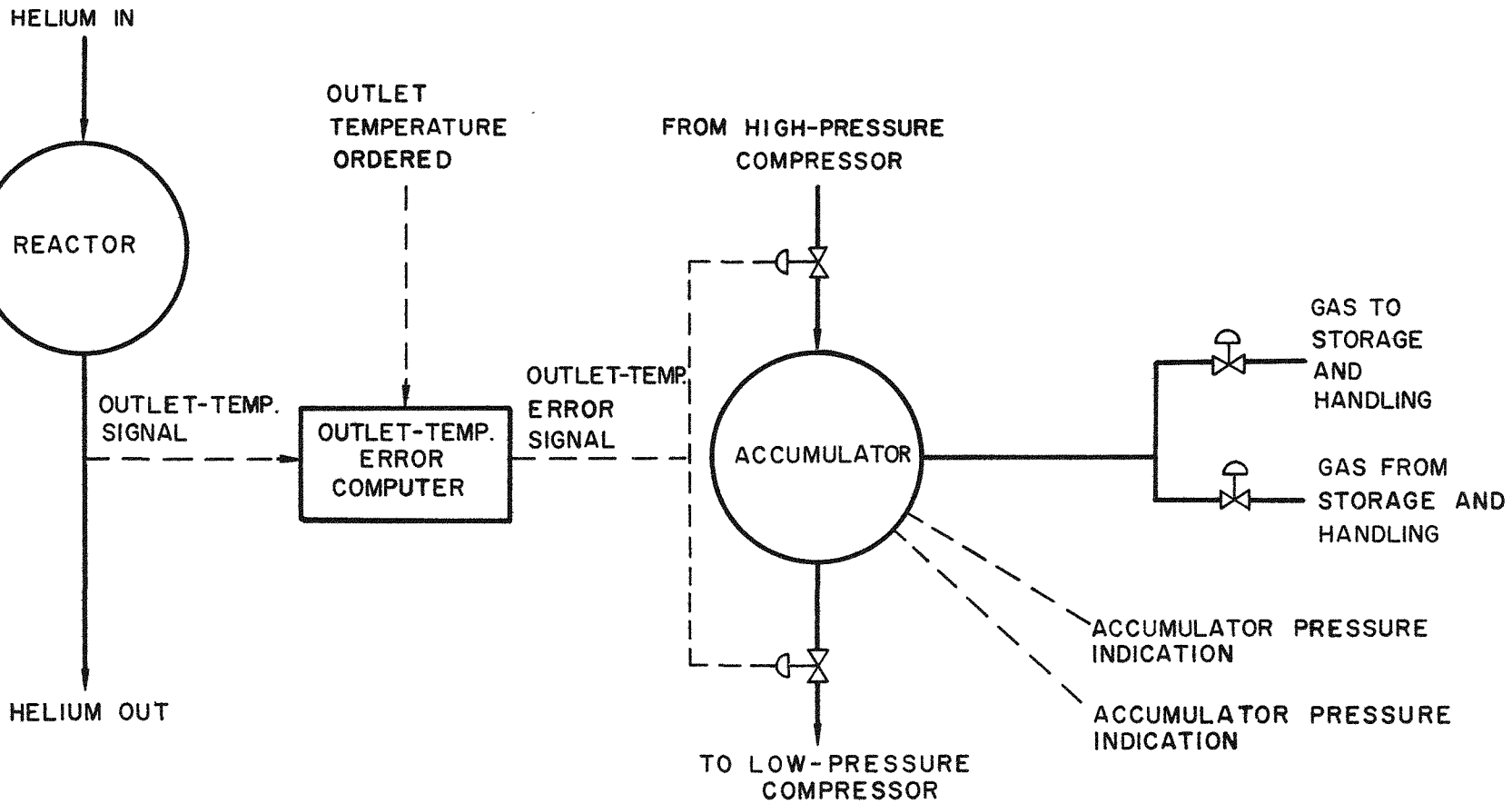

Fig. 2.5--Reactor outlet temperature and helium inventory control system

Response to two types of system disturbances have been obtained: (a) changes in reactor power and (b) changes in plant load. The most important findings are:

1. Increasing the reactor power from 100% to 120% in 2 sec at constant inventory results in no plant instability.
2. An instantaneous reduction in shaft load from 20,000 shp to zero results in the low-pressure turbine exceeding 106% of design speed in less than 1 sec and 120% of design speed in less than 2 sec. Currently, 106% of design speed has been designated the overspeed limit and 120% of design speed is approximately the overspeed limit of the turbine.

The first result indicates that the power portion of the system will not contribute to plant instability in the range of anticipated disturbances. The second result, which represents the change of load in the event of failure of the shaft or coupling between the low-pressure turbine and the reduction gear, indicates that a fast low-pressure turbine bypass system must be designed.

The results reported above are those which will occur with no control system operating. Later studies will incorporate the equations of the control system in the plant dynamic equations.

Effect of Heat Exchangers on System Control

Families of heat exchangers, which meet preliminary cycle design conditions of pressure drop and heat transfer, were designed during this quarter in support of transient analysis, establishment of the working cycle, and arrangement studies. The internal geometry, the external dimensions, and the weight of the precooler, intercooler, and regenerator have been developed for use in current plant arrangements.

A variety of exchanger internal geometries was investigated, including finned-tube exchangers. It was determined that those finned-tube exchangers which appear theoretically advantageous require fin-tube geometries which

are not commercially available. The development of new fin-tube geometries is a long and expensive process. Many that appear to be theoretically desirable are not economically feasible. As a consequence, all preliminary design exchangers employ bare tubes.

A study of the precooler and intercooler has been made, which shows the effects of an increase in the cooling-water temperature in the precooler and intercooler above its current 15°F value. Such an increase may permit a reduction in circulating water pump capacity at the cost of increased length and diameter of the heat exchanger.

Equations have been written for the transient behavior of the regenerator. They are sufficiently general to be applied to the precooler and intercooler with only slight modification. The partial differential equations describing the heat exchangers have been written as difference equations for numerical solution.

FLUID-MECHANICAL SYSTEMS (B. Lund, J. H. Pilliod, M. R. Fishkind, and J. W. Justusson)

A description has been prepared for each fluid-mechanical system which outlines the functions of the systems. Schedules were established which indicate significant commitment dates. In accordance with these scheduled commitment dates, preliminary engineering specifications have been established for the following systems: (1) main coolant, (2) emergency and shutdown cooling, (3) steam generating, (4) coolant purification, (5) coolant storage handling, (6) coolant charging and make-up, and (7) condensate.

Cost estimates of these systems were prepared for the revised prototype plant cost estimate. This required preparation of conceptual engineering sketches and preliminary condensed design descriptions for approximately 40 fluid-mechanical systems. The primary objective of the sketches is to furnish a design reference datum on which to base the cost estimate. Although prepared for this purpose, the sketches also

form a basis for future detailed systems development. The primary objective of the descriptions is to outline system functional requirements and briefly describe how each system is designed to accomplish its function(s). Off-haul systems required for prototype site facilities were also outlined for cost-estimating purposes.

Preliminary sizing (and rating, if possible) of all principal system components has been completed on a "rough approximation basis." This information was used to support the revised prototype plant cost estimate and also to develop initial power plant arrangement studies. A preliminary arrangement study has been completed, and plans have been prepared for both the containment area and auxiliary machinery spaces. The plans show a shipboard type of arrangement. However, "shipboard only" and "prototype only" equipment is identified. More detailed machinery arrangement plans will be developed, using the initial arrangement plans as a basis.

Design and development of long lead-time equipment has been initiated and is currently in progress. Such equipment includes the bypass steam generator, main coolant heat exchangers, coolant purification equipment, and special coolant valves. A program for preparing specifications, testing, evaluating, and procuring small valves (4 in. and under) for coolant (helium) service was initiated and is in progress. This program includes establishing valve requirements, surveying industry for commercial availability, testing and evaluating several types and makes of valves, and establishing helium valve standards for all applications in the sizes noted. A preliminary fluid-mechanical components list was prepared and this will form the basis for a more detailed and complete component list currently in progress.

COOLANT PURIFICATION AND ANALYSIS

A preliminary study was made of various means of purifying helium in both the storage tank and the main loop. Several methods of purification

were considered, including the following:

1. Low-temperature (-320°F) adsorption:
   a. Molecular sieves,
   b. Activated carbon.
2. Chemical reactants:
   a. High-temperature getters,
   b. Liquid baths (sodium or NaK).
3. Diffusion through a porous medium.

Of the various methods considered, two were selected and recommended for a laboratory study program. These are low-temperature adsorption using a molecular sieve material and high-temperature gettering using titanium. The major equipment items in the low-temperature adsorption system are

1. A room-temperature adsorption bed for removal of water and oil (two in parallel),
2. A low-temperature (-320°F) adsorption bed (two in parallel),
3. A heat exchanger to cool the incoming helium with the outgoing helium,
4. A liquid nitrogen recondenser.

The major equipment items in the high-temperature gettering system are

1. A high-temperature (1,800°F) titanium getter bed (nonregenerative),
2. A low-temperature (750°F) titanium bed for hydrogen removal (regenerative),
3. Suitable heat exchangers for heating the incoming helium with the outgoing helium.

The low-temperature adsorption system will remove inert contaminants, e.g., argon and krypton, and it is regenerative. However, it may give a radioactive gaseous waste on regeneration. The high-temperature gettering system has no moving parts and has a lower initial cost. However, it is not regenerative and does not remove the rare gases.

Analytical instrumentation is available commercially for continuous monitoring of most of the impurities down to 1 ppm. The analytical

methods that can be used are as follows:

Impurity	Method
O_2	Trace oxygen analyzer (Baker or Beckman)
N_2 and A	Concentration-chromatography combination
CO, CO_2, and oil	IR analyzers
H_2	Deoxo indicator (Baker)
H_2O	Electrolytic hygrometer

It may not be necessary to analyze for all of the impurities listed above when monitoring the shipboard plant, but it may be sufficient to analyze for certain key components, e.g., oil, CO, and H_2O.

PROPULSION PLANT ELECTRICAL SYSTEMS (W. V. Datkiw, B. Lund, and T. J. Gerken)

Task descriptions have been written for each of the eighteen propulsion plant electrical systems, and a schedule for completion of diagrams was prepared.

A block diagram for each system shows the hardware presently anticipated. A description has been prepared for each system to supplement the block diagrams. These descriptions and diagrams define the system configurations used for this cost estimate and form a datum plane for future cost estimates and system engineering and design. Electrical system components were then sized and preliminary ship arrangement plans were developed. It is anticipated that a shipboard arrangement will be utilized for the prototype. Shipboard-only or prototype-only items are defined on the arrangement plans.

A limited amount of planning for prototype location of electrical systems was accomplished. This included analysis of such "off-hull" requirements as the design of the basic electric power distribution system, stand-by diesel generator capacity, sizes of various load center distribution panels, and various shop, laboratory, and recording instrumentation requirements.

The electrical load analysis was revised during this reporting period, and is presently undergoing another revision to include additional operating conditions and changes resulting from the prototype cost estimate work. It appears that it may be necessary to increase the tentative size of the ship generators. However, this will be discussed in the next reporting period when the analysis is complete. The off-hull emergency diesel generator installation requirements will be included. The ship generators are presently sized as follows: (1) 750-kw turbine generator set, (2) 750-kw main diesel generator, (3) 100-kw emergency diesel generator.

Engineering of the electric power distribution system has produced a preliminary system description and a list of items that require description. Engineering of the electric plant control system was begun.

A preliminary investigation was conducted to determine the operating temperature limits and the maximum permissible ambient temperature for various types of electrical equipment which will be located in the containment area. Results of this investigation indicate that a normal maximum operating containment area ambient temperature of 140°F can be considered safe for electrical equipment which has no special cooling provisions.

PLANT ARRANGEMENT STUDIES OF STRUCTURE AND SHIELDING

(A. C. McClure and I. H. Kabler)

Drawings have been developed which show the machinery arrangement, including the containment area and auxiliary machinery spaces.

The primary effort in arrangement studies has been directed toward eliminating or minimizing relative thermal expansion by logical placement of components to fit the system requirements and then grouping them in rigid-body assemblies.

The reactor is located forward of the centerline of the ship. The rotating machinery is in-line; i.e., the power turbine is located aft adjacent to and coaxial with the compressors and high-pressure turbine. The generator consists of two parallel U-shells interconnected by inlet

and outlet headers located directly below the rotating machinery, with the shell side inlet below the power turbine. This allows a discharge directly from the power turbine to the regenerator shell with a minimum of connecting piping. The precooler and intercooler are vertically mounted bare-tube heat exchangers with the precooler connected directly to the upper regenerator header. All other components are located in the most convenient positions relative to their respective piping connections.

Access for retubing the two sea-water heat exchangers (precooler and intercooler) is through openings in the top of the containment area, or secondary shield. Vertical mounting facilitates tube removal. Access to the water boxes for cleaning heads and tubes, or for tube plugging, may be accomplished from within the containment area.

In conjunction with the containment area arrangement, plans have been made of the engine room and auxiliary machinery spaces showing all shipboard components in their proper positions. Some of these components are for shipboard installation only and will not appear in the prototype. Others will be replaced by an equivalent component, e.g., the ship's reduction gear will be placed by a high-speed power absorber.

A study has been made of ways to support the reactor so as to allow fore and aft movement during thermal expansion of the high-pressure turbine-reactor duct, and thus to minimize reactions on the turbine. Possible methods are to use sliding supports, bar linkage, or flex-plates; the flex-plates are currently preferred.

Main turbine-compressor and regenerator foundation requirements are being investigated. The main turbine-compressor foundation is currently conceived as a deep fore-and-aft bridge-type structure supported at the after end by the containment structure and near the forward end by columns. Additional work is in progress to determine the best type of support for other components.

EMERGENCY COOLING SYSTEM (B. Lund, J. H. Pilliod, and M. R. Fishkind)

An auxiliary circulating loop, using helium under high pressure or air at low pressure, will accomplish the emergency cooling. The gas pumping for both high-pressure helium and low-pressure air can be done by a single blower having a two-speed drive. Accordingly, the design calls for two identical blowers, each equipped to handle either high-pressure or low-pressure gas.

The use of air as a coolant is contemplated for the emergency cooling system when it is not possible to hold high pressure in the loop. Because air would react with hot graphite, it will be necessary to precool the reactor core with some inert medium before introducing air. Preliminary design work was carried out on a cool-down system in which a stored inert coolant, such as nitrogen, carbon dioxide, or steam, is introduced into the core at low temperature and high flow rate. It may be necessary to introduce this coolant through a separate connection at the top of the reactor vessel in order to avoid rapid cooling and high thermal stress in the reactor pressure vessel. It is estimated that a nitrogen cool-down system would require storage of about 50,000 lb of nitrogen.

III. REACTOR PHYSICS

CONTROL RODS (J. Stein, H. Vieweg, and J. Seibold)

Two-group PDQ calculations were run to obtain estimates of control-rod worth for the preliminary design core under cold, clean conditions. These calculations were run in XY-geometry with the rods in the form of thermally black cruciforms; axial bucklings for the cases were derived from axial flux distributions obtained in PDQ calculations of the unrodded core in RZ-geometry. The results are given in Table 3. 1.

Table 3. 1

RESULTS OF PDQ CALCULATIONS FOR THERMALLY BLACK CONTROL RODS

	Number of Cruciform Rods Fully Inserted		
	0	25	16
Rod span (in.)	-----	6. 50	7. 22
Rod center-to-center spacing (in.)	-----	12. 64	14. 44
Rod-blade tip separation (in.)	-----	6. 14	7. 22
K_{eff} (cold, clean)	1. 173	0. 872	0. 943
$\Delta K/K_{rods\ in}$	-----	0. 344	0. 244

Rough estimates obtained during the evaluation program indicated that twenty-five 6. 5-in. -span rods were required to yield a 2% shutdown margin; however, this estimate was based on crude extrapolation of core parameters to cold conditions, which resulted in a large overestimate of the total absorption cross section in the core.

The $\Delta K/K_{rods\ in}$ worth of the rods in the cases considered is proportional to the rod span; on this basis, sixteen 6. 5-in. -span rods

would have a $\Delta K/K_{\text{rods in}}$ worth of 0.220, yielding an adequate shutdown margin of 3.8% (K_{eff} rods in = 0.962).

Curves of rod worth versus position were obtained for the hot, clean and the cold, clean preliminary design core. PDQ calculations in XY-geometry with sixteen 6.5-in.-span thermally black rods were run to obtain the equivalent uniform poison cross section for the rods under cold and hot conditions. The cross sections were then used in PDQ calculations in RZ-geometry to represent the rods as a poison blanket with different insertions in the core. Critical rod positions obtained were 26.6 in. from the bottom of the 76.4-in. core under hot, clean conditions and 15.4 in. from the bottom under cold, clean conditions.

Normalized curves of the fraction of rod worth inserted versus fraction of rod length inserted are given in Fig. 3.1. The curves demonstrate the higher incremental worth of the rods in the cold core as compared to that in the hot core.

POWER DISTRIBUTION

Calculations are under way to establish a synthesized three-dimensional power distribution for the preliminary design core under hot, clean conditions. Radial distributions for the rodded and unrodded portions of the core will be obtained from PDQ calculations in XY-geometry. These results will be combined with the axial distributions from the RZ calculation of the core with the rod blanket in the critical position.

Figure 3.2 shows the centerline axial power-density distribution in the hot, clean core with the rods banked in their critical position, i.e., 26.6 in. from the bottom of the core. The maximum-to-average power-density ratio of 3.32 occurs at the bottom core-reflector interface. Modifications of the composition and structure of the lower reflector might be necessary if this peak is unacceptable.

Although the rods are inserted nearly two-thirds of the way into the core under hot, clean conditions, the rodded region generates 39.7% of the

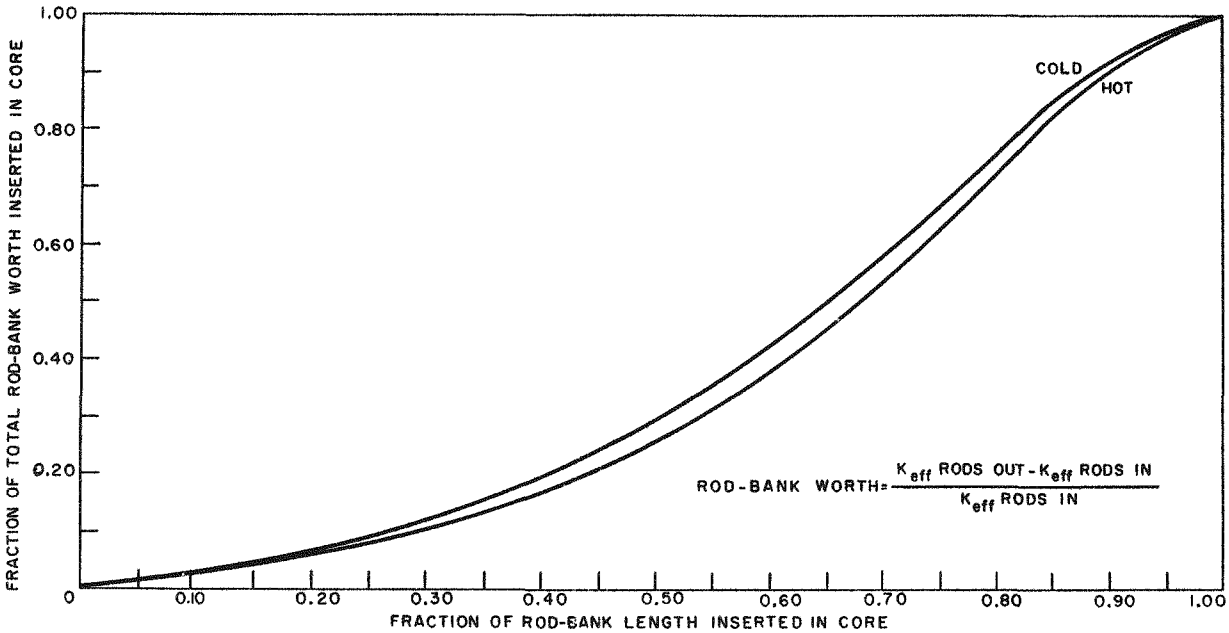

Fig. 3.1--Rod worth inserted versus rod length inserted for preliminary design core

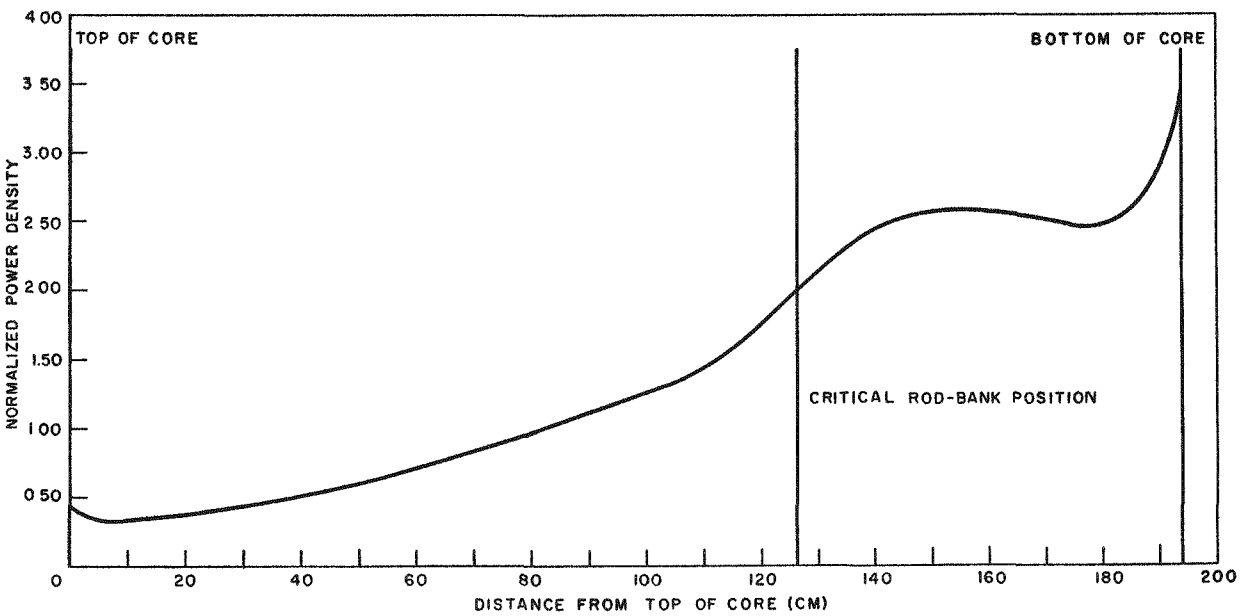

Fig. 3.2--Centerline axial power-density distribution for preliminary design core

total power. This is a consequence of the rod spacing being larger than the rod span.

CORE LIFE AND REACTIVITY REQUIREMENTS

Revision of the estimated core life was made by introducing corrections to the equivalent resonance escape probability and thermal nonleakage probability for a reactor in the analytical burnup model. These corrections, described in GAMD-610,* incorporate the effectiveness of the reflector in bypassing resonance absorption in the core. For the preliminary design core, the lifetime at full power was reduced by these corrections from 603 to 572 days.

BURNABLE-POISON STUDY

Analytical hand calculations of criticality and burnup were employed in studies of the variation of U^{235} loading with natural boron content.

Prior to the survey calculations, a detailed lifetime calculation was made for the preliminary design heterogeneous core (128.3 kg of U^{235} and 500 kg of U^{238}); 428 g of natural boron was considered to be uniformly distributed in the fuel elements, reducing K_{eff} (initial, hot, poisoned), from 1.097 to 1.009. The core lifetime at full power was consequently reduced from 572 to 533 days.

Figure 3.3 shows the variation in K_{eff} with days of full-power operation for the core with and without boron for cold and hot conditions. In calculating the cold K_{eff} during life, a conservative approach was used by ignoring all equilibrium and permanent fission-product absorption. The maximum K_{eff} is seen to occur later in life in the cold system than in the reactor at operating temperature; this is a result of omitting fission-product poisoning in the cold reactor.

---

*J. M. Stein and H. A. Vieweg, Effect of Reflectors on Resonance Escape Probability, General Atomic Report GAMD-610, December 5, 1958 (internal document).

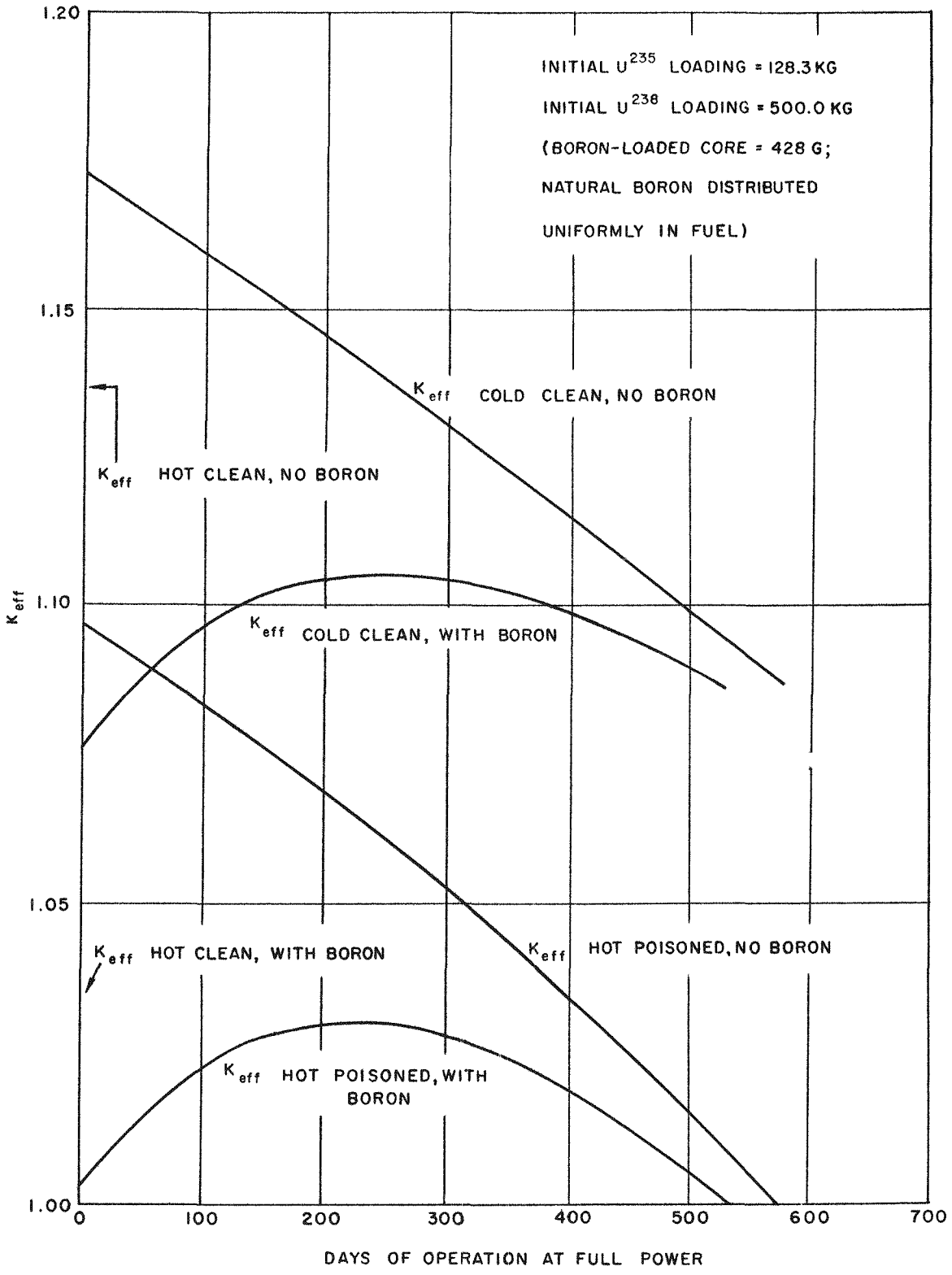

Fig. 3.3--MGCR preliminary design core reactivity (lifetime curves)

The maximum K_{eff} (cold) of 1.105 in the borated core (compared with 1.173 in the core without boron) would permit a reduction from sixteen to ten and four-tenths 6.5-in.-span rods. Choosing the next lowest number of rods in a symmetrical array yields nine 7.5-in.-span rods.

The advantages of the reduction in number of rods will be appraised in the light of metallurgical complications introduced by the use of burnable poison. Another advantage which will be weighed in reaching a decision on the use of burnable poison is the reduction in the fraction of the core which must be blanketed with control rods during hot operation.

The survey calculations completed thus far relate the boron and U^{235} loadings for full-power core lifetimes of 572 days (preliminary design), 2 years, and 2-1/2 years. The end-of-life K_{eff} was made to be unity; an upper limit to boron content was established by setting a lower limit of 1.01 for K_{eff} (initial, hot, poisoned). Figure 3.4 gives the results for a heterogeneous core with a fixed U^{238} loading of 500 kg; Fig. 3.5 gives the comparable results for a fully enriched core. Stainless steel, void, and moderator volumes were maintained at their values in the preliminary design.

In estimating the fuel-cycle costs, no additional fabricating cost was considered for the homogeneous distribution of boron in the fuel elements.

For the range of lifetimes covered in these studies, the maximum permissible boron-to-U^{235} atom ratio is about 0.1 in the partly enriched core and about 0.075 in the highly enriched core.

Fuel-cycle costs are somewhat higher in the partly enriched core for the 572-day and 2-year lifetimes because of the higher inventory charge for the larger U^{235} content; at a lifetime of 2-1/2 years, the fuel-cycle cost is slightly lower in the partly enriched core, because the plutonium credit and reduced burnup costs overcome the higher inventory charge. However, in all cases, the fuel-cycle costs vary less than 10% for the lifetime and loading ranges considered.

Calculations will probably be completed during April, 1959, which

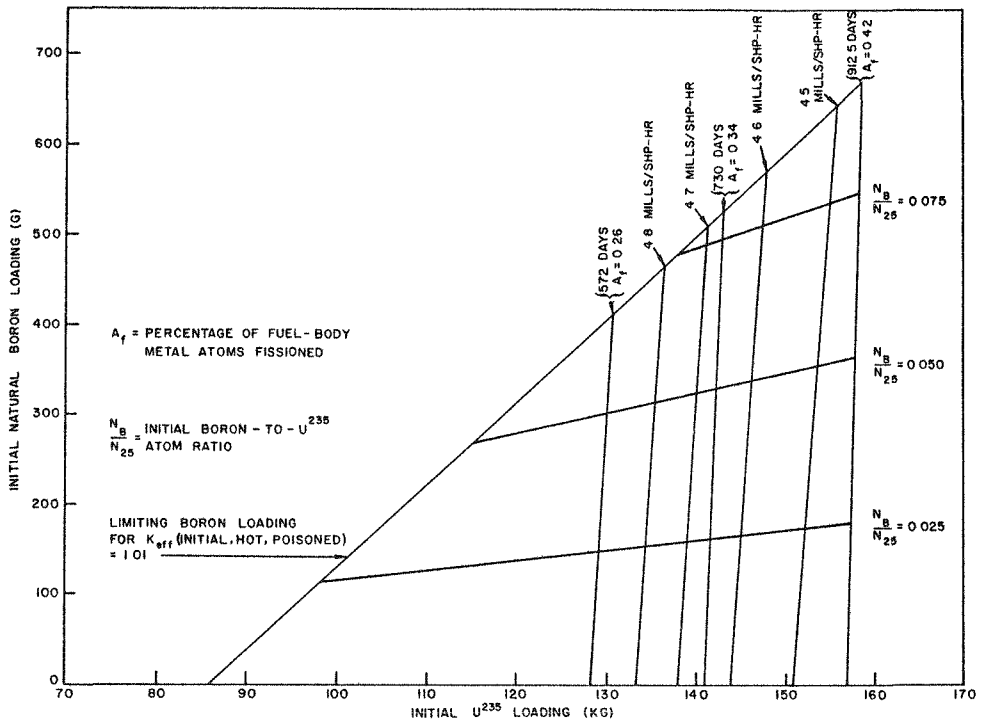

Fig. 3.4--Boron versus U^{235} loading for preliminary design core with 500 kg U^{238}

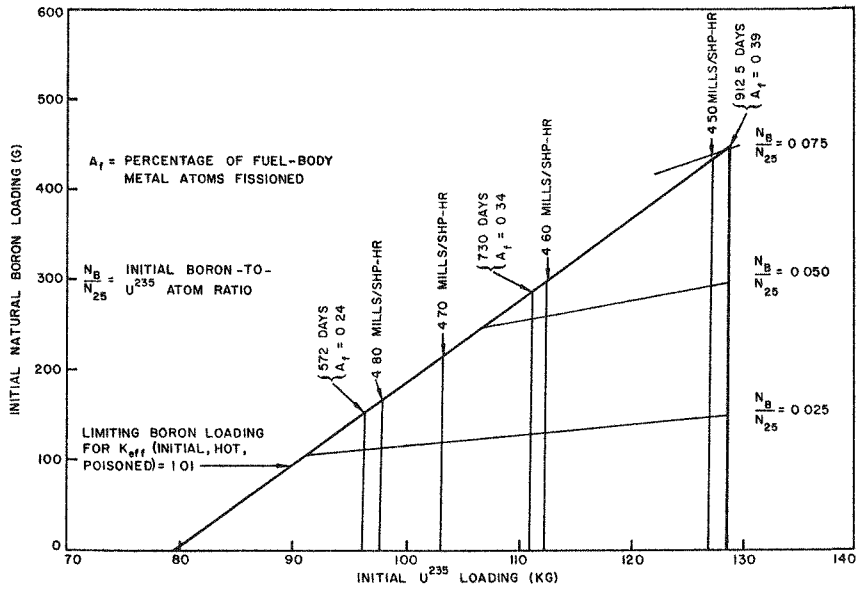

Fig. 3.5--Boron versus U^{235} loading for preliminary design core with no U^{238}

will add curves of constant number of control rods to the results given in Figs. 3.4 and 3.5. A decision on the use of burnable poison is expected to be made by the end of the next quarterly period.

MGCR CRITICAL EXPERIMENTAL PROGRAM

Critical Experiments at General Atomic

During the present reporting period, funds were made available and work was resumed on an MGCR critical experiment at General Atomic.

The facilities will be located in the buildings formerly used for the CIRGA experiments. These include a reactor building, a control building, and a fuel-storage facility, all of which will have to be modified to some extent.

The original critical experiments program is being re-evaluated and modifications are being made to accommodate our current schedule requirements. The earliest tie-in of this program with the design program was found to be the establishment of pressure-vessel requirements by spring, 1960. To meet these conditions, a series of experiments requiring six months for completion is necessary. The experimental program should start in October, 1959. It is estimated that an additional six months of experimental work will be necessary to complete the entire program of critical experiments.

The design of the experimental facilities has progressed to a 50% completion point during the present reporting period. The experimental setup is shown in Fig. 3.6. The procurement of materials and equipment has been started on long-lead items.

Work has been initiated on the preparation of a safeguards report, and project personnel have met with General Atomic's Criticality Safeguards Committee for preliminary review of the concept. A number of suggested changes in design and analysis are being incorporated in the MGCR critical experiments program.

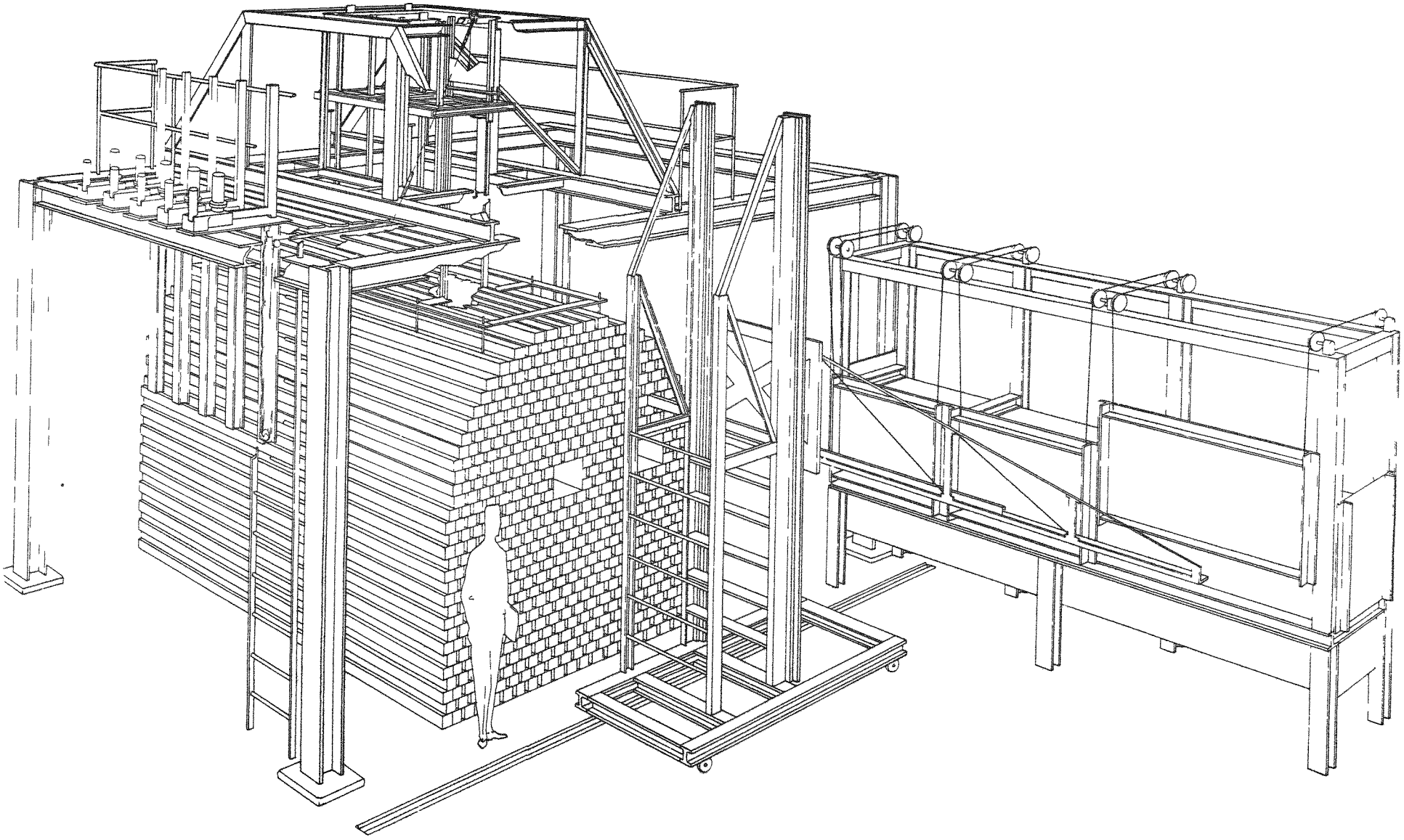

Fig. 3.6--Proposed critical facility

To expedite procurement, the facility components have been grouped into the following packages:

1. General Contractors' Package: modifications to the reactor building doors and windows, the pouring of a heavy concrete pad for critical-assembly support, the installation of heating and ventilating equipment, alterations in lighting and wiring, and the surfacing of outside approaches to the buildings.
2. Structural-steel Package: (a) overhead steel for the support of rod drives, shock absorbers, and control cables; (b) the installation of rails for the movable loading platform; (c) modifications to the pit, which consist of steel covering and supports; and (d) the ladder required at the rear of the reactor building.
3. Outside Fabrication Package: the loading platform and the loading bench, both of which will be fabricated outside General Atomic.

All other fabrication, except specific stock components procured outside, will be done in General Atomic's shop.

In addition to the three major packages listed above, procurement of enriched uranium-aluminum foils is under way. Bids were received from a number of manufacturers, and Babcock and Wilcox has been selected to fabricate the fuel.

MGCR Experiments in Lawrence Radiation Laboratory "Hot Box"

Although the LRL experiments provide data on temperature dependence of reactivity associated with thermalization, leakage, and thermal-neutron absorption, the limitation to highly enriched systems results in a lack of data for temperature dependence of strong absorbers in the resonance range. Since current plans for the MGCR involve (1) the use of U^{238} in the fuel elements to obtain a prompt negative temperature coefficient, and (2) the use of rare earths for control rods, such information would be of great value.

To augment the present experimental program, it is proposed that a series of experiments be performed in the hot box, which would provide these data for the MGCR program. Specifically, it is proposed that we prepare elements containing U^{238} and rare earths in the form of rods which can be inserted into the assembly. These rods will be in groups of various sizes and compositions, so that the influence of both "lumping" and temperature can be evaluated. The nuclear materials used for these experiments will be the same as those being ordered for the MGCR critical experiments.

The first phase of these experiments, involving highly enriched graphite assemblies, has been completed. The test data are in the process of reduction, and a comparison with analysis will be completed during the next quarter. These data should afford an excellent check on our analytical methods for calculating neutron thermalization, since the temperature over the range from room temperature (at which crystalline effects are important) to $1,200^{\circ}F$, where the heavy-gas model is also being used, should be applicable.

In addition to providing these data, the experiments will provide a check on our methods of calculating self-shielding and flux depression of various arrays of materials.

During the next quarter, work will continue on other graphite assemblies with reflectors, and possibly some of the first work on beryllium oxide systems will be undertaken.

IV. MATERIALS DEVELOPMENT

FUEL MATERIALS (W. P. Wallace)

Irradiation Stability of MGCR Fuel Materials (D. E. Johnson)

Work on this portion of the MGCR fuels program was conducted at Battelle Memorial Institute during this quarter. The fabrication of fuel-bearing specimens (UO_2 + BeO, UC + graphite, UC_2 + graphite) for irradiation testing was completed. The design and fabrication of the first irradiation capsule was completed, and irradiation in the BRR began on April 8, 1959.

Some of the results obtained during the fuel fabrication studies indicate that for graphite bodies containing uranium monocarbide, the conversion of the monocarbide to the dicarbide can be observed beginning at a temperature of 2,350°F.

Fuel bodies consisting of a dispersion of UO_2 particles in BeO were successfully fabricated. Two techniques for incorporating the UO_2 grains were used: in one, presintered and crushed UO_2 was incorporated into the matrix; in the second, unsintered UO_2 agglomerates were incorporated into the bodies. The densities obtained were estimated to be 94.8% and 96.8% of theoretical density, respectively. Some "dusting" of the unsintered UO_2 agglomerates occurred during the blending with the BeO powder. The extent and consequences of such dusting have not been determined.

Fuels Development (D. E. Johnson, F. H. Lofftus, A. R. Miller, B. A. Czech, and R. J. La Porte)

The initiation of a systematic program at General Atomic on the study of the sintering behavior of alumina in hydrogen atmospheres was noted in the previous quarterly report, GA-744. This study was continued during this quarter. The data obtained are being evaluated and will be presented in a separate report. Some of the more general conclusions

reached during the course of the study are summarized here.

The study of grinding efficiency during ball-milling as a function of solution pH did not yield conclusive results. The data tend to indicate that the highest sintered densities are obtained with alumina that is ball-milled for 8 hr in an aqueous hydrochloric acid solution. The optimum pH of the grinding solution (before adding the alumina powder) appears to be about 2.5.

As expected, the sintered density of the alumina pellets increased with increasing compacting pressure up to 60,000 psi. However, pellets compacted at 120,000 psi crumbled and could not be conveniently handled. The reason for this behavior is not known, although it is suspected that the type or amount of binder may have been a contributing factor.

The density of sintered pellets increased with sintering time up to 8 hr. The average density for ten pellets sintered 8 hr at 1,700°C was about 96.6% of theoretical density. The lowest density value observed for this lot was 95.7% of theoretical.

The density of sintered pellets also increased with a sintering temperature up to 1,750°C.

As a result of the experience gained in these experiments, it is felt that high-density alumina pellets can be produced by the following procedure:

1. Ball mill alumina powder in a water-hydrochloric acid solution (pH = 2.5 before adding alumina) for 8 hr.
2. Dry, granulate, and add binder (1 wt-% of polyethylene glycol was added for the binder in this series of experiments).
3. Dry and compact at 40,000 psi.
4. Sinter for 6 hr at 1,700°C in a hydrogen atmosphere.

The pellet densities obtained with this procedure should be approximately 95% to 96% of theoretical density.

The continuation of this work will be directed toward the development of techniques for placing a dispersion of UO_2 particles in the alumina matrix.

The effect of certain additives on the sintering rate of the alumina will also be studied. As fuel-bearing pellets are produced, they will be tested to determine their fission-product retention behavior by the activation and post-irradiation annealing techniques which are already in use.

Fission-product Retention by Fuel Bodies (A. R. Miller and D. E. Johnson)

The release of fission products from fuel materials has been studied by numerous workers.[1-11]* However, most of these studies have been conducted on bulk sintered UO_2. Since the fuel being considered for use in the MGCR consists of a dispersion of fairly large particles in a ceramic matrix, an understanding of the fission-product release behavior of this type of system and of each of its components is required.

An apparatus was assembled during this quarter for the study of fission-product release from fuel materials. This apparatus consists of a helium gas purification train, a furnace capable of operating at 1,400°C, a trapping system for the collection of the evolved fission products, and a single-channel analyzer for use in monitoring the fission-product gamma activity in the traps. Numerous tests were made to check out the equipment.

The procedure used in the study of fission-product release behavior of reactor fuels is as follows: UO_2 pellets are compacted and sintered to obtain high-density fuel material. The pellets are then crushed and screened to obtain the desired particle-size fractions for the experiments. One-gram samples of the desired particle-size fractions are irradiated in the TRIGA reactor for 1 hr at a reactor power level of 100 kw. The irradiated specimens are "cooled" for a period of about two weeks to allow the short-lived fission products to decay. The samples are then heated to a temperature of about 1,400°C, for selected time periods, and the iodine evolved during heating is collected in a warm copper trap. The xenon is adsorbed on the activated charcoal at liquid-nitrogen temperature and is subsequently monitored by a scintillation crystal and counting equipment.

*References are listed at the end of this section.

At the present time, analysis is being made only for xenon, and the results obtained during the quarter are noted below in tabular form. They are also presented graphically in Fig. 4.1.

Table 4.1

FISSION-PRODUCT XENON RELEASED FROM UO_2 PARTICLES

Screen Size (mesh)	Particle Size (μ)	Xenon Collected in Trap (%)
-28 to +35	588 to 417	0.12
-60 to +80	250 to 180	0.14
-60 to +100	250 to 150	0.14
-100 to +200	150 to 75	0.66

The xenon collected was that which was released during an 18-hr annealing treatment of the UO_2 at 1,400°C. The pellets that were crushed for this study exhibited densities of about 95% to 96% of theoretical density.

It is planned that this study will be continued and will include experiments on the fission-product release behavior of fused UO_2, of sintered UO_2 of various densities, of UO_2 dispersed in other ceramic materials such as alumina, and of the uranium carbides. A special high-temperature furnace is also being designed which will make possible experimentation at temperatures up to about 2,000°C.

Uranium Oxide Chemistry (U. Merten, L. Dykstra, P. Winchell, and J. Dixon)

Some of the difficulties encountered in conducting experiments on uranium oxide ceramic systems have been concerned with the development of suitable techniques for preparing samples and their examination by X-ray techniques at high temperatures. Considerable progress has been made toward solving these problems. Samples are being prepared as small tablets, approximately 1/4 in. diameter by 1/16 in. thick, by cold pressing and sintering. The sintering is carried out in a tungsten-wound

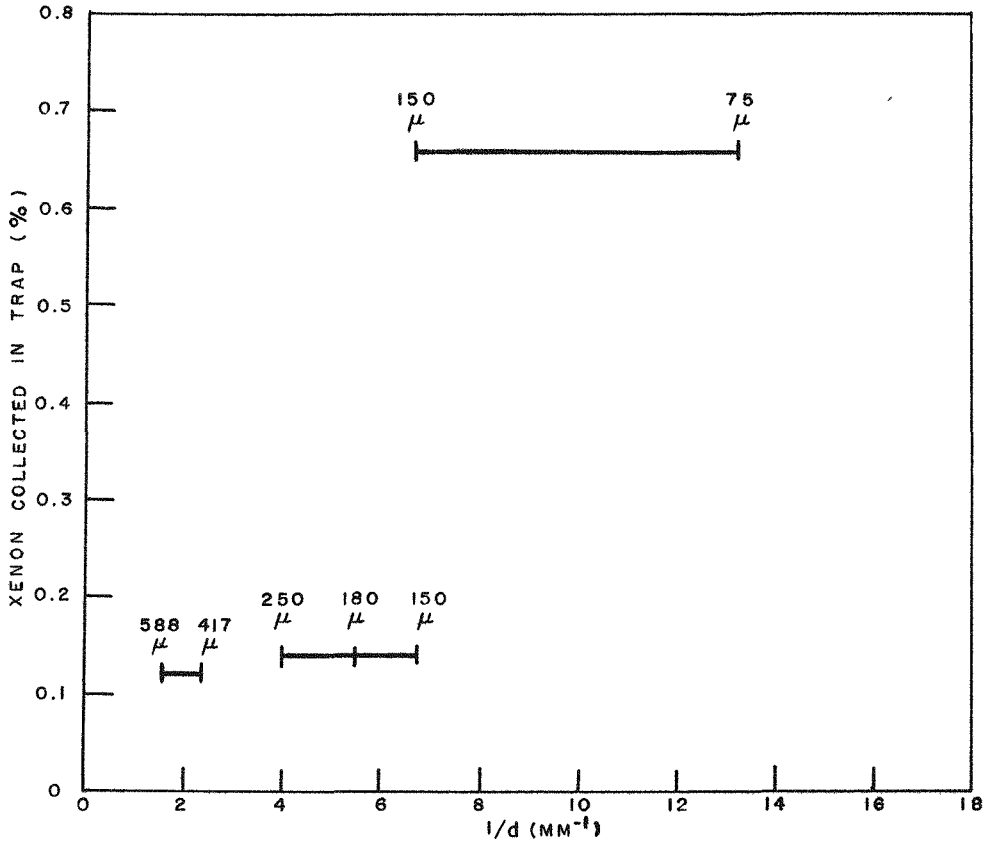

Fig. 4.1--Fission-product xenon released from sintered UO_2 as a function of the reciprocal of particle diameter

furnace enclosed in a vacuum chamber and the sintering can be done at any temperature up to approximately 2,000°C.

The X-ray camera has now been completed and is being tested. In it, the specimen "tablet" is placed between two alumina discs, 3/4 in. across, in which platinum windings are imbedded. The use of the two relatively large discs facing each other, with only a narrow gap between them, allows the specimen in this gap to be brought to a very nearly uniform temperature, which can be measured by an optical pyrometer or a Pt-PtRh thermocouple. With the platinum windings it should be possible to work up to approximately 1,400°C. (In the future, more refractory metal windings will be tried in an effort to increase this limit.) The camera is so designed that a well-collimated X-ray beam strikes the specimen at a grazing angle, and the diffraction pattern is recorded on film in a conventional manner. The entire furnace assembly is enclosed in a water-cooled, vacuum-tight container so that the oxygen pressure over the samples can be controlled. The film, which is separated from the vacuum space by a beryllium window, is mounted in a film cassette which allows four exposures on a single strip of film.

Preliminary experiments made with the camera indicate that it operates satisfactorily at 800°C. Tests at higher temperatures are in progress.

Fuel-element Manufacture and Evaluation (D. E. Johnson, A. Miller, F. Lofftus, B. Czech, and R. La Porte)

A project covering the development and production of fuel-bearing graphite pellets was conducted during this quarter. These pellets were used in the fabrication of a nuclear mockup of a test element for the Hanford in-pile loop. Testing this mockup in the Hanford test pile will provide information to determine the fuel loading required to obtain the desired thermal performance. The pellet size was approximately 1/2 in. in length and diameter.

The process used for fabricating the pellets was as follows: graphite flour and UO_2 powder were blended in appropriate proportions to obtain a uniform mixture. Pitch binder was added to this mixture as a solution in benzene and mixed thoroughly. The benzene was then volatilized. During the volatilization, the mixture was stirred occasionally to prevent the pitch binder from concentrating at the top. The resulting cake was granulated and then warm compacted at a pressure of 10,000 psi and a temperature of about 80°C. Enough pellets were fabricated to provide 3 ln ft of fueled graphite for each fuel loading. Out of each lot of approximately forty pellets, three were selected for chemical analysis to determine the uniformity of the fuel loading. The results of the chemical analysis are presented in Table 4.2.

Table 4.2

CHEMICAL ANALYSIS OF FUEL-BEARING PELLETS

Sample No.	Nominal Loading (g UO_2/ft)	Loading Analysis (g UO_2/ft)
1A		26.0
1B	24.4	26.4
1C		26.2
2A		41.0
2B	36.6	41.9
2C		40.7
3A		12.5
3B	12.2	12.6
3C		12.4
4A		6.2
4B	6.1	6.65
4C		6.2

After the fuel-bearing compacts were measured and weighed, the pellets were sprayed with a thin coat of aluminum paint to minimize the

loss of fuel and the associated spread of contamination that might occur as the pellets were rubbed against other surfaces.

Hot-cell Facility (F. Brown, B. Turovlin, G. Torgison, and L. Bailey)

The construction of the General Atomic Hot Cell is continuing on schedule. A strike at the supplier's plant will delay the installation of the in-cell crane manipulator in the high- and low-level cells. The length of the delay is unknown at this time. Operation without these items will be hampered, but not entirely prevented. Operation that would tend to contaminate the cells will be avoided, as the manipulator and crane installation must be made in a clean cell. This requirement will limit operations to simple manipulations, viewing, and macrophotography. Operation will also be limited to relatively small samples which require a minimum of in-cell handling.

Some difficulty was experienced at the Corning Glass Works; a melt of nonbrowning glass for the viewing windows did not meet specifications and was scrapped. The completion of the cell will probably not be delayed because of the lack of windows unless complications arise in the second melt.

Effort has been directed toward the acquisition of remote operating equipment. Thus far the equipment is primarily intended for metallurgical examinations. A mockup of one section of the cell structure has been constructed to aid in the equipment development.

Supporting equipment also has been ordered for the machine shop and the health physics laboratory.

Cladding Materials (J. C. Bokros, D. G. Guggisberg, and W. H. Ellis)

A new series of graphite-metal compatibility experiments has been initiated at 1,700° and 1,850°F. Experiments are being run in impure and gettered helium. Materials being evaluated in these tests include nickel, nickel-copper alloys, niobium alloys, and molybdenum alloys.

The effect of carburization on the room-temperature tensile properties was determined on representative alloys selected from each alloy

group (except the niobium alloys). Tensile specimens were machined from 0.031 in. sheet with a 1-1/2 in. gauge length and a 1/4 in. gauge width. Two-thirds of these specimens were pack carburized in a mixture of 5% $BaCO_3$ + 95% graphite at 1,600° to 1,700°F for 500 hr. The carburization was done in a stainless steel capsule which had been evacuated and filled with helium prior to heating to the carburization temperature. The resulting atmosphere at equilibrium at the carburization temperature was carbon monoxide and helium at a gauge pressure of about 5 cm of Hg. Carbon analysis of the tensile specimens was made before and after carburization. The balance of the specimens were used as controls and given the same thermal treatment as the carburized specimens in vacuum. The specimens were tensile tested in an Instron testing machine at room temperature.

The carburized nickel specimen showed an increase from 0.064% to 0.300% carbon, and the Monel specimen showed an increase from 0.069% to 0.170% carbon. In each case the strength was increased, whereas the ductility was unaffected. The carburized nickel specimen gave a serrated stress-strain curve, probably attributable to a very fine precipitate in the grain-boundary region.

Duranickel (95.5 Ni-4.5 Al) was completely embrittled by the carburization. The microstructure indicated that the aluminum had been internally oxidized.

Type 314 stainless steel was strengthened during the carburization and slightly embrittled. The ductility of Types 430 and 316 stainless steel was significantly reduced by the carburization.

Carburization increased the strength and decreased the ductility of Inconel and decreased both the strength and ductility of Inconel X. The microstructure of Inconel showed about 10% carbide, whereas the microstructure of Inconel X showed only a slight grain-boundary carburization.

Carburization of molybdenum resulted in a 0.0003-in. carbide coating which cracked severely during testing. The carburized specimen

showed an increase in strength and a decrease in ductility. The yield point evident in the stress-strain curve for the control sample did not appear in the curve for the carburized specimen.

Nickel and alloys of nickel and copper appear to be the best choice for a graphite cladding material. Neither nickel nor copper forms stable carbides and both are in equilibrium with graphite to their melting temperatures. Carburization results only in solid-solution strengthening with no sacrifice in ductility. (A description of all of the graphite-metal results is given in Ref. 12.)

Four niobium-clad graphite capsules enclosed in an outer graphite can were thermal-cycled 15 times from 200°F to 1,600°F in 500 to 1,050 psi helium. Two of the capsules were 1/2 in. in diameter and two were 3/8 in. in diameter. Both were 2 in. long and had a cladding thickness of 0.010 in. The capsules were held for 92 hr at 1,600°F. The graphite was not outgassed and the helium was taken directly from a tank without purification. Two of the four capsules failed in a brittle manner. One end of each of the two capsules which failed was broken off in the heat-affected zone of the weld and one of the capsules split longitudinally. Figures 4.2 and 4.3 are photographs of the disassembled test fuel elements which failed during test. Each of the two capsules which did not fail decreased in diameter by 0.001 in. and decreased in length by 0.006 in. in one case and 0.012 in. in the other. The chemical analysis of the helium after the test is given in Table 4.3.

A test fuel element clad with 0.005 in. of Monel was cycled 19 times from 200° to 1,600°F and held for 264 hr at 1,600°F. The pressure varied from 800° to 1,400°F during cycling. The cladding material was very ductile after cycling. Photomicrographs of the Monel cladding and the nickel end cap, taken so the graphite-metal interface is visible, are shown in Figs. 4.4 and 4.5. The familiar fine precipitate which forms in the grain-boundary region of nickel and nickel-copper alloys when they are exposed to graphite is evident and appears to be more extensive in the

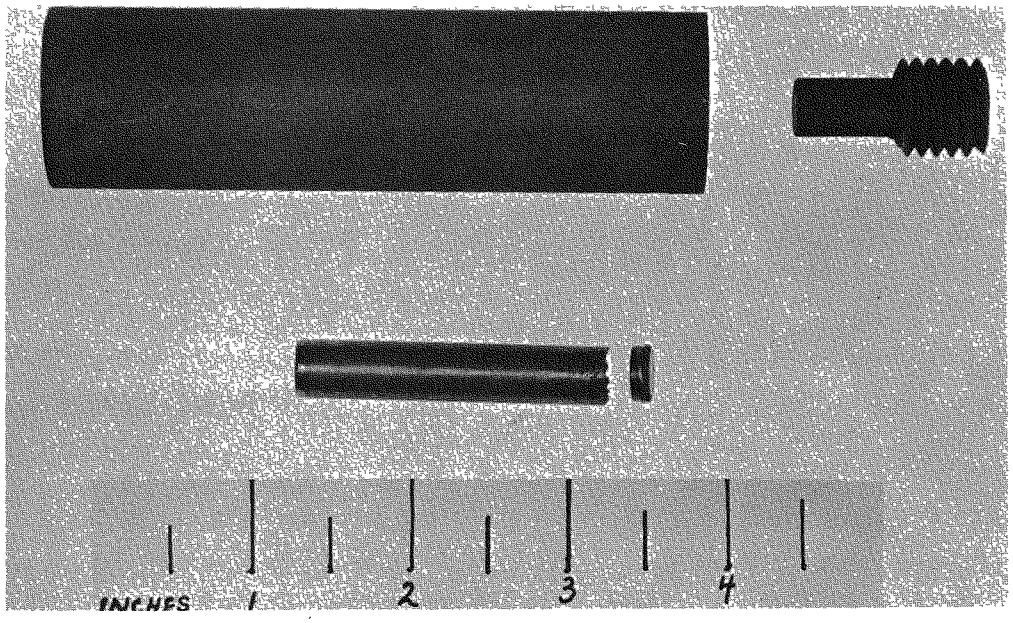

Fig. 4.2--Niobium-clad graphite cycled 15 times from 200° to 1600°F in 1200-psi helium. End cap failure

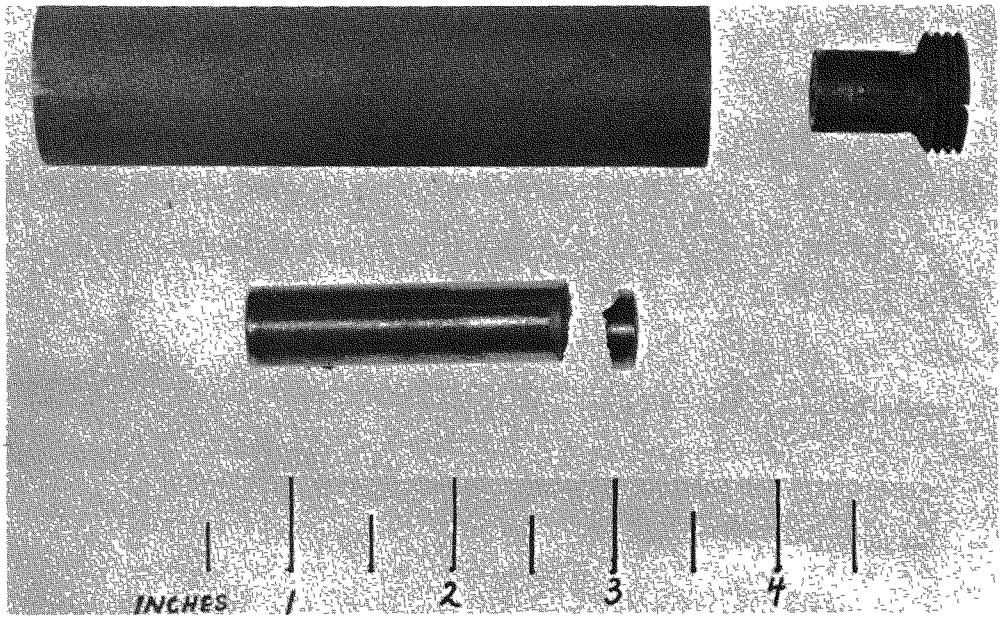

Fig. 4.3--Niobium-clad graphite cycled 15 times 200° to 1600°F in 1200-psi helium. End cap and longitudinal failure

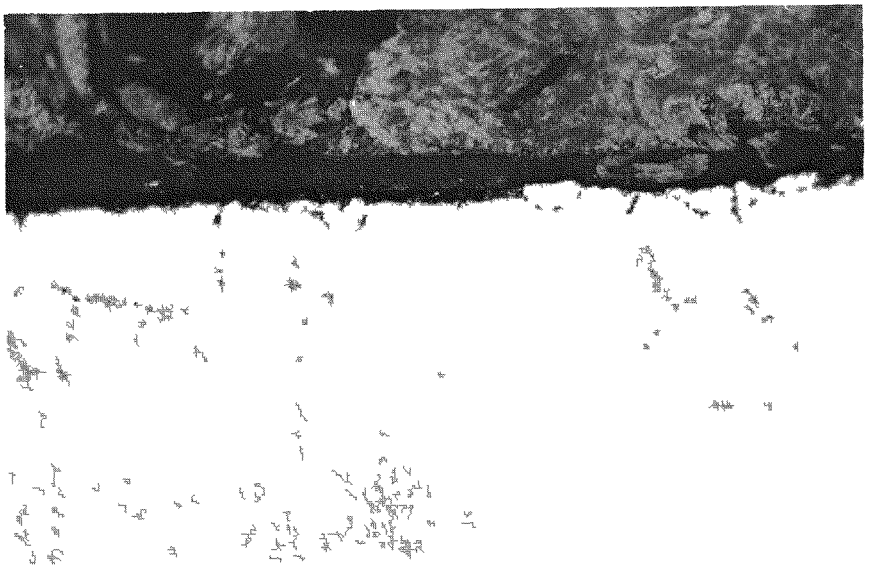

Fig. 4.4--Photomicrograph of 0.005 in. Monel cladding from a graphite fuel assembly cycled 19 times from 200° to 1600°F in 1200-psi helium. Fine grain-boundary precipitate extending to 1.0 mil (500X)

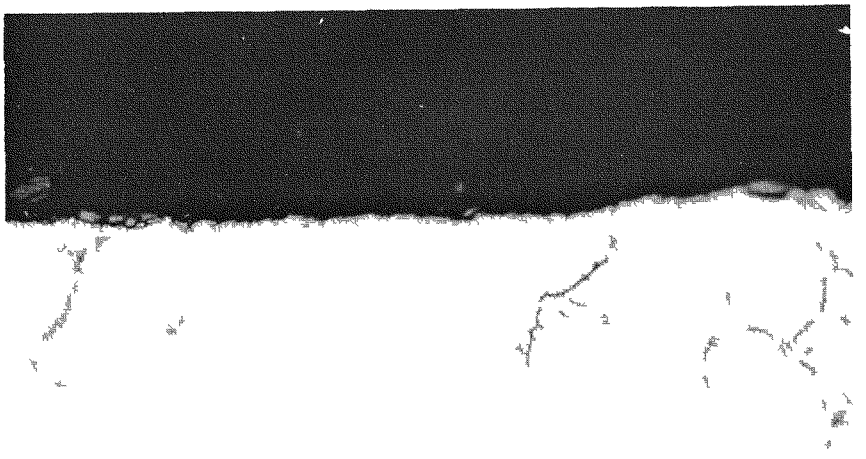

Fig. 4.5--Photomicrograph of nickel end cap from a Monel-clad fuel assembly cycled 19 times from 200° to 1600°F in 1200-psi helium. Fine grain-boundary precipitate extending to 2.0 mils (500X)

nickel. The clad graphite pin was originally 1/4 in. in diameter and did not decrease during cycling. The length, however, decreased by 0.012 in. (in 2 in.). Chemical analysis of the helium after cycling is shown in Table 4.4.

Table 4.3

CHEMICAL ANALYSIS OF HELIUM USED IN CYCLING THE NIOBIUM-CLAD TEST FUEL ASSEMBLIES

Impurity	Mol-%
Hydrogen	0.16
Oxygen	0.0082
Nitrogen	0.023
Methane	0.0008
Carbon monoxide	0.23
Carbon dioxide	------

Table 4.4

CHEMICAL ANALYSIS OF HELIUM USED IN CYCLING TYPE 348 AND 430 STAINLESS STEEL AND MONEL-CLAD TEST FUEL ASSEMBLIES

Impurity	Mol-%
Hydrogen	0.22
Oxygen	0.0011
Nitrogen	0.0105
Methane	0.0026
Carbon monoxide	0.0648
Carbon dioxide	0.019

The test fuel element clad with 0.010 in. of Type 348 stainless steel was cycled 19 times from 200° to 1,600°F and held for 264 hr at 1,600°F. The pressure varied during cycling from 800 to 1,400 psi. The capsule did not fail during cycling, but was carburized very badly. Figure 4.6 (p.72) shows a photomicrograph of the graphite-metal interface. A carbide

layer has developed between the graphite and the metal. The cladding is badly carburized throughout and failed in a brittle manner when it was stripped from the graphite core. The 1/4-in. capsule decreased in diameter by 0.003 in. and decreased in length by 0.025 in. (in 2 in.). Chemical analysis of the helium after the test is shown in Table 4.4.

Three test fuel elements clad with 0.010 in. of Type 430 stainless steel were cycled 31 times from 200° to 1,600°F and held for 454 hr at 1,600°F. The capsules did not fail during cycling, but were carburized. Figure 4.7 shows the graphite-metal interface. Similar to the Type 348 stainless steel, this alloy reacted with the graphite to form a carbide layer between the metal and the graphite. Massive carbides are evident in the microstructure, but have not as yet completely embrittled the alloy, i.e., the cladding was ductile enough to be stripped from the graphite core without fracture. The diameter of the capsules decreased from 0.002 in. to 0.003 in. during cycling.

A hexagonal graphite block containing six 4-in.-long, 1/4-in.-diameter graphite pin clad with Type 304 stainless steel was cycled 12 times from 200° to 1,600°F without failure. Metallographic results are not yet available.

Two hexagonal assemblies, each containing six 4-in.-long, 1/4-in.-diameter nickel-clad simulated fuel bodies, are now being cycled from 100° to 1,700°F in from 500- to 1,000-psi helium at the rate of one cycle per 10 hr. One of these contains graphite as the simulated fuel and the other contains 1/2-in.-long Al_2O_3 pellets.

MODERATOR-COOLANT COMPATIBILITY (W. L. Kosiba and C. R. Mungle)

A system for the study of graphite-gas reactions was designed and constructed during this quarter. This is a once-through system in which helium, with known amounts of impurities, will be passed over hot graphite; the graphite will be weighed at intervals and the changes in weight recorded.

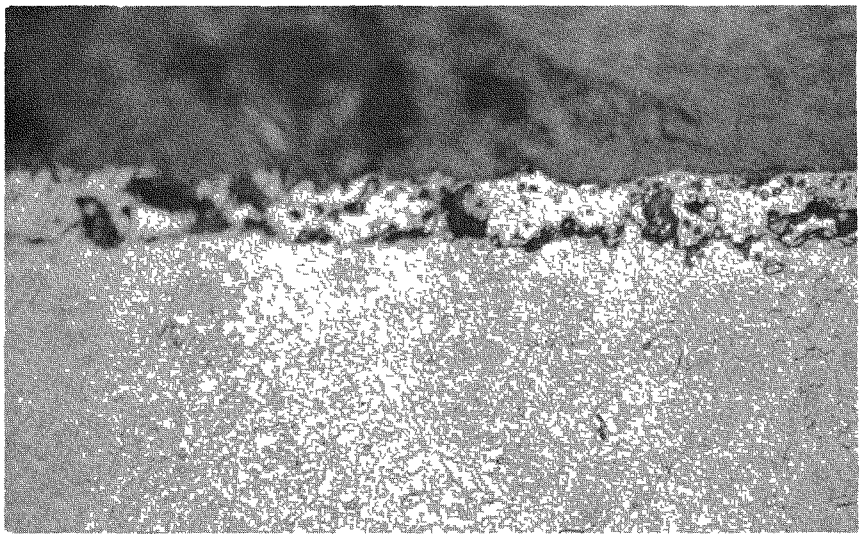

Fig. 4.6--Photomicrograph of Type 348 stainless-steel cladding stripped from a fuel assembly cycled 19 times from 200° to 1600°F in 1200-psi helium. Carbide layer formed between graphite and cladding. Cladding was completely carburized and very brittle (500X)

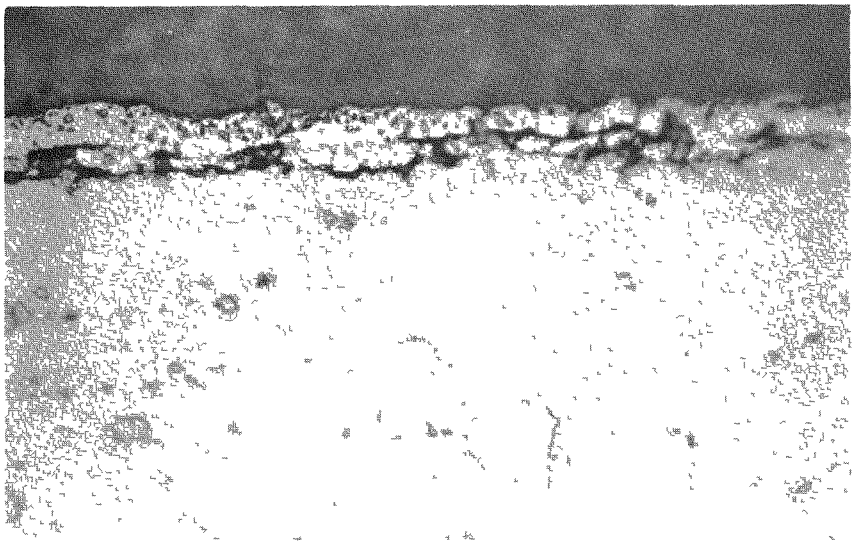

Fig. 4.7--Photomicrograph of 0.010 in. Type 430 stainless-steel cladding stripped from a fuel assembly cycled 31 times from 200° to 1600°F in 1200-psi helium. Carbide layer formed between graphite and steel and massive carbides formed in the microstructure (500X)

The first experiments with 0.3% impurities in helium have been initiated and the results will be reported subsequently.

CONTROL-ROD MATERIALS (B. Turovlin and J. R. Lindgren, Jr.)

Control-rod development work has been carried out utilizing two different approaches.

1. Flame-spraying of samarium-gadolinium oxide on a stainless steel tube, previously sprayed with Nichrome, has been done successfully. An inner graphite core was used to prevent rapid cooling of the stainless steel and it is believed to have been a contributing factor in securing the desired results. The integrity of the sprayed surface was spot checked by measuring the continuity with an ohmmeter.

2. A compact of 5% samarium-gadolinium oxide powder (the remainder of Type 304 stainless steel powder) was prepared and sintered for 3-1/2 hr in hydrogen at 2,300°F. A portion of the compact was canned in a stainless steel "picture frame," evacuated, sealed, and then rolled at 2,000°F to a 4:1 reduction in thickness. Breaks occurred in the stainless cladding. It is believed that thicker cladding would remedy the condition. Gadolinium oxide, alone, was flame-sprayed on stainless steel using the same techniques as with the samarium-gadolinium oxides. The gadolinium oxide was sprayed on the stainless steel to 1/2 g/in.^{2} of surface area.

STRUCTURAL-MATERIALS PROBLEMS RELATED TO THE WORKING FLUID (B. Lund, R. Shepheard, and J. Balass)

This program, concerning materials for the nonreactor portion of the MGCR plant, has been devoted to

1. A study of the effects of commercially pure helium on the properties of ducting and turbine materials at elevated temperatures.

2. The preparation for testing the ability of ducting materials to contain helium at operating temperatures and pressures.

3. A proposed program for evaluating effects of varying levels of impurities on stress-rupture properties of ducting alloys, depending on the results obtained from completion of tests under Item 1.

4. A proposed program of study on the mode of fracture and dependence of stress-rupture life on stress, temperature, and atmosphere of a chromium-molybdenum steel and Type 316 stainless steel.

5. The preparation of a summary report of the corrosion test work performed in 1958.

In order to learn the effects of commercially pure helium on the properties of ducting and turbine materials at elevated temperatures, the New England Materials Laboratory has been awarded a subcontract to perform preliminary stress-rupture tests in air of the tentative ducting alloys (1-1/4 Cr-1/2 Mo and 2-1/4 Cr-1 Mo steels and Type 316 stainless steel) and they will shortly begin tests in helium. The ultimate objective of these tests is to produce a log stress versus log rupture-time curve, in air and in helium, for each of these alloys at anticipated maximum operating temperatures, in order to establish the existence of an enviromental effect, its magnitude, and its stress dependence. Results thus far obtained and tests in progress at the New England Materials Laboratory are presented in Tables 4.5 through 4.7. Based on these results, the best heat treatment will be chosen to obtain stress versus rupture-life curves in air and in helium at 1,000°F, utilizing seven stress levels to obtain curves extending to 1,000 hr.

The data in Table 4.7 indicate no apparent effect of solution heat treatment. The second plate (Table 4.7), although it ruptured in similar time to the first, appears to have lower ductility. However, the microstructure is more homogeneous, and it is planned to use this second plate for obtaining air and helium log stress versus log rupture curves.

Preliminary high-stress rupture tests with as-received vendor heat-treated material for the tests in air indicated an apparent discrepancy in the rupture life of the above materials. Thus, a need for knowledge of

Table 4.5

STRESS-RUPTURE TESTS IN AIR OF 1-1/4 Cr-1/2 Mo STEEL AT A TEMPERATURE OF 1,000°F

Stress (psi)	Rupture Time (hr)	Elong. (%)	RA (%)	Remarks
40,000	0.4	28.8	72.0	1/2-in. plate, as received
40,000	0.4	39.8	79.0	
35,000	0.9	32.4	77.4	
30,000	27.0	48.5	74.7	
27,000	98.4	40.0	82.4	
25,000	97.1	40.1	71.0	
30,000	Being run			1/2-in. plate, norm 1750°F
30,000				1/2-in. plate, norm 1550°F
30,000				1/2-in. plate, norm 1750°F, D 1,350°F
30,000				1/2-in. plate, norm 1750°F, D 1,150°F
30,000				1/2-in. plate, norm 1550°F, D 1,350°F
30,000				1/2-in. plate, norm 1550°F, D 1,150°F
30,000	Run scheduled			1/2-in. plate, annealed 1650°F

Table 4.6

STRESS-RUPTURE TESTS IN AIR OF 2-1/4 Cr-1/2 Mo STEEL AT A TEMPERATURE OF 1,000°F

Stress (psi)	Rupture Time (hr)	Elong. (%)	RA (%)	Remarks
25,000	306.7	64.0	87.0	1/2-in. plate, as received
25,000	206.2	66.0	78.7	
25,000	160.5	49.0	81.3	
28,000	88.3	56.2	82.0	
30,000	35.9	37.4	83.6	
30,000	Being run			1/2-in. plate, norm 1750°F
30,000				1/2-in. plate, norm 1550°F
30,000				1/2-in. plate, norm 1750°F, D 1,350°F
30,000				1/2-in. plate, norm 1750°F, D 1,150°F
30,000				1/2-in. plate, norm 1550°F, D 1,350°F
30,000				1/2-in. plate, norm 1550°F, D 1,150°F
30,000	Run scheduled			Annealed 1650°F

Table 4.7

STRESS-RUPTURE TESTS IN AIR OF TYPE 316 STAINLESS STEEL AT A TEMPERATURE OF 1,300°F

Stress (psi)	Rupture Time (hr)	Elong. (%)	RA (%)	Remarks
20,000	29.0	42.0	44.8	1/2-in. plate, as received
20,000	48.4	54.0	52.9	
20,000	42.5	54.0	57.0	
18,000	50.6	41.2	44.9	
20,000	49.1	49.2	51.4	Same plate, solution heat treat 2,100°F, W.Q.
20,000	37.5	17.8	27.0	Second plate, solution heat treat 2,100°F, W.Q., different chemistry

the effects of heat treatment and microstructure on these particular alloy heats appeared necessary, and tests of the chromium-molybdenum steels with various heat treatments are now being run. From these tests in air and in helium, an indicated optimum heat treatment will be determined to obtain log stress versus log rupture-life curves.

The Westinghouse Industrial Gas Turbine Department is performing comparative air and helium stress-rupture tests of turbine blade and disc materials.

The helium-containment test system has been completed and the experiments will begin after system checkouts.

A series of tests with controlled levels of oxygen, nitrogen, water vapor, carbon monoxide, and oil vapor in helium are scheduled for the near future in order to reveal any gross effects of these impurities and their concentrations on the stress-rupture life of materials.

MODERATOR DEVELOPMENT (W. L. Kosiba)

During discussions with graphite suppliers, it was learned that one of them has had some degree of success in cementing large pieces of graphite. Joints which are as strong as the parent graphite body can be obtained if great care is used in the process. Equally strong joints have been obtained by mechanically interlocking the pieces, and this is preferred. Cementing is recommended only as a last resort because the cement layer is about 15 mils thick and contracts 4 to 6 mils when fired, which makes it difficult to maintain close tolerances. The machining characteristics of the cement bond are the same as those for the base material.

The arch-type support structure that has been suggested as one core design is feasible and can be made in the size that is required. This could be made out of sections cemented together. One graphite supplier has had experience in making similar structures. High-strength graphites are not

made by any special process by National Carbon, but are selected pieces from standard grades. Small pieces are readily available; large pieces are also available, but an added cost is incurred because of more involved selection and inspection. Another supplier makes high-strength graphite by a special process and some of our crude tests show that they have achieved a 5,000-psi tensile strength; this value, however, is questionable. Tensile strengths of 2,000 to 2,500 psi have been achieved by graphitizing at lower temperatures. The cost of high-strength graphite is unknown at present. The thermal expansion coefficient of high-strength graphite is about twice that of normal-grade graphites.

CORROSION AND MASS TRANSPORT TESTS IN HELIUM (J. C. Bokros and H. E. Shoemaker)

The major reaction which might cause mass transport in the reactor is oxidation of carbon in the reactor core. This would form carbon monoxide which may partially disproportionate in the cooler regions of the reactor to deposit free carbon and thus leave carbon dioxide, which may further oxidize the core.

The first experiments were therefore designed to study these reactions, together with the corrosion of various metals which may be present in the reactor.

The apparatus constructed for this investigation is shown in Fig. 4.8. With this system, it is possible to pass helium test gas through a titanium and a uranium trap to remove the oxidizing impurities. A trace impurity may then be added to the pure helium through the controlled leak. The exhaust gas bubbles out through a mercury bubble trap and thus a positive pressure of 1 to 2 psi is maintained in the system. Each quartz chamber is heated in a resistance furnace with the temperature maintained by a controller. Two recorders are used to measure the temperature at numerous points in the tubes.

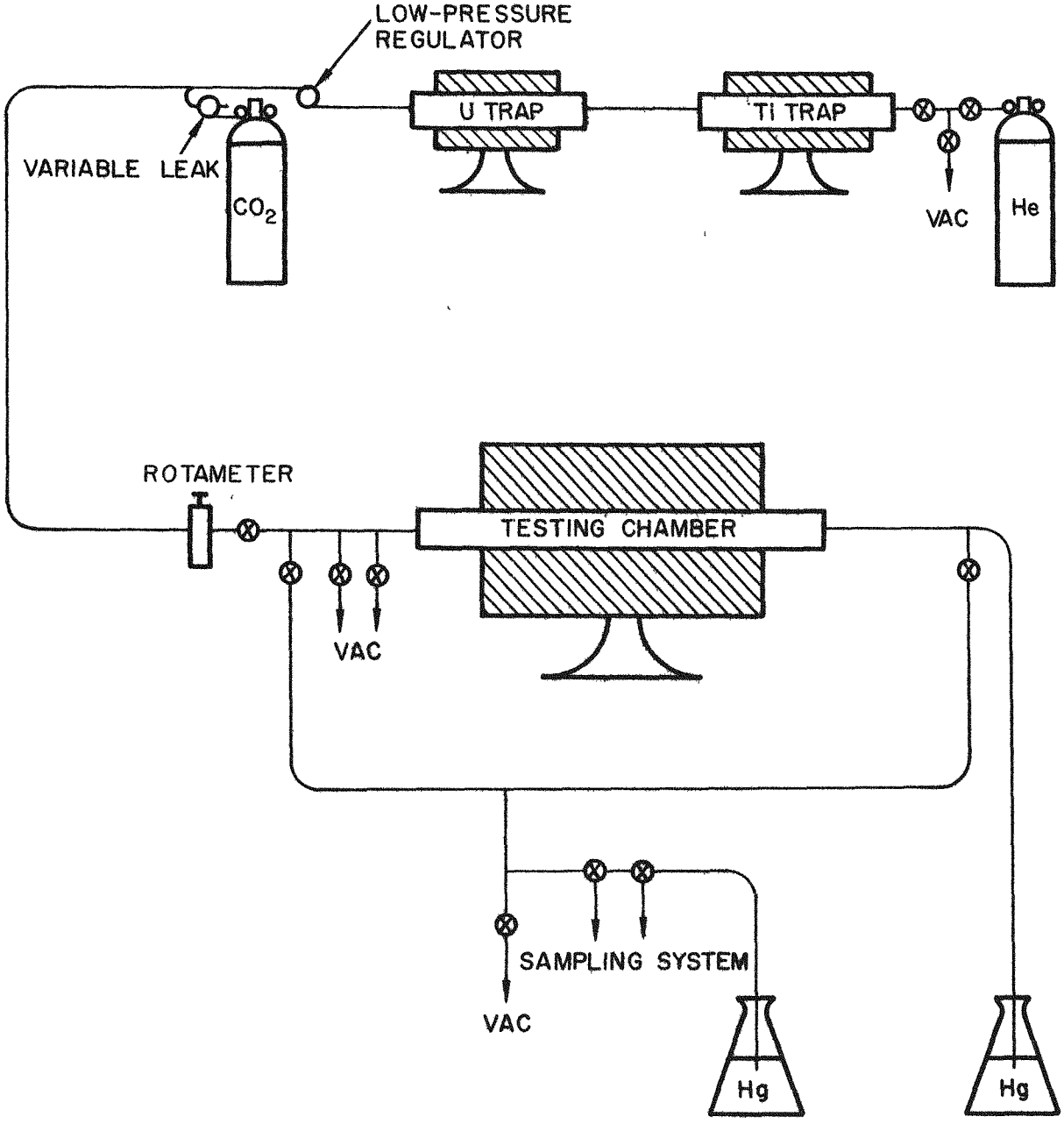

Fig. 4.8--Schematic diagram of apparatus for testing helium impurity reactions with graphite and metal

The metals tested were those of interest for such applications as fuel cladding, turbine blades, etc., and included niobium and niobium alloys, nickel and nickel alloys, an austenitic stainless steel, and a ferritic stainless steel. The samples were prepared by rolling the metal into sheets less than 30 mils thick.

The graphite used in these tests was all machined from AGOT graphite; the helium used was Bureau of Mines grade A (99.995% pure prior to the hot-trap purification); and the carbon dioxide used as a contaminant was welding grade, 99.9% pure.

The chemical analyses were conducted with a Burrell Model K-2 Kromotog gas chromatograph. The inlet helium was found to contain traces of neon and hydrogen, 200 ±100 ppm of oxygen, and 200 ±100 ppm of nitrogen. After passing the helium through the hot traps, it was impossible to detect, with any degree of accuracy, the remaining impurities. The total oxidizing impurity was only a few parts per million. The major difficulty in the analysis was that the argon comes out with the oxygen, so that the effect of the two is recorded simultaneously, and thus it was impossible to achieve any high degree of accuracy for oxygen analysis in the low ppm range.

The chemical analyses of the gases were not precise enough to permit a material balance. They did show, however, that the exhaust carbon monoxide concentration was approximately twice the inlet carbon dioxide concentration, which was 80 ±20 ppm, indicating that any loss of oxygen due to reaction with the metals was not great enough to alter the impurity level in the gas. No carbon dioxide was detected in the exhaust gas. The absence of carbon dioxide indicated that the quench of the exhaust gases was too rapid to permit the disproportionation of the carbon monoxide to deposit carbon in detectable quantities. An inlet and exhaust concentration of 5 ±2 ppm N_2 was observed with no apparent change in concentration.

The weight changes of the materials are the most significant results at this time. Since the surface area calculated from the graphite dimensions would not be the actual available surface area of the graphite, the weight loss was determined in milligrams per gram rather than milligrams per square centimeter. The sample-testing space was divided into four areas with Zone 1 at the gas inlet and Zone 4 at the exhaust. The weight losses of the samples were then plotted to show the difference in corrosion relative to the placement of the sample in the chamber.

At 1,700°F, the weight loss of the graphite discs was fairly uniform throughout the tubes. This loss amounted to approximately 0.2 mg/g in 500 hr. At 1,500°F, the weight loss of the graphite was high at the inlet and approached equilibrium at the end of Zone 2. This was the middle of the reaction chamber, so the atmosphere would have been somewhat oxidizing in the first two zones. The weight losses are plotted in Fig. 4.9 for the chamber containing the niobium samples and in Fig. 4.10 for the chamber containing the nickel samples. At 1,700°F, the perforated graphite plugs at the inlet to the graphite cylinders accounted for nearly 75% of the weight loss of the graphite in the system. These plugs had an average weight loss of 2 mg/g in 500 hr. The oxidation of carbon was obviously much slower at 1,500°F, as these porous plugs accounted for less than 25% of the total graphite weight loss. These plugs had an average weight loss of only 0.3 mg/g in 500 hr. Disproportion of carbon monoxide to carbon dioxide plus carbon was not observed at the exhaust of any of the chambers. This was in agreement with the gas analysis and indicated that the quench was too rapid to permit a detectable amount of the reaction.

The weight gains of the metal samples are plotted in Figs. 4.11 through 4.24. Each line indicates the zone in which the sample was tested. Zone 1 was at the gas inlet end of the reaction chamber and the zones run consecutively to the exhaust. Each figure contains two unconnected points. One of these points indicates the weight gain of a sample at 100 hr, at which time it was removed for analysis and metallography, and the 400-hr point is for the sample which replaced it in the reaction chamber.

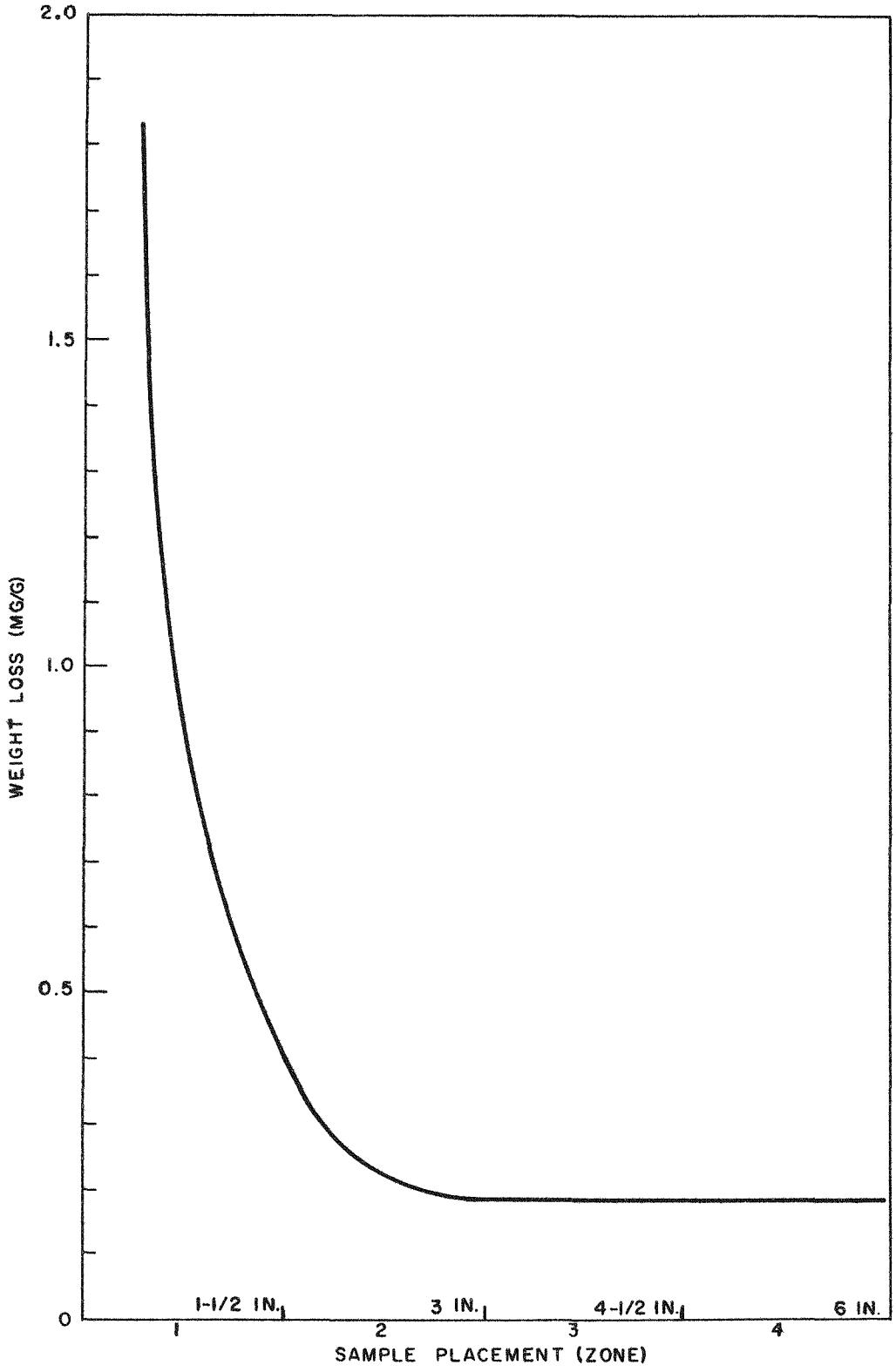

Fig. 4.9--Graphite weight loss at 1,500°F in helium and carbon oxides (average of 12 points). Niobium cladding

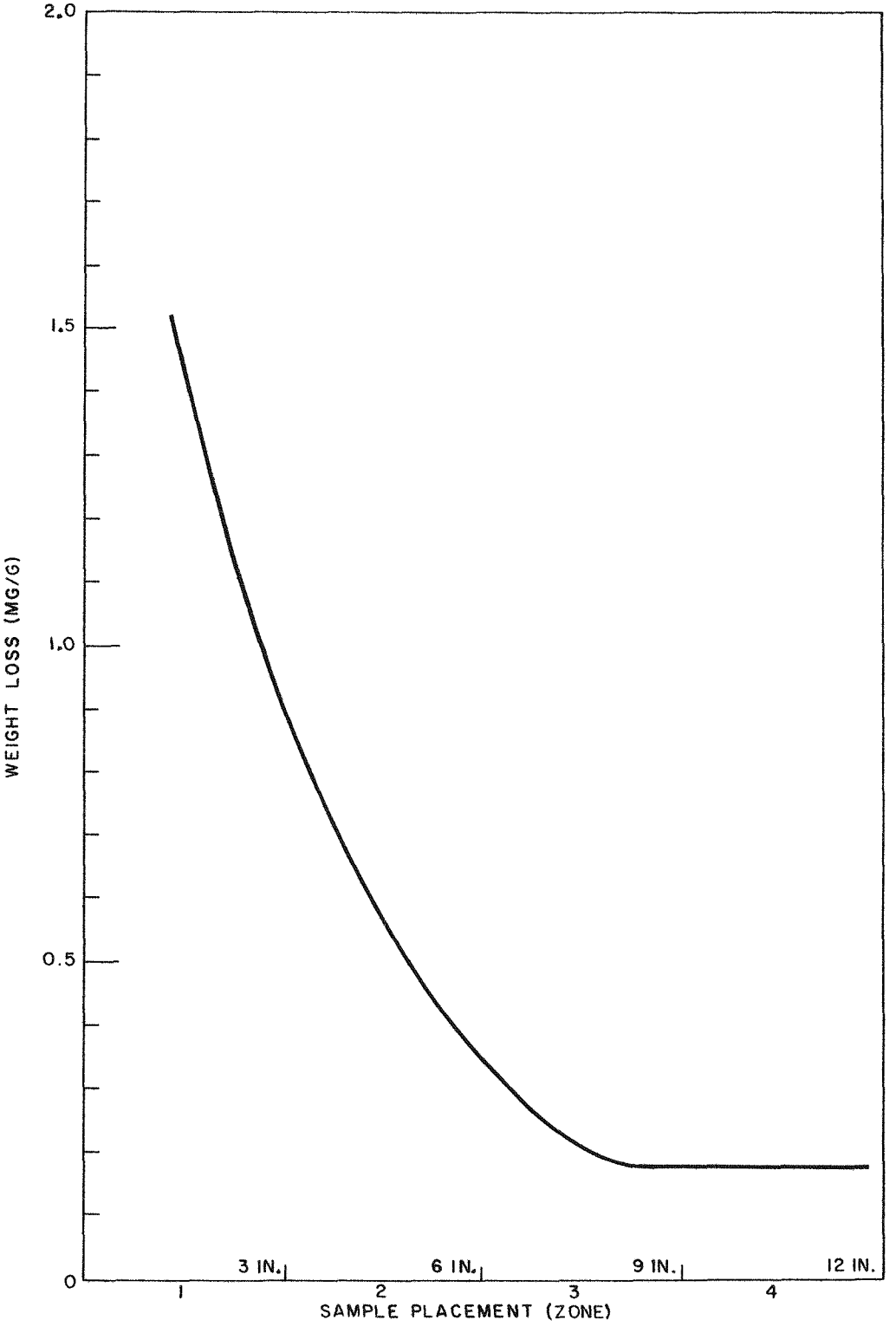

Fig. 4.10--Graphite weight loss at 1,500°F in helium and carbon oxides (average of 24 points). Nickel cladding

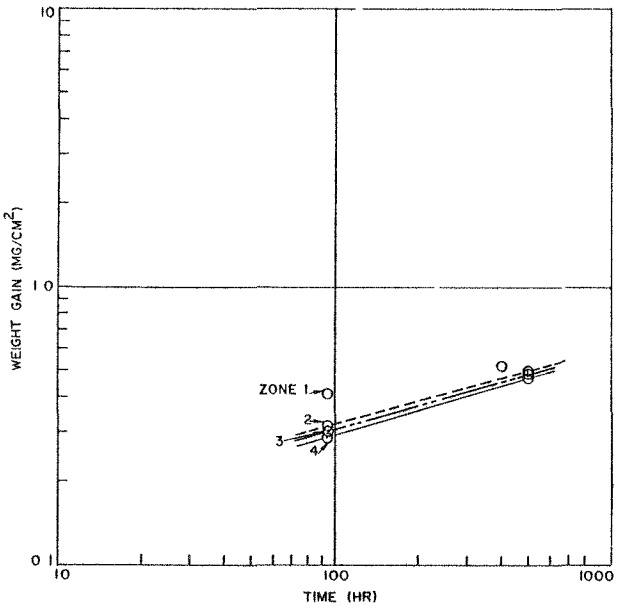

Fig. 4.11--Weight gain versus time for niobium +1% zirconium in helium $+2 \times 10^{4}$ atm $P_{CO} + 2\ P_{CO_2}$ at 1,700°F

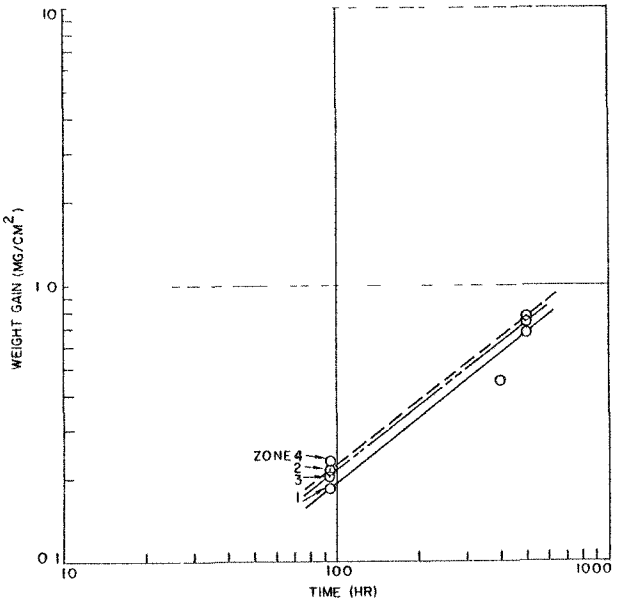

Fig. 4.12--Weight gain versus time for Type 430 stainless steel in helium $+2 \times 10^{4}$ atm $P_{CO} + 2\ P_{CO_2}$ at 1,700°F

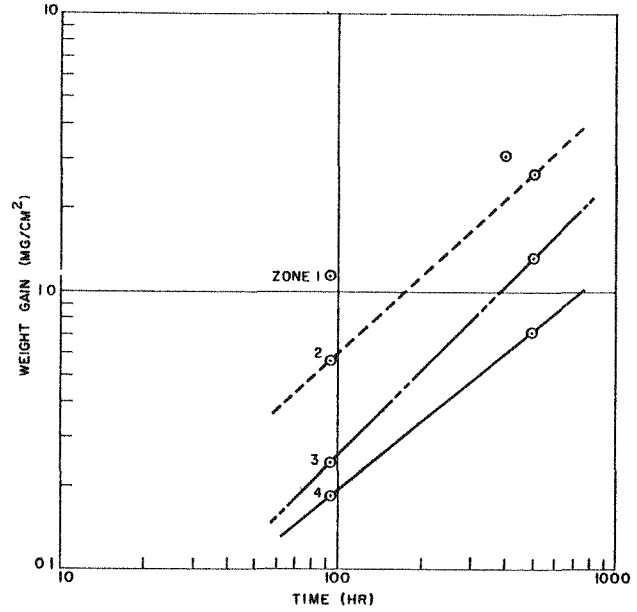

Fig. 4.13--Weight gain versus time for niobium + 1% zirconium in helium $+2 \times 10^{4}$ atm $P_{CO} + 2\ P_{CO_2}$ at 1,500°F

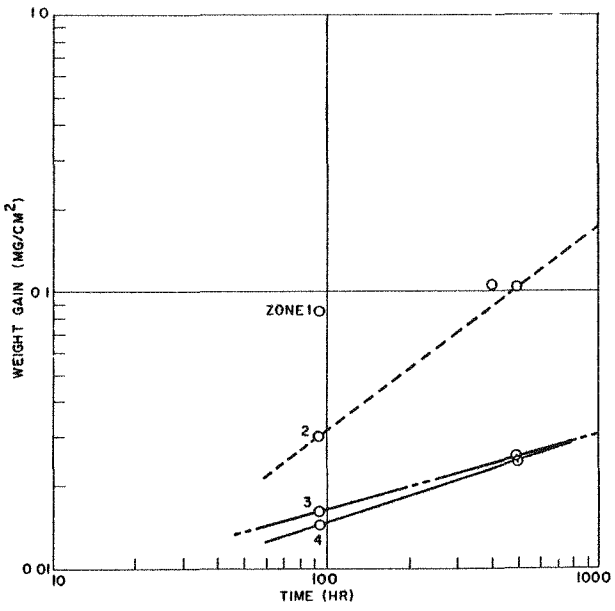

Fig. 4.14--Weight gain versus time for Type 430 stainless steel in helium $+ 2 \times 10^{-4}$ atm $P_{CO} + 2\ P_{CO_2}$

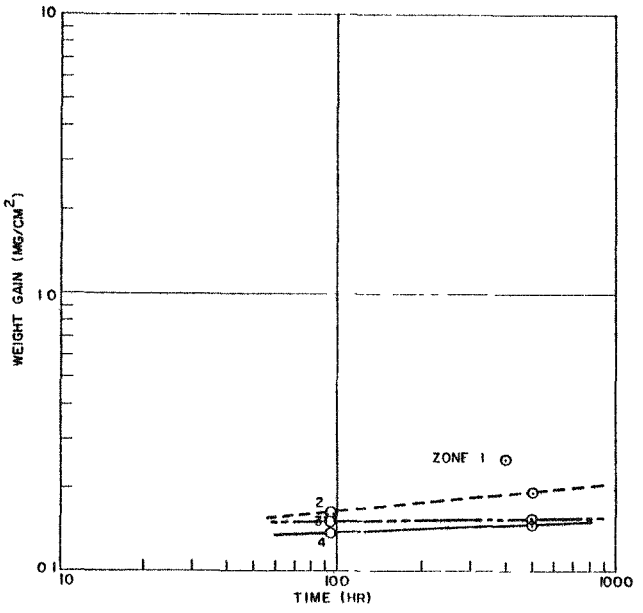

Fig. 4.15--Weight gain versus time for Type 316 stainless steel in helium $+2 \times 10^{-4}$ atm $P_{CO} + 2\ P_{CO_2}$ at 1,500°F

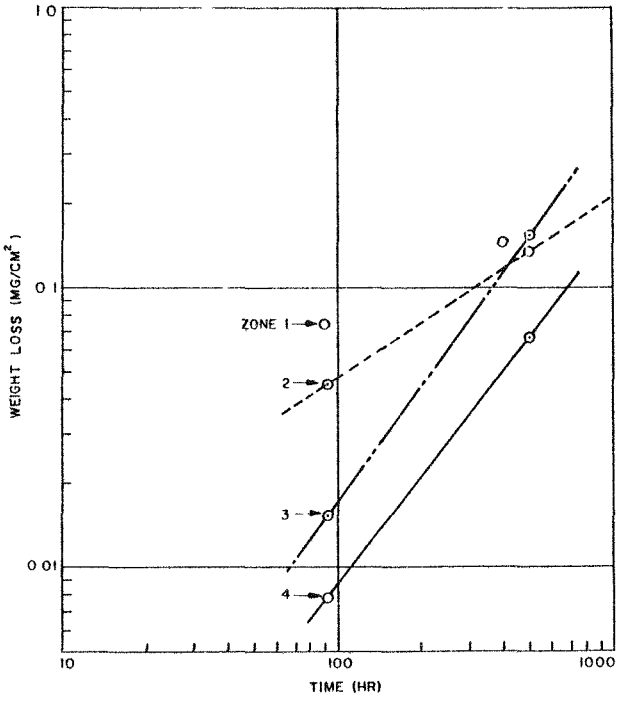

Fig. 4.16--Weight loss for "A" nickel in helium $+2 \times 10^{-4}$ atm $P_{CO} + 2\ P_{CO_2}$ at 1,500°F

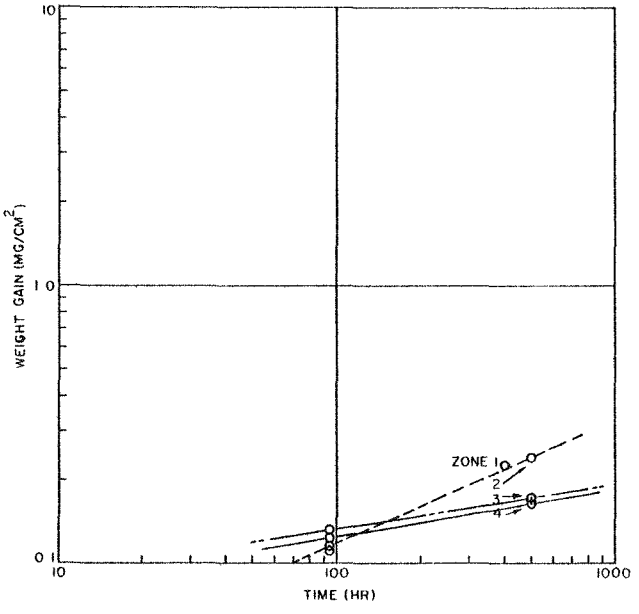

Fig. 4.17--Weight gain versus time for Inconel in helium + 2×10^{-4} atm $P_{CO} + 2\ P_{CO_2}$ at 1,500°F

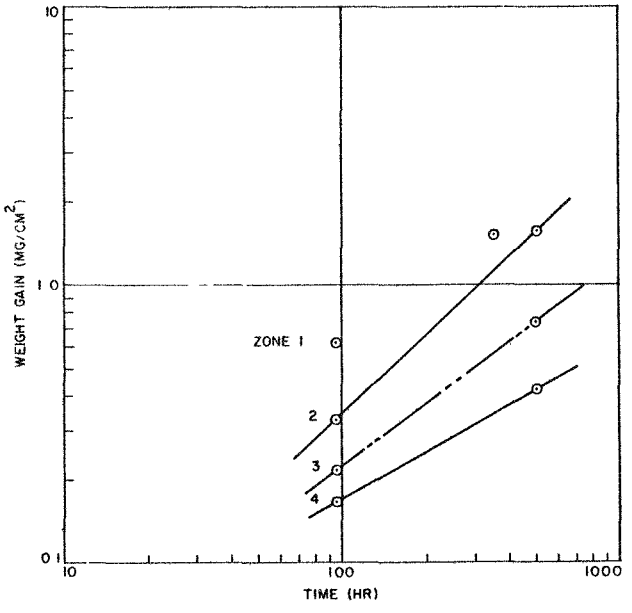

Fig. 4.18--Weight gain versus time for niobium in helium + 2×10^{-4} atm $P_{CO} + 2\ P_{CO_2}$ at 1,500°F

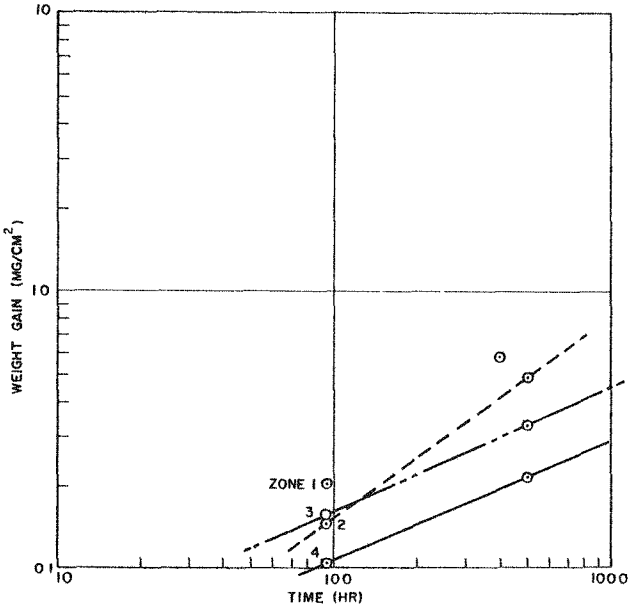

Fig. 4.19--Weight gain versus time for Inconel X in helium + 2×10^{-4} atm $P_{CO} + 2\ P_{CO_2}$ at 1,700°F

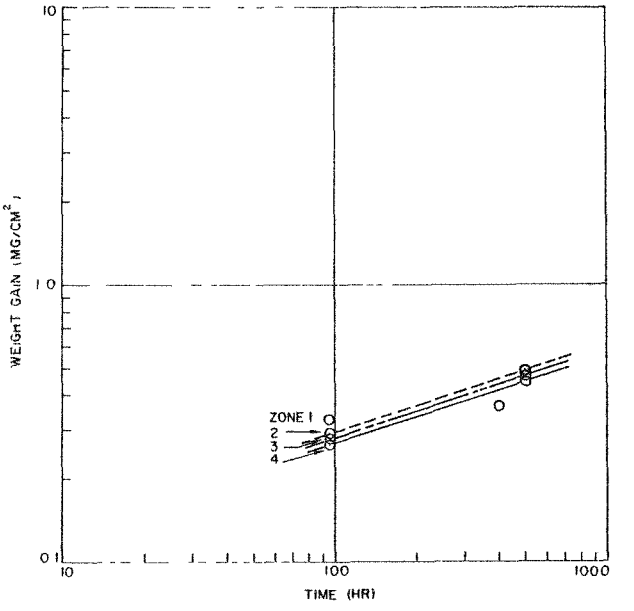

Fig. 4.20--Weight gain versus time for niobium in helium + 2×10^{-4} atm $P_{CO} + 2\ P_{CO_2}$ at 1,700°F

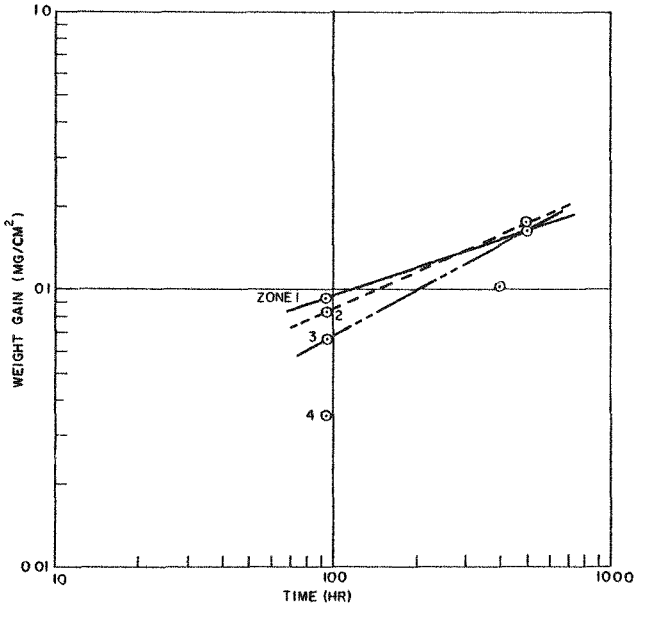

Fig. 4.21--Weight gain versus time for Inconel X in helium + 2×10^{-4} atm $P_{CO} + 2\ P_{CO_2}$ at 1,700°F

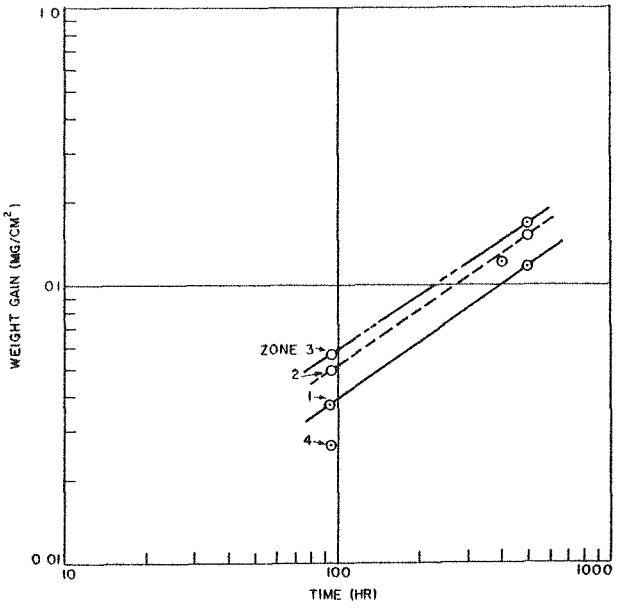

Fig. 4.22--Weight gain versus time for Inconel in helium + 2×10^{-4} atm $P_{CO} + 2\ P_{CO_2}$ at 1,700°F

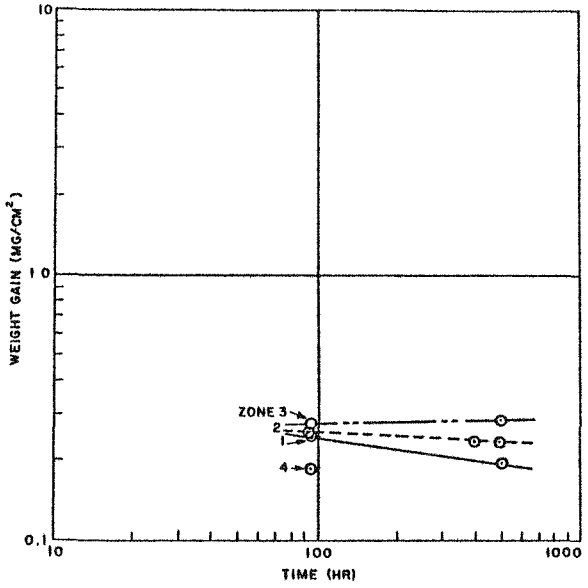

Fig. 4.23--Weight gain versus time for Type 316 stainless steel in helium $+2 \times 10^{-4}$ atm $P_{CO} + 2\,P_{CO_2}$ at 1,700°F

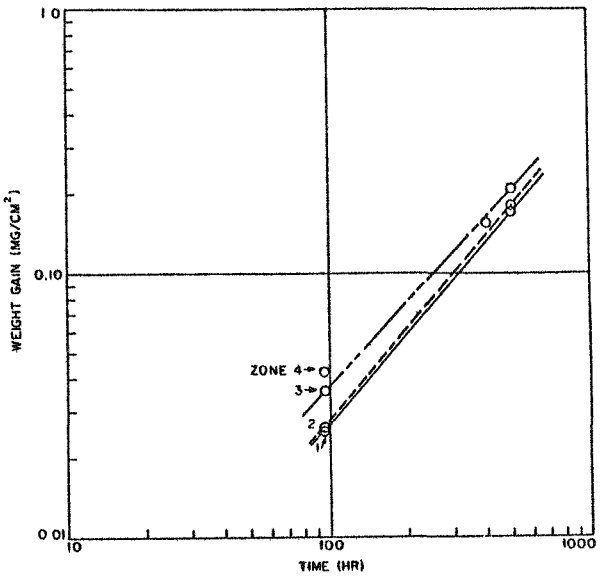

Fig. 4.24--Weight gain versus time for "A" nickel in helium $+2 \times 10^{-4}$ atm $P_{CO} + 2\,P_{CO_2}$ at 1,700°F

Samples of Duranickel and Monel were added to the tubes containing the nickel samples. The weight changes of these samples are given in Table 4.8.

Table 4.8

WEIGHT GAINS IN HELIUM PLUS 200 PPM CO FOR 400-HR TEST

(In milligrams per square centimeter)

Sample	Testing (°F)	Zone 1	Zone 2	Zone 3	Zone 4
Monel	1,700	-0.213	-0.177	-0.179	-0.164
	1,500	-0.045	-0.120	-0.216	-0.069
Duranickel	1,700	0.153	0.120	0.455	0.242
	1,500	0.585	0.336	0.177	0.112

No detectable dimensional changes were observed for any of the materials. The chemical analyses of the metal samples have not been completed. X-ray analyses of the niobium samples indicated the formation of NbC, and metallographic examination has been started.

Experiments will be conducted in which the exhaust gas will be cooled slowly at carbon monoxide levels of 1% and 100% to determine both the catalytic effect of various metals on the carbon monoxide disproportionation and the optimum temperature at which this reaction occurs.

EFFECTS OF IRRADIATION ON CORROSION BY COOLANT OR COOLANT-CARRIED IMPURITIES (W. L. Kosiba and C. R. Mungle)

Preliminary work was performed to determine the most feasible experimental arrangement for the graphite-metal-helium system. Two experimental arrangements were considered: (1) a straight tube and (2) a circular thermal convection harp (a torus). After some analytical considerations, the convection harp appeared to have the most advantages.

Several features of the test capsule require some discussion. The thermocouples do not "see" the internal torus temperatures. Thus, it was decided not to penetrate the quartz walls with thermocouples. This would avoid complicating the torus geometry. The spacers used to separate the metal specimens in the torus will be quartz. The four tori are loosely supported on the heat barrier and will be removed in one piece from the outer shell for the hot-cell examination.

As part of a brief bench study of graphite outgassing in preparation for the irradiation experiment, it was found, in agreement with the experience at General Atomic, that helium will filter through fused quartz. At 1,500°F, a quartz tube having a 1/16-in.-thick wall and approximately 0.4 in. ID allowed 35% of the initial helium at 1 atm to escape in 64 hr. In the same quartz tube at 800°F, 3% of the helium escaped in 32 hr.

Some information has been obtained at BMI on the outgassing of graphite specimens 3/4 in. OD by 4 in. long cut from bar stock. After the specimen in the quartz tube was vacuum-outgassed for 48 hr at 1,000°F, the specimen was heated to 1,500°F in 1 atm of tank helium and samples of the helium were analyzed with a mass spectrometer. When very dilute nitrogen and carbon monoxide impurities are present, each impurity is not readily distinguishable in the BMI mass spectrometer. Therefore, all nitrogen concentrations reported include a small (relative to nitrogen), but unknown, carbon monoxide contribution. The largest impurity in the tank supply was 0.06 vol-% nitrogen, together with 0.02, 0.02, 0.003, and 0.01 vol-% of H_2, CO_2, O_2, CO, and H_2O, respectively, which are the limits of sensitivity in our routine mass spectrometry. After a 24-hr exposure of the graphite, the nitrogen content increased to 0.26 vol-% and did not change after an additional exposure of 62 hr. During these two heat treatments, concentrations of the other impurities did not exceed the limits of sensitivity listed above. If a plateau concentration of nitrogen is verified in the next incremental exposure (100 hr), it is planned to stop this experiment and repeat it with a fresh graphite specimen and a zirconium foil in the quartz tube. The results obtained so far in this phase of the program indicate that in-pile release of gases from vacuum-outgassed graphite will make a significant contribution to the capsule impurities.

To measure the integrated fast-neutron exposure in the irradiation experiment, nickel wires will be located on the heat barrier. To supplement this information, fast-neutron and gamma-ray intensity in the empty core position will be measured before the capsule is irradiated. The total radiation received by the graphite can be estimated with adequate precision by using these dosimetry procedures.

Graphite specimens will be machined from the graphite bar supplied by General Atomic. The metal specimens will be nickel, Monel, niobium + 1% Zr, and Types 316 and 446 stainless steel.

A crude measurement of the time required for the helium to make one complete cycle around the torus was made by investigating convective gas flow in a simple glass mockup of the torus. The BMI estimate for the loaded torus is 2 min.

Several tori and specimen parameters which are of interest are listed in Table 4.9. A torus volume has been selected which is one-tenth the volume (25.9 $in.^3$) of the straight-tube capsules previously used. Reductions by this factor were made in the weights and volumes of the graphite and in the areas of the metal specimens, but not in the weights and volumes of the metal specimens.

Table 4.9

TORUS AND SPECIMEN PARAMETERS

Volume of empty torus, $in.^3$	2.58
Inside surface area of empty torus, in.	20
Torus (OD), in.	0.5
Torus wall thickness, mm	1.5
Volume of graphite specimen, $in.^3$	0.2
Surface area of graphite specimen (minus centerline hole), $in.^2$	2.27
Weight of graphite specimen, g	5.5
Graphite dimensions (nominal), in.	1/4 OD x 0.078 ID x 4 long
Area of metal specimen (both sides), $in.^2$	0.06
Helium pressure at temperature, atm	1

The four tori have been completed at BMI and are scheduled to be placed in the reactor during the first part of April.

The graphite specimens were vacuum-outgassed at 1,000°F for 48 hr. Whenever possible, both before and during torus loading, the outgassed graphite specimens are stored and handled in helium. The metal specimens were cut from as-received sheet stock. Prior to torus loading, the specimens were degreased with carbon tetrachloride.

A few changes have been made in the capsule to improve thermal performance. Two semicylindrical heaters are separated from the outer capsule shell by a helium gap. A 1/16-in. plate has been placed in the gap adjacent to one of the heaters to reduce this gap from 1/8 in. to 1/16 in. The gap (5/32 in.) adjacent to the other heater remains the same.

The heat barrier on which the tori are loosely supported is a 1/16-in.-thick nickel-plated stainless-steel plate that was polished to a mirror finish. Two plates have been added on both sides of this heat barrier to further reduce heat transfer between the two compartments. These plates are 10 mils thick. One is polished stainless steel and the other is polished nickel. The two plates are 1/16 in. apart, and the one nearest the heat barrier is 1/16 in. from this barrier.

The thermal mockup data indicate that the 700°F temperature difference can be achieved in the torus arms. Helium circulation in the capsule body, which would tend to smooth out this temperature gradient, is avoided by packing the areas at the ends of the heat barrier with quartz wool. The capsule is loaded with 15-psia helium at room temperature.

A duplicate set of tori are being constructed at General Atomic to simulate the in-pile experiment. Similar conditions of temperature, impurities, and materials will be used.

EFFECT OF COOLANT AND IMPURITIES IN COOLANT ON MATERIALS

(J. C. Bokros and D. G. Guggisberg)

Exploratory thermal convection tests were run to determine if carbon transport or carburization of plant structural materials occurs in impure helium-graphite systems, and if they do, how effective gettering might be for inhibiting these reactions.

The experiment was conducted with apparatus described in the previous quarterly report, GA-744. Quartz tubes, 80 cm long and 30 mm ID, were used to contain the specimens. They were loaded as follows:

Tube 1

a. Graphite at 775° to 810°C,

b. Graphite at 365° to 590°C,

c. Helium at 1/2 atm.

Tube 2

a. Graphite at 775° to 810°C,

b. Graphite at 365° to 590°C,

c. Zirconium getter at 305° to 335°C,

d. Zirconium getter at 775° to 795°C,

e. Helium at 1/2 atm.

Tube 3

a. Graphite at 775° to 810°C,

b. Graphite at 365° to 590°C,

c. Metal (430 and 316 SS, Inconel, Nb, and Nb + 1% Zr) at 810°C,

d. Metal (430 and 316 SS, Inconel, Nb, and Nb + 1% Zr) at 560° to 635°C,

e. Helium at 1/2 atm.

Tube 4

a. Graphite at 775° to 810°C,

b. Graphite at 365° to 590°C,

c. Metal (430 and 316 SS, Inconel, Nb, and Nb + 1% Zr) at 560° to 635°C,

d. Metal (430 and 316 SS, Inconel, Nb, and Nb + 1% Zr) at 810°C,

e. Zirconium getter at 305° to 335°C,

f. Zirconium getter at 775° to 795°C,

g. Helium at 1/2 atm.

The duration of the experiment was 1,000 hr. There was no evidence of carbon deposits in the quartz. The weight changes of the graphite specimens in each tube are shown in Table 4.10. There were no dimensional changes in the graphite. Figure 4.25 shows the tube after removal from the furnace, and Fig. 4.26 shows a photograph of the metal and graphite samples and the zirconium getter after removal from the quartz tubes.

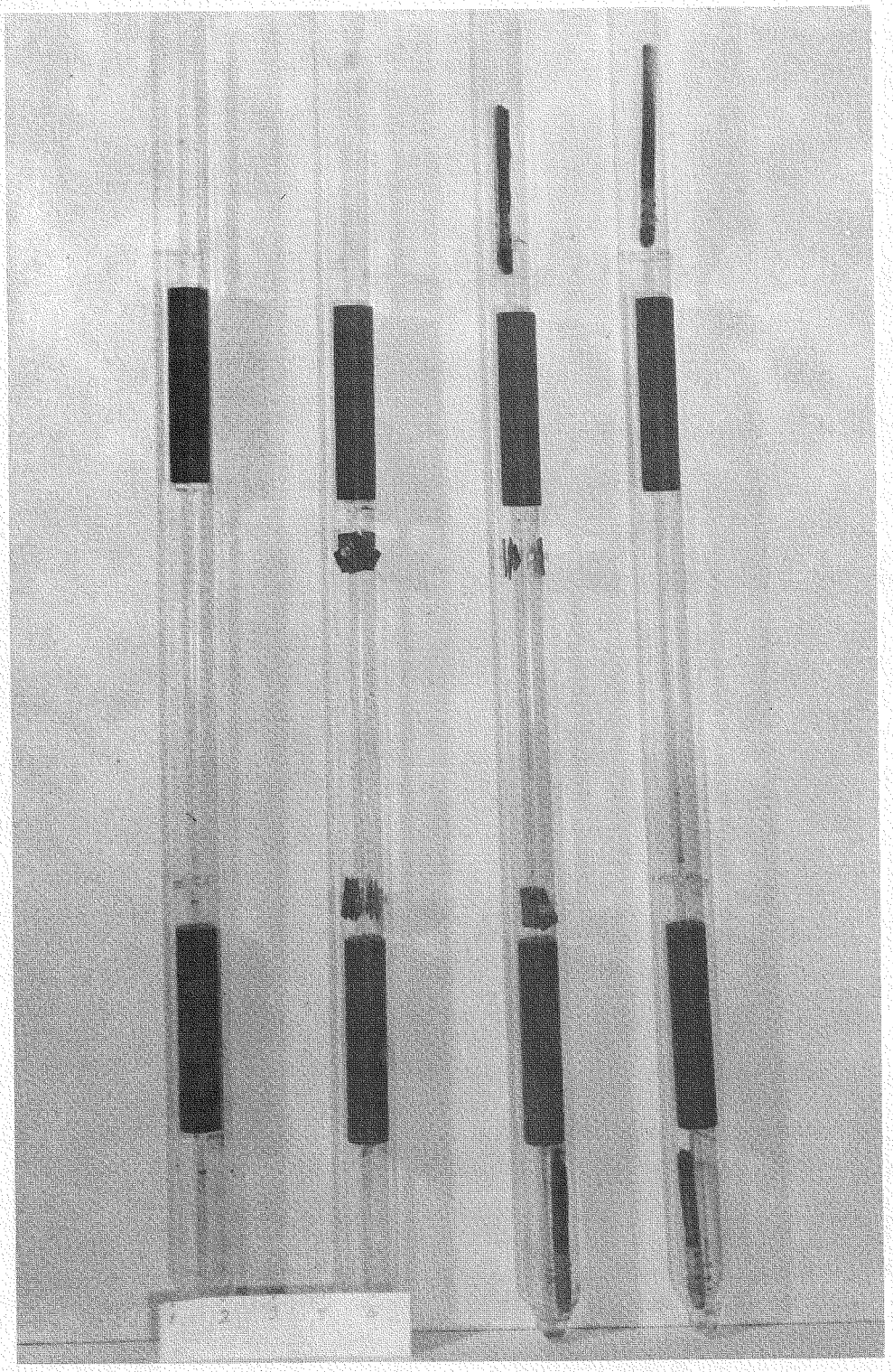

Fig. 4.25--Quartz tube after removal from furnace

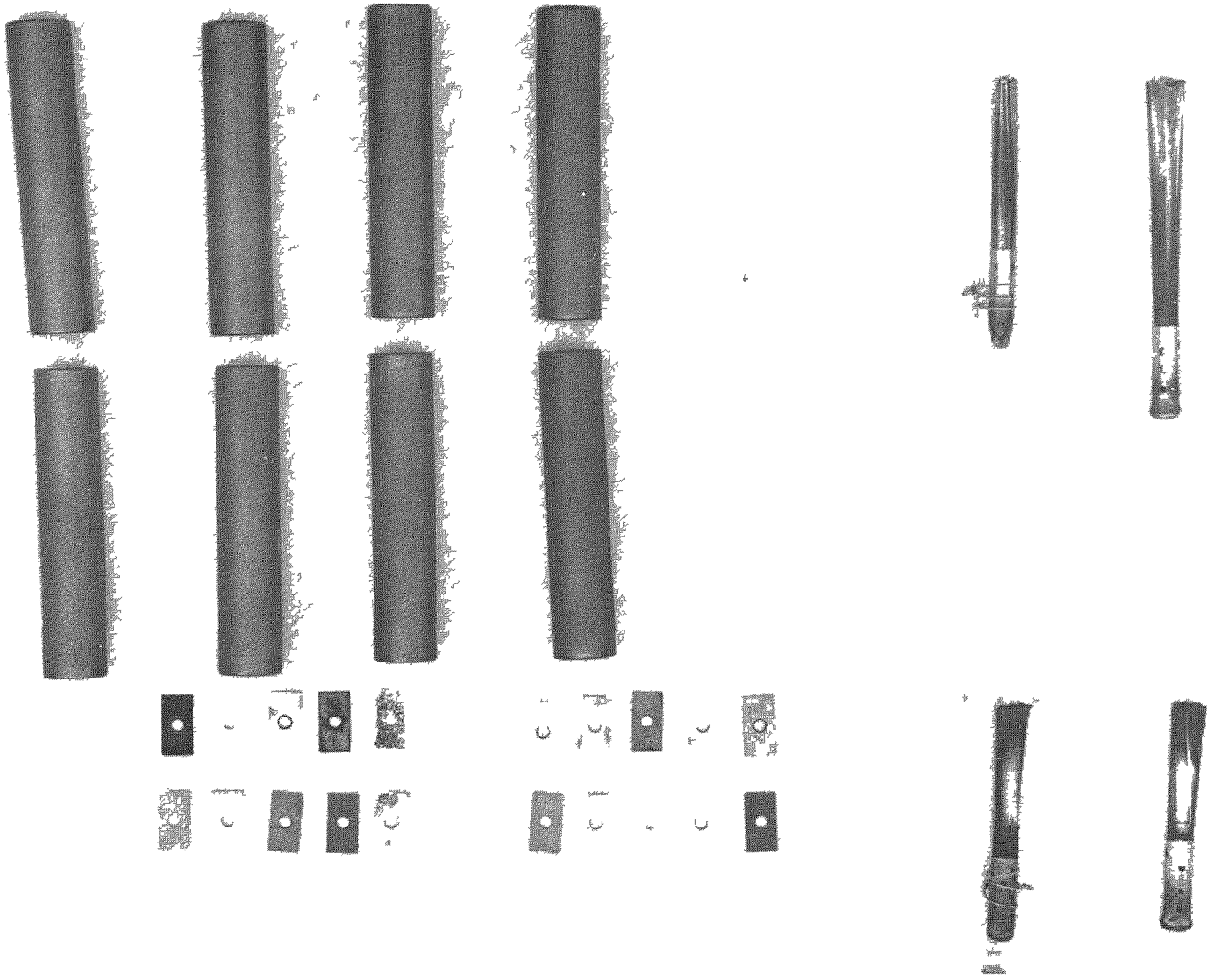

Fig. 4.26--Metal and graphite samples and zirconium getter

Table 4.10

WEIGHT CHANGES OF GRAPHITE AND GETTER

(In milligrams)

Tube No.	Graphite Specimen 775°-810°C	Graphite Specimen 365°-590°C	Zirconium Getter at 305°-335°C	Zirconium Getter at 775°-795°C
1	-15.6	-7.2	---	---
2	-15.1	-4.5	Lost	Lost
3	-17.0	-7.6	---	---
4	-11.7	-2.5	+0.5	-10.4

The analysis of the helium from each tube after the test is shown in Table 4.11. A mass spectrograph sensitive to impurities in excess of 0.005 mol-% was used.

Table 4.11

HELIUM ANALYSIS FROM EACH TUBE

(In mol-%)

Tube No.	H_2	He	N_2	CO	CO or N_2
1	6.77	89.10	0.12	4.01	------
2 (getter)	----	100.00	------	----	------
3	2.65	97.29	------	----	0.05
4 (getter)	----	100.00	------	----	------
Tank analysis	Trace	99.99+	0.0004	----	0.0004

The weight changes of the metal samples are shown in Table 4.12.

A preliminary metallurgical examination of the metal samples exposed in the four static carbon-transport experiments indicates that the impurities present in helium (CO and H_2) in equilibrium with graphite carburized Inconel, niobium, and niobium + 1% Zr in the ungettered capsule, but did not carburize these alloys in the gettered capsule. Hardness data obtained on these samples are given in Table 4.13.

Table 4.12

WEIGHT CHANGES OF METAL SAMPLES

(In milligrams)

Tube No.	Material	Area (cm^2)	Temperature (^oC)	Total Weight Change	Mg/cm^2
3	Niobium	3.9	810	+2.6	+0.67
3	Nb + 1% Zr	3.8	810	+4.7	+1.24
3	Inconel	3.9	810	+2.3	+0.59
3	318 SS	3.8	810	+1.2	+0.32
3	430 SS	3.7	810	+0.6	+1.6
3	Niobium	3.9	560 to 635	+1.3	+0.33
3	Nb + 1% Zr	3.8	560 to 635	+3.0	+0.79
3	Inconel	3.9	560 to 635	+2.2	+0.56
3	318 SS	3.8	560 to 635	+0.3	+0.08
3	430 SS	3.7	560 to 635	+0.4	+0.11
4	Niobium	3.9	810	+1.3	+0.33
4	Nb + 1% Zr	3.8	810	+1.6	+0.42
4	Inconel	3.9	810	+0.6	+0.15
4	318 SS	3.8	810	+2.0	+0.53
4	430 SS	3.7	810	+0.5	+0.14
4	Niobium	3.9	560 to 635	+0.8	0.21
4	Nb + 1% Zr	3.8	560 to 635	+0.2	0.05
4	Inconel	3.9	560 to 635	+0.1	0.03
4	318 SS	3.8	560 to 635	+0.2	0.05
4	430 SS	3.7	560 to 635	+0.5	0.14

These data show a significant difference in the hardness of niobium and of niobium + 1% Zr in the ungettered capsule compared with the gettered capsule. This change is attributed to carburization and/or solution of impurities in these metals. The small amount of carburization observed metallographically in Inconel did not affect the hardness significantly. No carburization was observed in the stainless steel experiments.

After the experiment, the tubes contained 0.57 atm of helium (at 300°C). Material balance for each tube, calculated from the gas analysis, and the weight change are shown in Table 4.14.

The graphite samples weighed about 54 g. The weight changes unaccounted for amount to about 0.01% and are believed to be insignificant. No carbon transport was observed.

Table 4.13

DPH OF SPECIMENS EXPOSED 1,000 HR

IN CARBON-TRANSPORT CAPSULES

Material	Gettered Helium				Ungettered Helium			
	Hot Zone		Cold Zone		Hot Zone		Cold Zone	
	Center	Edge	Center	Edge	Center	Edge	Center	Edge
Nb	165	162	139	132	213	218	171	153
Nb + 1% Zr	189	277	173	142	374	298	165	182
Inconel	189	203	193	195	166	189	177	188
318 SS	213	197	227	245	194	219	188	205
430 SS	183	192	170	168	166	147	228	192

Table 4.14

MATERIAL BALANCE

(In milligrams)

Tube No.	Material Loss of Graphite	Weight Increase of Impurities in Gas	Weight Gain of Metals	Weight Gain of Getter	Unaccounted For
I	-21	+13	---	---	-8
III	-25	+1	+19	---	-6
IV	-14	---	+8	+11	+5

REFERENCES

1. Booth, A. H., and G. T. Rymer, "Determination of the Diffusion Constant of Fission Zenon in UO_2 Crystals and Sintered Compacts," AECL-692, August, 1958.

2. Booth, A. H., "A Method of Calculating Fission Gas Diffusion From UO_2 Fuel and Its Application to the X-2-f Loop Test," AECL-496 (n.d.).

3. Booth, A. H., A. S. Bain, D. Kerr, and G. T. Rymer, "Collection and Measurement of Stable Fission Xenon in Sheath Puncture Experiments, Method and Results to Date," AECL-545, October, 1957.

4. Robertson, J. A. L., et. al., "Behavior of Uranium Oxide as a Reactor Fuel," Proceedings of the Second International Conference on the Peaceful Uses of Atomic Energy, Geneva, Switzerland, P/193, September, 1958.

5. Stubbs, F. J., P. J. Silver, and C. B. Webster, "The Release of Fission Product Rare Gases from Some Ceramic Materials," AERE-C/M-343, May, 1958.

6. Lustman, B., "Release of Fission Gases from UO_2," WAPD-173, March, 1957.

7. Markowitz, J. M., R. C. Koch, and J. A. Roll, "Release of Fission Gases from Irradiated Uranium Dioxide," WAPD-180, July, 1957.

8. Eichenberg, J. D., et. al., "Effects of Irradiation on Bulk UO_2," WAPD-183, October, 1957.

9. Moody, W. E., Jr., A. J. Taylor, and J. R. Johnson, "Preliminary Investigation of the Fission Product Retention Ability of Cermet Compacts," ORNL-1778, July 8, 1955.

10. Booth, A. H., E. W. Carruthers, and R. C. Hawkings, "A Preliminary Report of the Evolution of Rare-Gas Fission Products from Irradiated UO_2," Atomic Energy of Canada, Ltd., Report CRDC-598, July 5, 1955.

11. Wilson, J. E., "Diffusion of Fission Products from BeO Fuel Rod Material," Argonne National Laboratory Report CT-3765, March 16, 1947.

12. Bokros, J. C., Graphite-metal Compatibility at High Temperatures, General Atomic Report GA-782, June, 1959.

V. ECONOMIC ANALYSIS

With the aid of conventional-tanker costs furnished by the Maritime Administration, a revised cost comparison was made between conventional tankers and nuclear tankers in the three sizes and power ranges suggested by the Atomic Energy Commission and Maritime Administration. The new comparison showed a slight relative improvement for nuclear tankers, particularly for the large and high-powered ships. Total costs per ton of cargo carried are shown in Table 5.1 for the New York-to-Kuwait round trip. In this comparison, the capital charges are taken at 8.5% of initial cost. Present estimated costs for nuclear tankers are somewhat higher than costs for conventional ships. Also, these costs do not include profit, and allowance for this factor would tend to penalize nuclear ships, since they represent a higher initial investment.

Economic studies are continuing with the objective of determining the optimum size and power ranges for both nuclear and conventional ships.

Table 5.1

COST OF SHIPPING*

($/ton cargo)

Type	38,000 dwt 20,000 shp	60,000 dwt 27,500 shp	100,000 dwt 55,000 shp
Conventional ship	13.39	10.82	9.40
Nuclear ship, present design	14.45	11.24	9.63
Nuclear ship, advanced design	12.85	10.00	8.35

*New York to Kuwait and return, via Suez in ballast, via Cape of Good Hope loaded (20,000 nautical miles round trip).

VI. ADVANCED-DESIGN POWER PLANTS

A study of beryllium oxide-moderated reactors was initiated during the quarter as an advance-planning effort.

The use of beryllium oxide as a moderator in a homogeneous or semihomogeneous design affords greater safety in the event of a coolant pressure loss than is afforded by the use of a graphite moderator, because (1) beryllium oxide has a higher volumetric heat capacity than graphite, (2) it does not burn when exposed to air, and (3) it retains fission products. Also, because its slowing-down power is superior to that of graphite, the use of beryllium oxide makes it possible to design thermal or epithermal reactors of smaller diameter than the presently anticipated graphite-moderated MGCR.

The first of these potential advantages is of interest for a second-generation core design for the MGCR. The second advantage is of interest for other applications that require smaller and lighter reactors. Work during the quarter was confined to the investigation of beryllium oxide for second-generation MGCR cores, but work on smaller cores is planned for the future.

REVIEW AND INTERPRETATION OF LITERATURE ON BERYLLIA PROPERTIES

A survey of the unclassified literature on beryllium oxide and on UO_2-fueled beryllium oxide was made. Data were found on thermal conductivity, thermal-expansion coefficient, tensile strength, and creep strength as functions of temperature. A limited amount of data was also found on the effect of radiation on thermal conductivity, dimensional stability, and compressive strength. One reference was found which gave information on the ability of fueled beryllium oxide to retain fission gases. The data on thermal conductivity and its decrease under radiation have

particular significance for the design of a beryllium oxide-moderated and urania-beryllia-fueled reactor. Some of this information is presented in Tables 6.1 and 6.2. Interpretation of these data for design usage is

Table 6.1

THERMAL CONDUCTIVITY OF PURE BeO AS A FUNCTION OF TEMPERATURE*

Temperature ($^{\circ}$C)	Conductivity [Cal/($^{\circ}$C)(cm^2)(sec)]
400	0.166
600	0.091
800	0.070
1,000	0.046
1,200	0.040

*Data taken from Bernard Schwartz, Beryllia, Its Physical Properties at Elevated Temperatures, Report MIT-1083, Massachusetts Institute of Technology, February 27, 1952.

difficult, because the irradiations were carried out at lower temperatures than those which would exist in the hotter regions of the reactor. The following observations concerning the data were used as a basis for estimating conductivities in the reactor:

1. Thermal resistance tends to increase rapidly with respect to integrated flux to a level of five or six times the unirradiated value and tends to increase at a slow rate thereafter.
2. Part of the increased thermal resistance of the beryllium oxide can be "annealed out" after irradiation by a few hours exposure to temperatures of 600°C or above.
3. The maximum decrease in thermal resistance is achieved by a 7-hr exposure at 1,000°C. Longer times and higher temperatures do not further reduce the thermal resistance below 2.5 times its unirradiated value.

Table 6.2

EFFECT OF RADIATION EXPOSURE ON CONDUCTIVITY OF FUELED BeO*

Wt-% UO_2 in BeO	Density (g/cm^3)	Irradiation Temperature (°C)	Exposure (MWD/aT)	Integrated Flux (nvt)	U^{235} Burnup (%)	Total Atoms Fissioned (%)	Ratio of Thermal Resistivity, R_A/R_B†
0	2.9	40	54.4	----------	----	-------	1.33
2	2.85	40	54.4	3.2×10^{19}	1.75	0.0005	5.74
10	2.85	40	54.4	3.2×10^{19}	1.77	0.00027	4.14
0	2.9	40	109	----------	----	-------	1.46
2	2.85	250	109	7.8×10^{19}	4.23	0.00122	4.65
10	3.01	250	109	6.6×10^{19}	3.6	0.0056	6.04
10	2.85	250	109	6.6×10^{19}	3.6	0.0056	4.65
0	2.9	40	219	----------	----	-------	1.62
2	2.85	650 to 700	219	1.31×10^{20}	7.2	0.00204	6.56
10	3.01	650 to 700	219	1.15×10^{20}	6.2	0.00962	6.16
10	2.85	650 to 700	219	1.15×10^{20}	6.2	0.00962	5.66

Note: Effects on Post-Irradiation Annealing on Pure and Fueled BeO Thermal Conductivity

1. Annealing of 10-wt-% UO_2 specimens exposed for 219 MWD/aT for 7 hr at 1,000°C reduced the ratio of thermal resistivity after irradiation to thermal resistivity before irradiation from 6.75 to 2.5.
2. Annealing for longer periods than 7 hr or at higher temperatures produced no significant further decrease in thermal resistance.
3. Annealing of pure BeO specimens for 1.5 hr at 900°C restored pre-irradiation thermal resistance.
4. Threshold temperature for annealing effects was approximately 600°C.

*Data taken from J. R. Gilbreath and O. C. Simpson, "The Effect of Reactor Irradiation on the Physical Properties of Beryllium," Report P/621, Second United Nations Conference on the Peaceful Uses of Atomic Energy, United Nations, Geneva, 1958.

†R_A is thermal resistivity after irradiation; R_B is thermal resistivity before irradiation.

It was assumed that at 1,000°C, the annealing was sufficiently rapid to result in a thermal resistance of 2.5 times the unirradiated value. At 600°C and at lower temperatures, it was assumed that no annealing occurred and that the thermal resistance was 6.0 times the unirradiated value. A curve was faired between 1/6 the unirradiated conductivity at 600°C and 1/2.5 the unirradiated conductivity at 1,000°C. The conductivity is approximately constant at 3.3 Btu/(hr)(ft)(°F) along this curve. For unfueled beryllium oxide, a conductivity of 60% of the unirradiated value was assumed below 600°C, a value equal to the unirradiated value above 900°C, and a faired transition was assumed between 600° and 900°C.

It should be noted that the data given in Table 6.2 are for uranium oxide particle sizes of 2μ or less. It is entirely possible that much smaller effects of radiation would be encountered if uranium oxide particles having a size of the order of 100 μ were used. In that event, the ligaments of beryllium oxide between particles of uranium oxide would be too thick to be penetrated by fission fragments.

The data on fission-gas retention that are summarized in Table 6.3 have an important bearing on the feasibility of a reactor employing a large volume of clad beryllium oxide-uranium oxide as fuel. The reference on which Table 6.3 is based derives the diffusion coefficients tabulated from measurements of fission-gas release. To extend these data to the temperatures that would exist in the reactor, the Eyring rate equation was fitted to the data, as indicated in Table 6.3.

The data given in Table 6.3 are for fueled beryllium oxide compacts fabricated in 1947. With new techniques, denser beryllium oxide compacts that would contain fewer flaws and a more uniform fuel distribution can be fabricated. There is every reason to believe that better compacts would reduce the loss of fission gas.

Table 6.3

FISSION-GAS RETENTION CAPABILITY OF FUELED BERYLLIUM OXIDE*
(90% BeO - 10% UO_2)

Density (g/cm^3)	Annealing Temperature (^oC)	Xe Diffused Out in 3 hr (%)	Log Diffusion Coefficient	Log Diffusion Coefficient Predicted by $0.136\, e^{[(-26,500)/T]}$
3.1	1,000	0.1	-10.00	-9.92
3.1	1,100	0.4	- 8.52	-9.24
3.1	1,200	0.4	- 8.70	-8.70
3.1	1,325	0.5	- 8.48	-8.95
3.1	1,450	1.4	- 7.70	-7.52
0.5	100	0.8	------	-----
2.7	1,000	0.9	------	-----
2.9	1,000	0.8	------	-----

*J. E. Wilson, Diffusion of Fission Products from Beryllia Fuel Rod Material, Argonne National Laboratory, Report CT-3765, January 17, 1947.

CONCEPTUAL DESIGN

The conceptual design was largely determined (1) by the necessity for limiting the volume of stainless steel in the core to about 2% in order to retain the nuclear advantages of beryllium oxide as a moderator and (2) by the necessity for limiting the temperature of the cladding to 2,000°F following loss of coolant pressure. Other factors, such as the minimum volume of fuel required to give an adequate negative temperature coefficient at the end of core life and the maximum permissible thermal stresses in beryllium oxide, could not be considered owing to lack of information. A time of 2,000 sec after shutdown was selected as being adequate to start emergency cooling. Thus, a surface temperature of 2,000°F or less at 2,000 sec was desired. The volume fraction of stainless steel was determined for given heat-transfer conditions by specifying a cladding thickness of 0.010 in. As shown in Fig. 6.1, the surface temperature for a given volume fraction of stainless steel is at a minimum when the

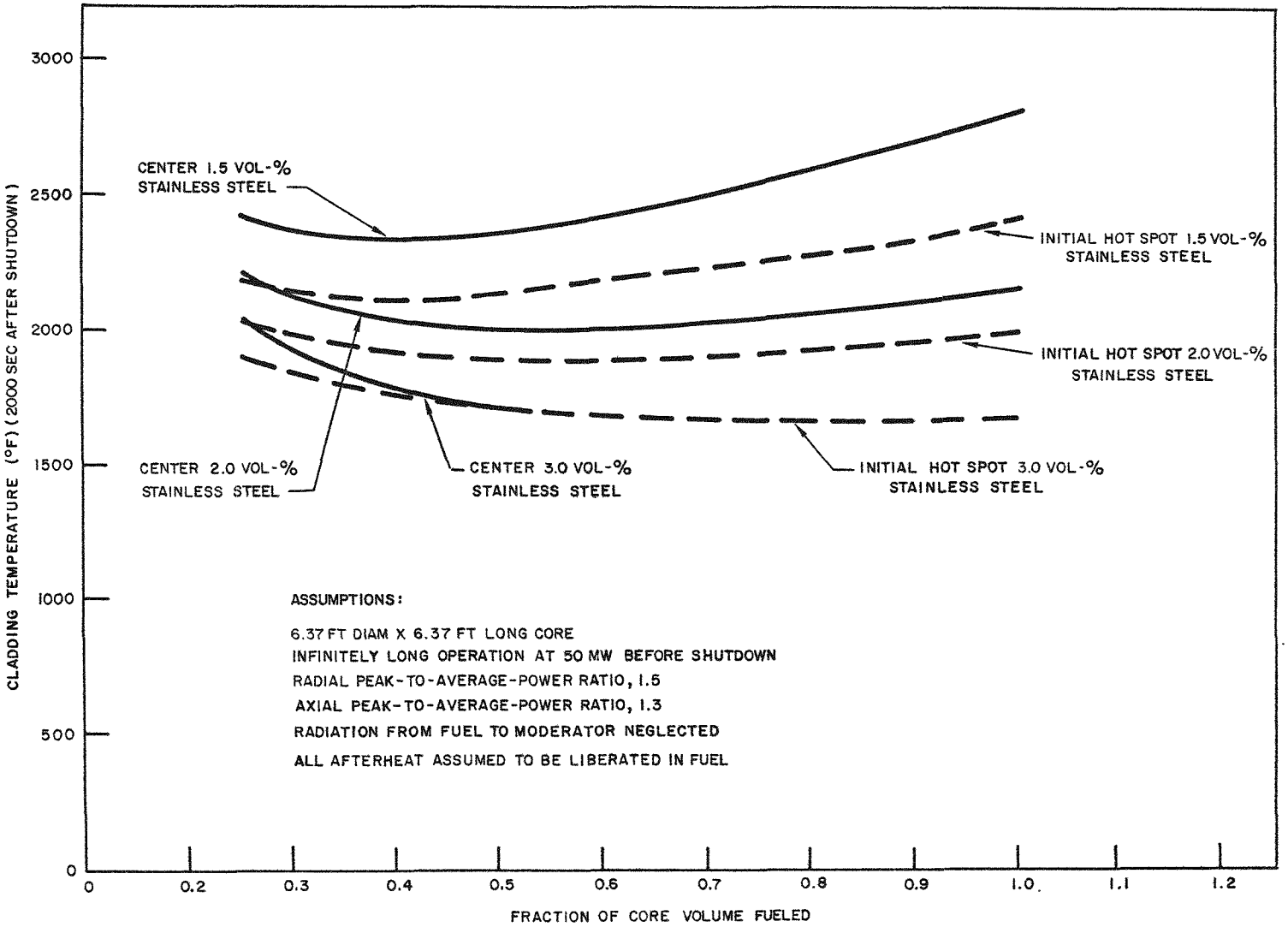

Fig. 6.1--Parametric study of cladding temperatures after loss of coolant in BeO-moderated reactors

fueled volume fraction is between one half and one third. The minimum point exceeds 2,000°F when the volume fraction of stainless steel is less than 2%. Two per cent stainless steel and one-third fueled volume were selected for the conceptual design. An arrangement of 151 hollow hexagonal moderator blocks, each containing 19 fueled beryllium oxide rods, 0.8 in. OD, was specified for the core. This arrangement fits into the same space as the proposed MGCR graphite cores. A conceptual layout study is in preparation.

FUEL-CYCLE COSTS

A program of calculations of neutronics, designed to determine the fuel inventories and lifetimes of comparable beryllium oxide-moderated and graphite-moderated reactors, is in progress. These calculations will be used to arrive at comparative fuel-cycle costs. From partial results, it is apparent that the use of beryllium oxide reduces the amount of neutrons lost by fast leakage. This advantage may be exploited (1) by introducing more U^{238} into the core for a given mass of U^{235}, thus reducing the enrichment and increasing the conversion ratio; and (2) by reducing the U^{235} inventory. It is not known whether reduced inventory or reduced enrichment and longer life will compensate for the cost of the beryllium oxide required in the fueled region.

STRUCTURAL PROBLEMS

Structural problems associated with thin cladding affect the feasibility of the semihomogeneous beryllium oxide reactor. The most serious problems are considered to be (1) rupture of the cladding due to fission-gas pressure following loss of coolant pressure, (2) failure of the cladding as a result of the strain cycling caused by the disparity in thermal-expansion coefficients of the fueled beryllium oxide and the cladding, and (3) local buckling of the cladding at the end of the fuel rod.

An analysis of the first problem has been made by utilizing the diffusion data presented in Table 6.3. In order for a void volume of 1% of the core to collect fission gas, the required pressure at the hottest point is computed to be only 1 atm. However, a helium pressure several times as great is probably necessary to preserve a reasonable thermal bond between the fuel and the cladding. Assuming 4 atm absolute pressure, a stress of 1,800 psi is predicted. This stress is less than both the short-time tensile and the 1-hr rupture strengths of AISI Type 310 stainless steel, which indicates that this type of stainless steel probably could be used. It is about equal to the short-time tensile strength of AISI Type 446 stainless steel, which indicates that this latter type material probably could not be used.

Analyses of problems (2) and (3) are in progress.